In vitro construction of liver sinusoid-like tissues by spatio-temporal control of hepatic stellate cells

March 2012

A thesis submitted in partial fulfilment of the requirements for the degree of
Doctor of Philosophy in Science (Engineering)

Keio University

Graduate School of Science and Technology
School of Integrated Design Engineering

Junichi Kasuya

Abstract

Development of tissue-engineered liver is an ongoing study for the future therapy of liver diseases. Its major challenge is reconstruction of sinusoidal structures. The sinusoids are functional multicellular complex composed of hepatocytes, hepatic stellate cells (HSCs) and endothelial cells (ECs), and responsible for highly differentiated functions of the liver. Therefore, the reconstruction of the sinusoidal structures is essential to achieve the functional liver tissues *in vitro*. However, the reconstruction of the sinusoidal structures has not been achieved yet. The role of HSCs in the sinusoid formation *in vivo* has been increasingly recognized. Therefore, this dissertation focused on a reconstruction of liver sinusoids *in vitro* using small hepatocytes (SHs) *i.e.*, hepatic progenitor cells, HSCs and ECs and elucidating the HSC's role in the reconstruction process.

Chapter 1 summarizes the background and purpose of this dissertation.

Chapter 2 summarizes the previous studies.

Chapter 3 summarizes the materials and methods.

Chapter 4 describes a reconstruction of HSC-mediated sinusoidal structures *in vitro*. In the sinusoids, HSCs mediated between layers of hepatocytes and EC capillaries. These HSC-mediated sinusoidal structures are essential to form the functional complex of these cell types. SHs and HSCs were first isolated from adult rat livers and cultured on polyethylene terephthalate (PET) microporous membranes. The SHs formed single-layered colonies on the membranes while HSCs resided in the micropores. Thereafter, ECs were inoculated on the opposite side of the membranes, resulting in a formation of the HSC-mediated structures. To obtain these structures, spatial control of HSC behavior by changing the pore size was critical. Furthermore, HSCs were confirmed to mediate the SH–EC communication in terms of EC morphogenesis. These

results indicate that the SH-HSC-EC physiological complex can be achieved in the reconstruction of the HSC-mediated structures.

In chapter 5, an effect of direct contacts between HSCs and ECs on EC capillary formation was determined in the SH-HSC-EC tri-culture. The HSC–EC contacts are increasingly recognized for their roles in EC capillary morphogenesis. However, the hypothetical role of HSC–EC contacts in morphogenesis remains unclear in the tri-culture. HSC–EC contacts were shown to inhibit EC capillary morphogenesis, suggesting that the HSC–EC contacts may be an important factor in EC capillary formation. In addition, ECs responded to the induction of capillary morphogenesis before the formation of HSC–EC contacts, suggesting that both spatial and temporal, of HSC behavior is a key engineering strategy for the reconstruction of sinusoidal tissue *in vitro*.

Chapter 6 describes the reconstruction of HSC-incorporated sinusoidal structures. In the sinusoids, HSCs surrounded the outer surface of EC capillary structures. To achieve these structures, heterotypic cell–cell interactions across the membranes need to be improved. To overcome this problem, poly (*D,L*-lactide-*co*-glycolide) (PLGA) microporous membranes were used. When pore size and porosity of the membranes were optimized, HSCs surrounded the EC capillary structures, resulting in the reorganization of sinusoidal-like structures. This model will provide a basis for the construction of functional, thick, vascularized liver tissues *in vitro*.

Finally, Chapter 7 summarizes the results of this study and describes its future prospects.

Abstract (Japanese)

将来的な肝臓病治療にむけて組織工学に基づいた機能的な肝臓組織の再生が試みられている．その最大の課題は，類洞の再構築である．類洞は肝細胞，星細胞，血管内皮細胞が形成する機能的な複合体であり，高次の肝機能を担保している．そのため，生体外で機能的な肝臓組織を再生するためには類洞の再構築が不可欠である．しかし，未だ類洞の再構築方法は確立されていない．一方，これまでに星細胞が生体内の類洞形成において重要な役割を果たすことが明らかになってきた．そこで本研究では，肝前駆細胞の一種である小型肝細胞と，星細胞および血管内皮細胞を用いて類洞構造を生体外で再構築し，再構築過程における星細胞の関与を明らかにすることを目的とした．

第 1 章に，本研究の背景と目的を記載した．

第 2 章では，基礎事項および従来の研究を概説した．

第 3 章には，実験方法を記載した．

第 4 章では，類洞の再構築の第一段階として星細胞による仲介構造の再構築を試みた．類洞では，星細胞が肝細胞の層状構造と血管内皮細胞の血管構造の間を仲介している．この星細胞による仲介構造は，3 者が生理学的な複合体として機能するために必須である．成熟ラットから分離した小型肝細胞と星細胞をポリエチレンテレフタラート多孔性薄膜上で培養すると，小型肝細胞は層状のコロニーを形成し，星細胞は微小孔内に分布した．その後，血管内皮細胞を薄膜の反対側に接着させることで，星細胞による仲介構造を再構築した．ここで，星細胞の挙動を微小孔の孔径によって空間的に制御することが，仲介構造の再構築に必須であることが分かった．さらに，仲介構造における星細胞は血管内皮細胞の形態形成において肝細胞と内皮細胞間のコミュニケーションを仲介した．すなわち，星細胞の挙動を空間的に制御し，星細胞による仲介構造を形成することで 3 者の生理学的な複合体を再構築できることが分かった．

第 5 章では，血管内皮細胞による血管構造の構築を試みた．生体外での血管構造の形成には，星細胞と血管内皮細胞の接触が大きく影響することが知られているが，3 者の共培養下におけるその役割は不明である．そのため，上記の共培養において星細胞と血管内皮細胞の接触が血管形態形成に与える影響を検討した．その結果，星細胞と血管内皮細胞の接触は血管形態形成を抑制することが分かった．そこで，まず血管形態形成を誘導し，その後星細胞との接触を形成させると，血管内皮細胞は毛細血管様ネットワークを形成できることが分かった．すなわち，3 者の共培養において血管構造を形成させるためには，星細胞の挙動の空間的な制御に加え，時間的な制御が不可欠であることを明らかにした．

第 6 章では，星細胞による裏打ち構造を再構築した．類洞では星細胞が細胞突起を伸ばして血管構造を裏打ちしている．この星細胞による裏打ち構造を再構築するためには，より活発な薄膜を介した異種細胞間相互作用が必要である．そこで，従来の多孔性薄膜より薄く，空隙率の高い生分解性ポリ乳酸 - ポリグリコール酸共重合体（PLGA）多孔性薄膜を作製し，この薄膜を用いることによって星細胞による裏打ち構造を形成することができるか検討した．その結果，適切な形状の薄膜を用いることによって，星細胞は毛細血管様ネットワークを裏打ちし，生体内の類洞に類似した組織を形成できることが明らかになった．さらに，この類洞様組織内の小型肝細胞は，肝細胞分化マーカーの mRNA を発現しており，肝細胞機能の指標となるアルブミン分泌量も高いレベルを維持していた．これらの結果は，PLGA 多孔性薄膜が異種細胞間相互作用を促進させ，機能的な肝類洞様組織の再構築に有効な細胞足場であることを示している．

最後に，第 7 章では各章で得られた内容をまとめ，本研究の成果を要約した．さらに本研究の今後の展望を述べた．

Contents

List of abbreviations

2D: two-dimensional (2-4)*

3D: three-dimensional (1-1)

α-SMA: α-smooth muscle actin (2-2-4)

*Alb***: albumin (2-4)

BC: bile canaliculi (2-1-1)

BPMEC: bovine pulmonary microcapillary endothelial cell (3-3-3)

BrdU: bromodeoxyuridine (3-4-1)

*Bsep***: bile salt export pump (3-8)

C/EBPα: CCAAT/enhancer binding protein α (2-4)

*Cebpa***: CCAAT/enhancer binding protein α (2-8)

CK: cytokeratin (2-4)

CMI: capillary morphogenesis index (3-5-5)

CO: carbon monoxide (2-2-2)

DAPI: 4',6-diamidino-2-phenylindole (3-4-1)

DMEM: Dulbecco's modified Eagle's medium (3-3-1)

DMEM/F12: 1:1 Mixture of Dulbecco's Modified Eagle's Medium and Ham's F-12 (2-4)

DMSO: dimethyl sulfoxide (3-3-4)

DNA: deoxyribonucleic acid (2-3)

DPPIV: dipeptidylpeptidase IV (2-4)

EC: endothelial cell (1-2)

ECM: extracellular matrix (2-2-1)

EDTA: ethylene diamine tetraacetic acid (2-4)

* Sections where the abbreviation first appears

** Gene symbols

EGF: epidermal growth factor (2-4)

EGFP: enhanced green fluorescent protein (3-3-1)

ELISA: enzyme-linked immunosorbent assay (3-7)

FBS: fetal bovine serum (3-3-1)

Gapdh[*]: glyceraldehyde-3-phosphate-dehydrogenase (3-8)

GFR: growth factor reduced (3-3-5)

HA: hyaluronic acid (2-4)

HCl: hydrochloric acid (3-6)

HEPES: 4-(2-hydroxyethyl)-1-piperazineethanesulfonic acid (3-3-1)

HGF: hepatocyte growth factor (2-4)

HNF: hepatic nuclear factor (2-4)

Hnf4a[*]: hepatic nuclear factor-4α (3-8)

HSC: hepatic stellate cell (1-1)

LEC: liver epithelial cell (2-4)

LETF: liver-enriched transcription factor (2-4)

MH: mature hepatocyte (2-4)

mRNA: messenger ribonucleic acid (3-8)

MRP2: multidrug-resistance associated protein 2 (2-4)

Mrp2[*]: multidrug-resistance associated protein 2 (3-8)

$NaHCO_3$: sodium hydrogen carbonate (3-3-1)

NH_4Cl: ammonium chloride (3-7)

NO: nitric oxide (2-2-1)

NPC: non-parenchymal cell (1-1)

PBS: phosphate-buffered saline (3-3-5)

PDGF: platelet-derived growth factor (3-4-1)

* Gene symbols

PET: polyethylene terephthalate (1-2)

PFA: paraformaldehyde (3-4-1)

PG: prostaglandin (2-2-2)

PHx: partial hepatectomy (2-3)

PI: propidium iodide (3-4-1)

PLGA: poly (*D,L*-lactide-*co*-glycolide) (1-2)

QPCR: quantitative real-time polymerase chain reaction (3-8)

RBP: retinol-binding protein (2-2-4)

ROI: region of interest (3-5-7)

RNA: ribonucleic acid (3-8)

RT: room temperature (3-4-1)

RT-PCR: reverse transcription polymerase chain reaction (2-4)

SD: standard deviation (3-6)

SD rat: Sprague-Dawley rat (3-3-1)

SDH: serine dehydratase (2-4)

SEC: sinusoidal endothelial cell (1-1)

SEM: Scanning electron microscopy (3-2-2)

SEP: subendothelial process (2-2-2)

SH: small hepatocyte (1-2)

SL: sinusoidal lumen (2-2-2)

SMC: smooth muscle cell (4-3)

Tat[*]: tyrosine aminotransferase (3-8)

TEM: transmission electron microscopy (2-4)

TO: tryptophan 2,3-dioxygenase (2-4)

To[*]: tryptophan 2,3-dioxygenase (3-8)

* Gene symbols

VE-cadherin: vascular endothelial-cadherin (3-4-1)

VEGF: vascular endothelial cell growth factor (2-2-3)

ZO-1: zona occludens-1 (2-4)

Chapter 1. General introduction

1-1. Introduction

Liver is the key organ with metabolisms of sugars, proteins/amino acids and lipids, detoxification of exogenous chemicals, production of bile acids, and storing of various other essential chemicals such as vitamins or irons (Ross *et al*., 2003). Therefore, its failure often results in a fatal threat to our life. About 3.5 million people in Japan are estimated to have liver disorder, with roughly 16,000 deaths registered annually due to liver disease (Vital and Health Statistics Division, Statistics and Information Department, Minister's Secretariat, Ministry of Health, Labour and Welfare of Japan, 2010). To date orthotopic liver transplantation is the only clinically accepted therapy for liver failure. Although about 2,200 patients are added to the waiting list each year, only about 500 patients undergo transplantations each year in Japan. Even if the patients fortunately find appropriate donors, they need to take an immunosuppressive drug whole life long since their immune systems reject the transplanted livers. Therefore, the need for alternative therapies to the liver transplantation is extremely urgent.

A tissue-engineered liver is expected to be developed as an alternative method to the liver transplantation. Tissue engineering is the process of creating functional three-dimensional (3D) tissues using cells combined with scaffolds or devices that facilitate cell growth, organization and differentiation, and is expected to serve as an alternative to organ transplantation (Langer and Vacanti, 1993). The tissue-engineered organs alleviate the shortage of donor organs for transplant. Additionally, since the tissue-engineered organs are made from patients' own cells, their immune systems do not reject them.

Despite the increasing demand for the liver tissue engineering, it is far from its clinical application. In contrast, tissue-engineered products such as skin substitutes and cartilage replacement have already helped thousands of patients (Yamato, 2009; Khademhosseini *et al.*, 2009). Artificial tissues such as bladder, cornea, bronchial tubes, and blood vessels are in clinical trials (Yamato, 2009; Khademhosseini *et al.*, 2009). A major reason that engineered liver tissues is off from practical use is that they lack an extensive internal vasculature. The difficulty of providing a blood supply has limited the size of engineered liver tissues. Any tissue with more than a few 100 microns thickness needs a vascular system because cells in a tissue need to be close enough to be capillaries to be supplied the oxygen and nutrients from the capillaries. This can be explained by the simple oxygen diffusion and consumption around the blood vessel (Lovett *et al.*, 2009). In particular, an incorporation of the vascular system for engineered liver tissues is absolutely imperative due to a very high cellular oxygen consumption rate of hepatocytes, *i.e.*, liver parenchymal cells, about 10 times higher than that of fibroblasts (Smith *et al.*, 1996). Consequently, many researchers are focusing on constructing vascularized engineered liver tissues *in vitro*.

The liver sinusoids are the microvasculature of the liver and the site of the majority of the blood–tissue interface in the liver. Unlike the microvasculature in other tissue beds, the liver sinusoids have a highly specialized structures, where hepatocytes and sinusoidal lining cells including sinusoidal endothelial cells (SECs) and hepatic stellate cells (HSCs) intimately associate with each other and form a physiological complex (section 2-2-2). This is responsible for wide-ranging functions of the liver. Therefore, reconstruction of the liver sinusoidal architecture is urgently needed.

The significance of the HSC's role in the sinusoidal organization has been increasingly recognized both in *in vivo* (Enzan *et al.*, 1997; Martinez-Hernandez and

Amenta, 1995) and *in vitro* observations (Wirz *et al.*, 2008; Semela *et al.*, 2008; Soto-Gutierrez *et al.*, 2010), suggesting that HSCs might play a key role in reconstruction of the sinusoidal tissues *in vitro*. Although various co-culture models of hepatocytes and non-parenchymal cells (NPCs) including microvascular cells have developed (section 2-5), no studies have addressed any effective culture methods for the reconstruction of the sinusoids since they did not focus on the potentially key role of HSCs in the sinusoidal organization. Hence, little is known about the HSC's role in the context of *in vitro* sinusoidal reconstruction, resulting in lack of efficient engineering strategies for construction of liver sinusoids *in vitro*.

1-2. Objectives

This dissertation aimed to elucidate HSC's role in the reconstruction of the sinusoidal structures using small hepatocytes (SHs) *i.e.*, hepatic progenitor cells, HSCs and endothelial cell (ECs), and also aimed to propose a novel engineering strategy for construction of liver sinusoids *in vitro*.

In the liver, HSCs closely adhered to SECs, which line the liver sinusoids. HSCs also directly face hepatocytes. From this mediated position of HSCs, the cells are considered to facilitate and integrate cell–cell communications between SECs and hepatocytes. However, due to the lack of *in vitro* models, little is known about the mechanisms by which HSCs facilitate and integrate communications in the hepatocyte-HSC-SEC complex. Therefore, the HSC-mediated hepatocyte and EC tri-culture model was established. The HSC-mediated sinusoidal structures are considered to be responsible for highly differentiated functions of liver, since they are significantly different from the microvascular structures in the other parenchymal organs and unique to the liver. Considering above, the reconstruction of the HSC-mediated structures is the initial step toward the achievement of the liver sinusoidal tissues *in vitro*. SHs were used as a source of hepatocytes since they can form hepatic organoids with HSCs *in vitro*. Hence, SHs and HSCs were first cultured on polyethylene terephthalate (PET) microporous membranes to let them form the hepatic organoids. ECs were then inoculated on the other side of the membranes. The SHs and ECs on each side of the membranes may be bridged by HSCs through the pores, resulting in forming of a physiological complex. It was ascertained whether size of the membrane's pore affected to the HSC behavior and the consequent organization of the cells. Additionally, it was elucidated whether the HSCs could work as both facilitators and integrators of cell–cell communication between hepatocytes and ECs in terms of EC morphogenesis.

As a next step toward the achievement of the sinusoidal tissues *in vitro*, EC capillary formation in the above SH-HSC-EC complex is necessary. Direct contacts between HSCs and ECs are increasingly recognized for their roles in EC capillary morphogenesis. However, the hypothetical role of HSC–EC contacts in morphogenesis remains unclear in the tri-culture. Therefore, the effects of direct HSC–EC contacts on EC capillary formation were first determined in the complex. Following the above investigation, engineering strategy for inducing the capillary formation in the tri-culture was developed.

In the liver sinusoids, HSCs are located along the outer surface of the EC capillary structures. The HSC-incorporated sinusoidal structures are responsible for active heterotypic cell–cell interactions and result in highly differentiated liver functions. During its organization, active heterotypic cell–cell interactions are involved. However, HSC–EC interaction in the tri-culture above was limited due to the high thickness and low porosity of the PET membranes. Therefore, microporous membranes with high porosity and reduced thickness are required. To address this issue, poly (*D,L* -lactide-*co*-glycolide) (PLGA) membranes were fabricated and their topography such as thickness, pore size, and porosity were optimized. In the optimized condition, formation of the HSC-incorporated capillary structures was morphologically analyzed over culture time. Furthermore, it was ascertained whether liver-specific functions of SHs were promoted.

A complete review of background information related to this dissertation is presented in chapter 2. Materials and methods used in this dissertation are then presented in chapter 3. As mentioned above, in chapters 4 to 6, HSC's role is determined in the reconstruction of the sinusoidal structures using SHs, HSCs, and ECs. Furthermore, a novel engineering strategy for the construction of liver sinusoids *in vitro*

is proposed. In chapter 4, the HSC-mediated structures are first reconstructed. Then, the EC capillary formation is inducted in chapter 5. In chapter 6, to reconstruct the HSC-incorporated capillary structures, the PLGA microporous membranes are fabricated and its topography is optimized. Finally, these studies are summarized and the conclusions are described in chapter 7.

References

Enzan H, Himeno H, Hiroi M, Kiyoku H, Saibara T, Onishi S. 1997, Development of hepatic sinusoidal structure with special reference to the Ito cells. *Microsc Res Tech*, **39**: 336–349.

Khademhosseini A, Vacanti JP, Langer R. 2009, Progress in Tissue Engineering, *Scientific American*, **300**: 64–71.

Langer R, Vacanti JP. 1993, Tissue engineering, *Science*, **260**: 920–926.

Lovett M, Lee K, Edwards A, Kaplan DL, 2009, Vascularization strategies for tissue. *Tissue Eng Part B Rev*, **15**: 353–370.

Martinez-Hernandez A, Amenta PS. 1995, The extracellular matrix in hepatic regeneration. *FASEB J*, **9**: 1401–1410.

Ross MH, Kaye GI, Pawlina W. 2003, 'Digestive System III: Liver, Gallbladder, and Pancreas' in *Histology a text and atlas, 4th edition*, Lippincott Williams & Wilkins, Philadelphia, PA, USA; 532–563.

Semela D, Das A, Langer D, Kang N, Leof E, Shah V. 2008, Platelet-derived growth factor signaling through ephrin-b2 regulates hepatic vascular structure and function. *Gastroenterology*, **135**: 671–679.

Smith MD, Smirthwaite AD, Cairns DE, Cousins RB, Gaylor JD. 1996, Techniques for measurement of oxygen consumption rates of hepatocytes during attachment and post-attachment, *Int J Artif Organs*, **19**: 36–44.

Soto-Gutierrez A, Navarro-Alvarez N, Yagi H, Nahmias Y, Yarmush ML, Kobayashi N. 2010, Engineering of an hepatic organoid to develop liver assist devices. *Cell Transplant*, **19**: 815–822.

Vital and Health Statistics Division, Statistics and Information Department, Minister's Secretariat, Ministry of Health , Labour and Welfare of Japan. 2010, General mortality, *Vital statstics of Japan 2010*.

Wirz W. Antoine M. Tag CG, Gressner AM, Korff T, Hellerbrand C, Kiefer P. 2008,

Hepatic stellate cells display a functional vascular smooth muscle cell phenotype in a three-dimensional co-culture model with endothelial cells. *Differentiation*, **76**: 784–794.

Yamato M. 2009, Current Status of Regenerative Medicine from the Viewpoint of Tissue Engineering. *Trends in the sciences*, **14**: 36–43.

Chapter 2. Background

This chapter presents the background information that will define the rationale of the thesis study. Section 2-1 summarizes organ level and sub-organ level functions and structures of the liver and section 2-2 reviews the microenvironment and the cells in the sinusoids. Section 2-3 reviews the regenerating capability of the liver. In section 2-4, characteristics of a SH and its application for liver tissue reconstruction *in vitro* are then summarized. Finally, current liver cell culture models which aim to reconstruct the sinusoidal tissues are discussed with their limitations in section 2-5.

2-1. Liver functions and structures

2-1-1. Liver functions

Liver carries out a multitude of functions, which is essential for life and can be classified into following four major functions: detoxification, synthesis, storage, and excretion (Ross *et al*., 2003). 1) Detoxification: hepatocytes detoxify drugs and toxins, such as ammonia products and alcohols. They convert drugs and toxins into more water-soluble forms, which can be transported to the kidney and removed. 2) Synthesis: the liver metabolizes carbohydrates, fats, and proteins. It synthesizes various circulating plasma proteins: albumins, lipoproteins, glycoproteins, prothrombins, fibrinogens, and nonimmune globlines. Hepatocytes also synthesize glucose and release it into the bloodstream in liver microvessels, termed liver sinusoids in respond to demand. 3) Storage: the liver absorbs nutrients from blood that has already circulated from the intestine, and stores glycogen, proteins, and vitamins. 4) Excretion: hepatocytes produce bile and excrete it into bile canaliculi (BC). The secreted bile flows into bile ducts and it is finally excreted into the duodenum. The bile contains metabolites, such as urea and bile acids that help to digest fats. These wide-ranging functions are made possible by

the complex interactions between the bloodstream and the cells of the liver, facilitated by the complex architecture of the parenchyma and its cell arrangement.

2-1-2. Liver structures

The liver is the largest solid organ in the body, weighting about 1,500 g in the adult human. It lies in the right upper quadrant of the abdominal cavity, direct contact with the undersurface of the diaphragm. Liver is divided into right and left lobes of about equal size. A large amount of blood runs into the lobes and they are highly vascularized, which allows blood with the ingested substances to be metabolized or detoxified by the liver before the systemic circulation. Total hepatic blood flow in the adult human amounts to 25% of cardiac output. This afferent blood supply of the liver has dual origin: 75–80% of the supply is accounted for by the portal vein and the remaining 20–25% from the hepatic artery (Wynne *et al*., 1989). The hepatic portal vein collects blood from the small intestine, colon, and pancreas. The hepatic artery is the major branch of abdominal aorta and contributes half of the total oxygen supply to liver. This dually-supplied blood is united to stream into the liver sinusoids, the specialized capillaries in the liver. Subsequently, the blood flows through the sinusoids and empties into the central vein of each lobule. The central veins coalesce into the hepatic veins, which leave the liver.

The liver lobes can be further divided into functional components, termed hepatic lobules (Fig. 2-1A). The hepatic lobule is the smallest module of the liver and we can see this polygonal unit, about 0.7 mm in diameter and 2.0 mm long, in a histological section of the liver. The central veins locate in the center of the liver lobules while the portal triads composed of the hepatic artery, the hepatic portal vein, and the bile duct locate in the periphery. The main cell type in the liver, hepatocytes, are arranged into plates of single thickness, known as the parenchyma. These hepatocyte plates extend

from the portal triads to the central veins, and they are separated by liver capillaries termed sinusoids. Sinusoids are 7–15 μm in diameter and lined with SECs. HSCs are distributed within the space of Disse, forming cell–cell contacts both with hepatocytes and SECs. Kupffer cells are the resident macrophages in the liver, interact with SECs within the sinusoid. Thus, the several kinds of cells are assembled and organized into the liver tissues (Fig. 2-1B).

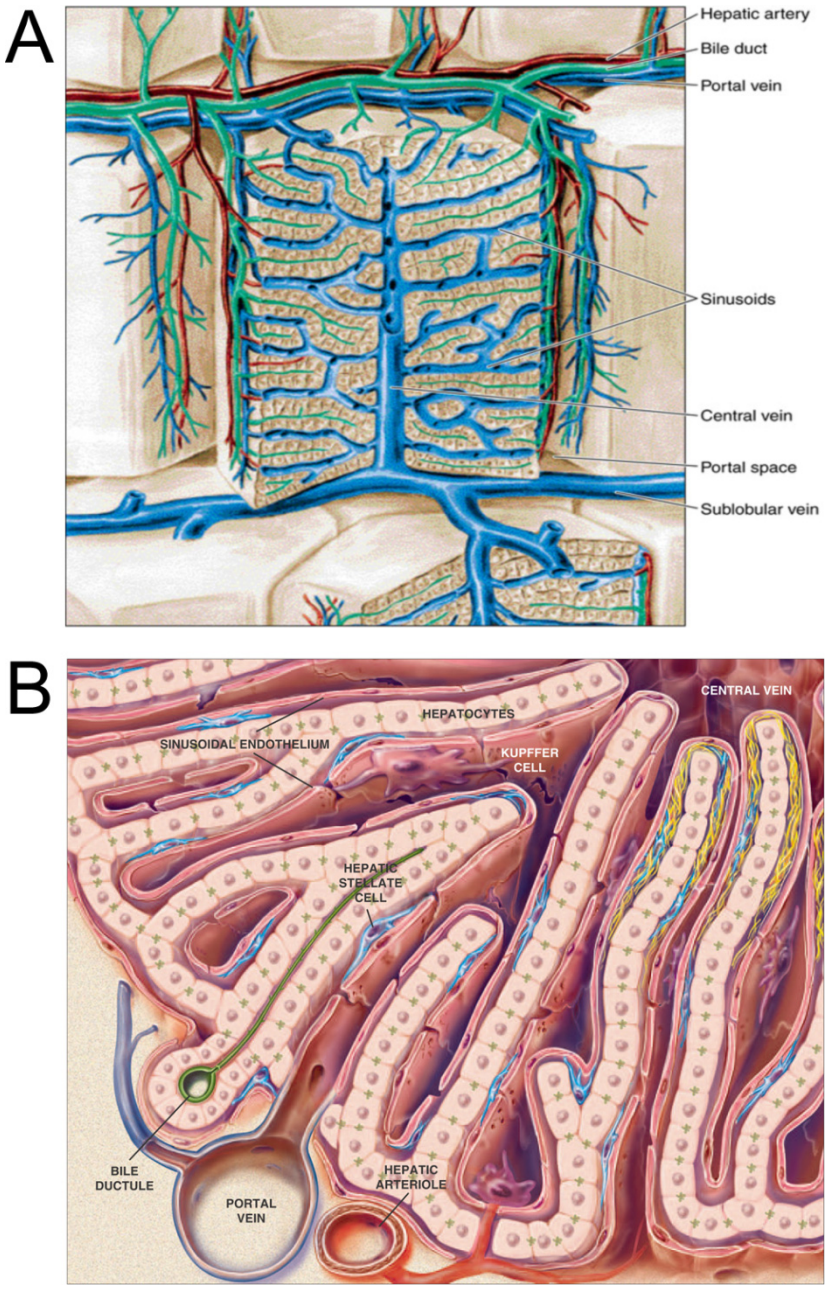

Figure 2-1. The structures of the liver's functional units, or lobules (*A*) (adapted from Mescher, 2010) and its detail (*B*) (adapted from Friedman and Arthur, 2002). Blood enters the lobules through branches of the portal vein and hepatic artery, then flows through sinusoids. The hepatocytes remove toxic substances from blood, which then exits the lobule through the central vein (*i.e.*, hepatic venue). In the liver lobules, several kinds of cells are organized into well-assembled tissues.

2-2. Liver microenvironment and cells

2-2-1. Liver Parenchyma

Hepatocytes are the most numerous cell type in the liver, constituting about 60% of total cells and composing about 80% by volume. They are highly differentiated cell type and responsible for most of the synthetic and many of the metabolic functions of the liver. Hepatocytes are shaped as complex polygon with several distinct surfaces that comprise functionally three distinct domains: the apical domain forms bile canalicular networks involved in secretion of bile components and metabolites of xenobiotics; the basal domain faces the extracellular matrix-rich (ECM-rich) region (the space of Disse) and is involved in cell signaling; the lateral domain forms tight junctions with neighboring hepatocytes.

The highly differentiated functions of hepatocytes are difficult to maintain for an extended period of time *in vitro*, mainly because the microenvironmental cues *in vivo* are not recaptured *in vitro*. These include homotypic and heterotypic cell–cell interactions, cell–ECM interactions, and mechanical stress signals. As mentioned before, unlike the parenchymal cells in other tissue beds, the hepatocytes are in close proximity to the sinusoids. These specialized structures are responsible for active heterotypic cell–cell interactions between hepatocytes and sinusoidal lining cells including SECs and HSCs, resulting in the highly differentiated functions of hepatocytes. Hence, recapturing the liver sinusoidal structures will not only contribute to the vascularization of engineered liver tissues *in vitro* but also address the above issues.

2-2-2. Liver sinusoids

The liver sinusoids are the microvasculature of the liver and the site of the majority of the blood–tissue interface in the liver. Unlike the microvasculature in other

tissue beds, the liver sinusoids have a highly specialized structure (Fig. 2-2A). As mentioned above, the liver cells are organized into the aciner-like structures with blood entering the sinusoidal space from the portal venules, surrounding both surfaces of the hepatic plate, and exiting via the hepatic venules. The sinusoids interconnect via SEC's fenestrations (for detail, see section 2-2-3), forming a labyrinth of vessels closely associated with the liver parenchyma. Note that the sinusoids are larger in caliber than the average extrahepatic capillaries and more closely associated with the parenchyma than the typical ECs (D'amore and Herman, 2001). SECs and hepatocytes are separated by the space of Disse, the extracellular space of the liver. HSCs reside in the space of Disse. As liver-specific pericytes, HSCs closely adhere to SECs and partly encircle sinusoids with their long cytoplasmic processes. A single SEC receives cytoplasmic processes from one to three HSCs. In addition, many thorn-like microprojections or spines extend from the subendothelial processes to make contacts with hepatocytes (Wake, 2006). One HSC entwines two or more sinusoids and about 20–40 hepatocytes. Thus, HSCs make physical contacts with both hepatocytes and SECs (Fig. 2-2B).

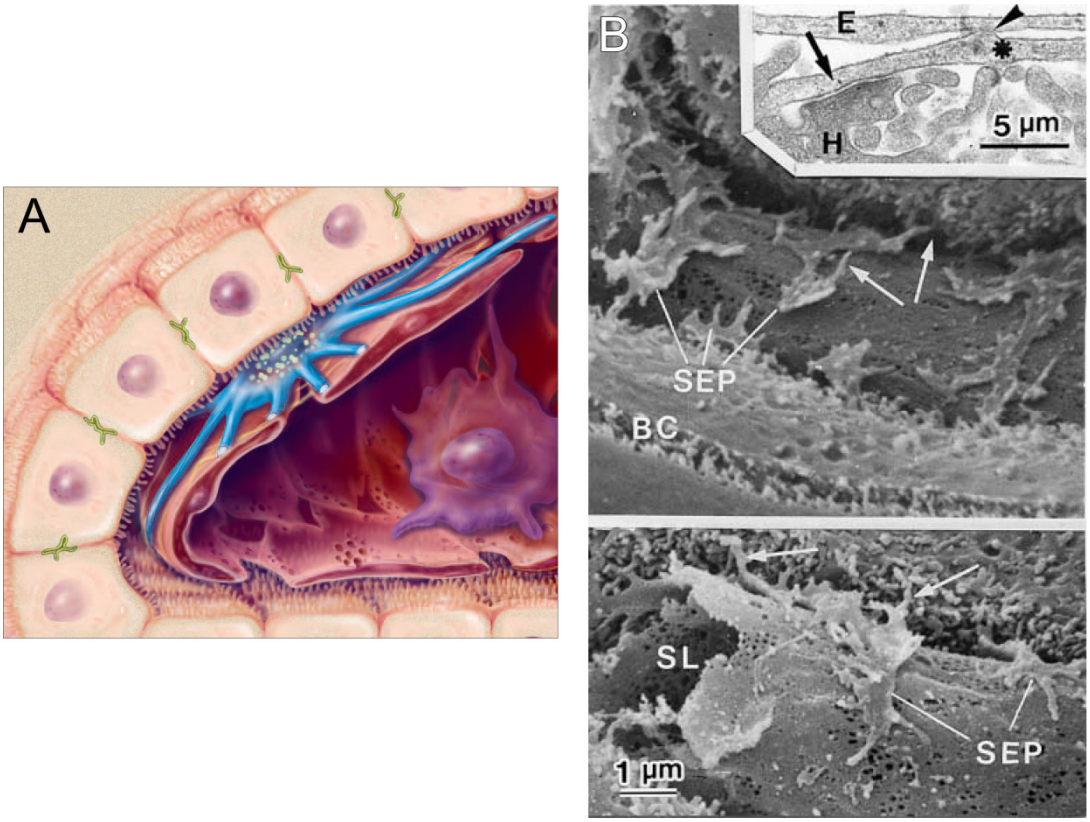

Figure 2-2. The HSC-mediated sinusoidal structures between hepatocytes and SECs. ***A)*** Within the normal hepatic sinusoid, HSCs (blue) are found in the space of Disse, located between the hepatocytes and the SECs. Quiescent HSCs are recognized by their perinuclear droplets, which contain vitamin A. Normal hepatocytes are lined with microvilli, and SECs have pores or fenestrations. A Kupffer cell (purple) lies in the sinusoid (Image A adapted from Friedman and Arthur, 2002). ***B)*** Scanning electron micrographs showing the Space of Disse and spines (arrows) of HSCs of the rat liver (Image B adapted from Wake, 2007). Spines project from lateral edges of the subendothelial processes (SEP) course obliquely through the Space of Disse and contact with hepatocytes. BC: bile canaliculus; SL: sinusoidal lumen. ×8,000. Inset: A transmission electron micrograph of a longitudinal section of the spine which extends from the subendothelial process (astarisk). The spine, crossing the space of Disse, adheres to both an EC (E) (arrowhead) and a hepatocyte (arrow). ×24,000.

Based on above *in vivo* observations for close proximity of hepatocyte, HSCs, and SECs, the concept of a hepatocyte-HSC-EC complex that functions as a unit for transduction between the bloodstream and the hepatic parenchyma was proposed (Wake, 2006, Suematsu and Aiso, 2001). Recent studies support a concept that HSCs serve a bridge that mediates bidirectional metabolic interactions between sinusoids and hepatocytes, utilizing prostanoids and/or gaseous mediators such as nitric oxide (NO) and carbon monoxide (CO) as signaling molecules. A typical example for the potential role of HSCs in alterations of sinusoidal function through hepatocyte-mediated mechanisms is a reception of CO secreted from hepatocytes by soluble guanylate cyclase in HSCs that contributes to maintenance of sinusoidal patency (Fig. 2-3A) (Goda, *et al*. 1998). Besides the CO-mediated maintenance of sinusoidal patency, a variety of vasoactive mediators such as endothelins, NO and prostaglandin (PG) E_2 are considered to transfer information at the sinusoidal side towards hepatocytes (Fig. 2-3B) (Suematsu, 1999). Although the hepatocyte-HSC-EC complex is thus increasingly recognized as a functional unit which integrates the bloodstream and hepatic parenchyma, few studies have addressed the above issue due to the lack of appropriate culture models which recaptured the structural and functional complex. This concept inspired the design of tri-culture in this study.

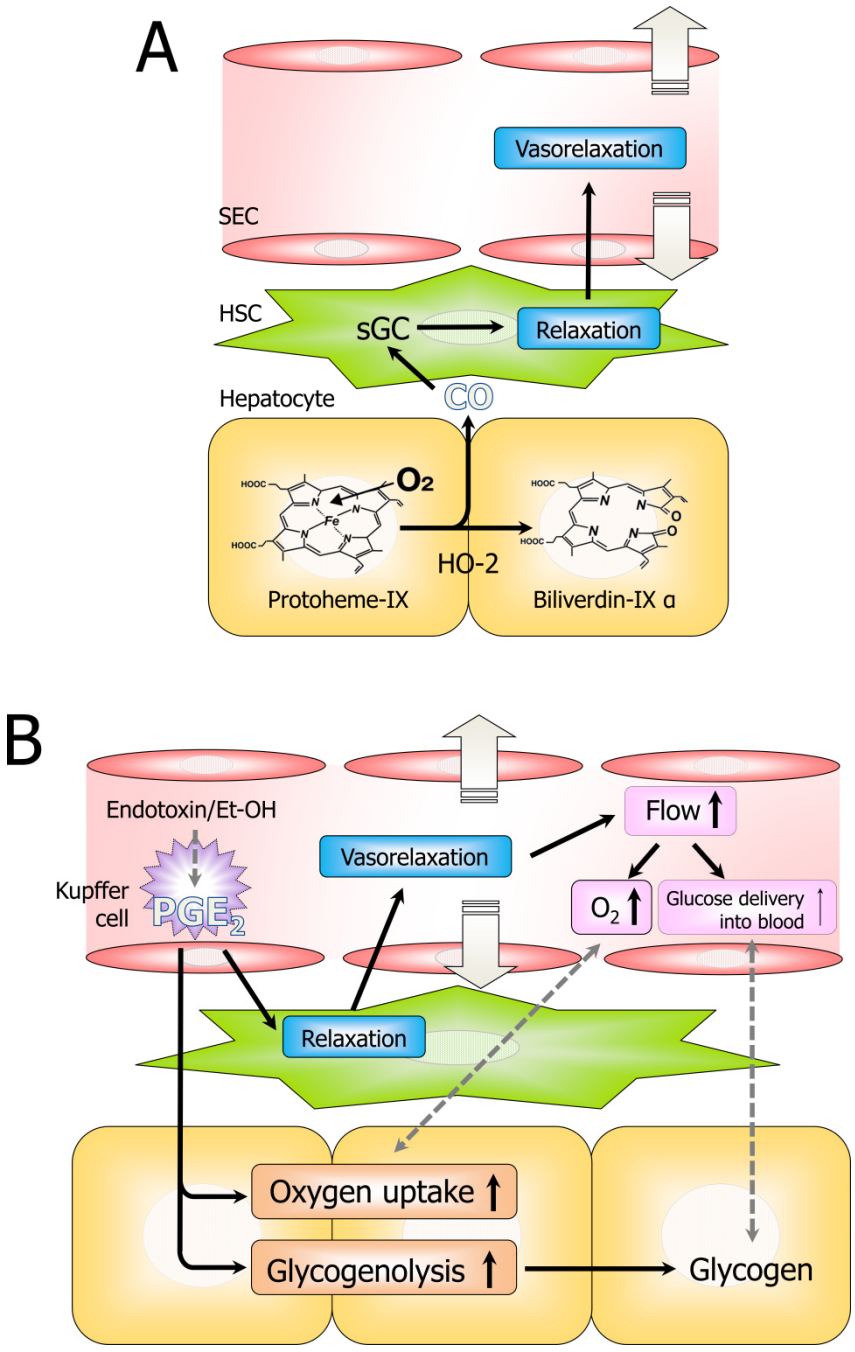

Figure 2-3. Schematic of the proposed concept of a hepatocyte-HSC-EC complex that functions as a unit for transduction between the bloodstream and hepatic parenchyma based on the studies by (*A*) Goda, *et al*. (1998) and (*B*) Suematsu (1999).

2-2-3. Sinusoidal endothelial cells

SECs form a continuous lining on the sinusoidal wall as a barrier between the parenchyma and blood (Braet and Wisse, 2002). They constitute about 19–21% of total cells, and comprise about 3% by volume. The thin cytoplasm of these flattened cells is penetrated by holes termed fenestrations, each about 150–170 nm in diameter, which form groups of 10–50 termed sieve plates (Braet and Wisse, 2002). The number and size of fenestrations vary in different zonations and can change in respond to a variety of hormones, drugs, toxins, and underlying ECM (Braet and Wisse, 2002). Unlike capillaries in other tissue beds, sinusoids lack a basement membrane, but have sparse ECM including collagen I, III, IV, and VI, laminin, heparin sulfate and dermatan sulfate proteoglycans, fibronectin, and chondroitin sulfate (Martinez-Hernandez and Amenta, 1993). The unique structures of SECs and sinusoids maximize delivery of blood fluid components, but the ECM in the space of Disse can bind some molecules.

Relating to the sinusoidal and SEC structures mentioned above, SECs provide the main pathway for clearance of effete molecules from the circulation. They clear effete proteins and colloids from the circulating blood through number of receptors involved in receptor-mediated endocytosis. These include the scavenger receptor, hyaluronan receptor, mannose receptor, and Fc receptor.

SECs do not adapt well to *in vitro* culture because of their poor survival (Takahashi *et al*., 2001). In serum-free, hormonally defined media, rat SECs plated on ECM survive less than a week, even when plated at high cell density, and lose fenestrae within a few days (Braet *et al*., 1994; Krause *et al*., 2000). Significant apoptosis of purified SEC is observed soon after plating *in vitro* even in the presence of serum and vascular endothelial growth factor (VEGF) (Ohi *et al*., 2006). Co-culture with primary hepatocytes, which secrete VEGF and other growth factors important for SEC survival,

improves maintenance of some phenotypic behaviors (DeLeve *et al*., 2004; Edwards *et al*., 2005), but fail to keep the cells alive much longer than a week (Nahmias *et al*., 2006). However, recent studies demonstrated that SECs survive longer than 13 days in 3D perfusion co-culture with hepatocytes and NPCs including HSCs (Hwa *et al*., 2007), and the cells survive at least two weeks in micropatterned co-culture with hepatocytes and fibroblasts (March *et al*., 2009). These studies suggest that SECs share an intimate relationship with hepatocytes and other NPCs in homeostasis of the liver.

2-2-4. Hepatic stellate cells

HSCs, located in the space of Disse and partly encircling sinusoids as liver-specific pericytes, comprise about 5–8% of all live cells (Greerts, 2001). Although HSCs do not account for large number of liver cells, they are multifunctional.

They play an important role in the metabolism of vitamin A together with hepatocytes and store ~50–80% of retinoids in the whole body as retinyl palmitate in lipid droplets in the cytoplasm (Bloomhoff, 1990). Dietary retinyl esters are first hydrolyzed to retinol in the intestinal lumen before absorption by enterocytes, and carotenoids are absorbed and then partially converted to retinol in the enterocytes. In the enterocytes, retinol reacts with fatty acid to form esters before incorporation into chylomicrons. Chylomicrons then reach the general circulation by way of the intestinal lymph, and chylomicron remnants are formed in blood capillaries. Chylomicron remnants containing almost all the absorbed retinol are mainly cleared by the hepatocytes. In hepatocytes, retinyl esters are rapidly hydrolyzed to retinol, which then binds to retinol-binding protein (RBP). A complex of retinol-RBP is secreted and transported to HSCs. HSCs store retinoids mainly as retinyl palmitate and secrete retinol-RBP directly into the blood (Senoo, 2004). Thus, HSCs regulate both transport and storage of retinoids. From the view of anatomy, the cytoplasmic storage of lipid

droplets is the most characteristic feature of quiescent HSCs in a physiological condition (Wake, 1971). In contrast, loss of the lipid droplets in HSCs is one of the markers of myofibroblastic phenotype (Friedman *et al*., 1993; Tsukamoto *et al*., 1996).

HSCs take the central role in synthesis and degradation of ECM components in the space of Disse (for information about the ECM components in the space of Disse in normal liver, see section 2-2-3). In contrast to their pivotal role in ECM metabolism in a healthy liver, HSCs are considered to commit liver fibrogenesis progression by producing abundant fibrous matrix into the space of Disse (Bedossa and Paradis, 2003). These quantitative or qualitative modifications of the ECM microenvironment will alter the HSC phenotype to myofibroblastic one, signed by their expression of α-smooth muscle actin (α-SMA), and further worsen a condition. Besides the phenotypic transition of HSCs, these ECM changes are also associated with modifications in the SEC phenotype including the loss of the fenestrae. These events are termed sinusoid capillarization. Furthermore, due to direct connections between hepatocytes and blood flow, the sinusoid capillarization will strongly impair the hepatocyte functions. These changes illustrate the role of HSCs as a coordinator of extracellular microenvionment and heterotypic cell–cell interactions.

2-2-5. Other cell types

Other liver cells include Kupffer cells and pit cells. Kupffer cells are the liver resident macrophages. They account for more than 50% of all macrophages in the body and about 8–12 % of all liver cells (Wisse, 1974a; Wisse; 1974b). They are located in the sinusoidal lumen, forming cellular projections over the SEC lining. Their extensions sometimes reach through the fenestration of SECs and into the hepatocytes. As a major immune defense cell type to preserve homeostasis of the liver, they remove foreign materials such as bacterial components, endotoxins, and immune complex from portal

blood through endocytosis, phagocytosis, and production of cytekines (Naito *et al*., 2004).

Pit cells are natural killer cells. They reside in the sinusoids and display mechanisms against viral infections and tumor metastasis (Nakatani *et al*., 2004).

2-3. Liver regeneration

The liver is the only internal organ capable of natural regeneration of lost tissue. Extensive functional damage created by loss of tissue drive proliferative processes that eventually restore liver function and architecture (Michalopoulos, 2007). In terms of partial hepatectomy (PHx) in a human living-donor trasnplantation, the volume of the residual liver of the donor doubles within 7 days (Fausto, 2001). PHx is commonly accepted as experimental model for studying liver regeneration. In PHx, lobes comprising two third of a rat liver are removed. The residual lobes enlarge to make up for the lost mass within 5–7 days. At the cellular level, deoxyribonucleic acid (DNA) synthesis of hepatocytes within the remnant rat liver first initiates 10–12 hours after PHx and peaks at 24 hours (Fig. 2-4A). This is followed by biliary epithelial cells at 36–48 hours, Kupffer cells and HSCs at 48 hours, and finally SECs at 96 hours (Michalopoulos and DeFrances, 1997).

The liver regeneration is accompanied by intrahepatic angiogenesis and at least in part, an angiogenesis-dependent phenomenon (Drixler *et al*., 2002). At 72 hours after PHx, single cell wide plates of hepatocytes have grown to avascular clusters of 10–12 hepatocytes (Fig. 2-4B). HSCs then extend their cytoplasmic processes and invade into the hepatocyte clusters and secrete ECM rich in laminin (Martinez-Hernandez and Amenta, 1995). Surrounding SECs follow and infiltrate into these avascular islands and

proliferate, resulting in reestablishment of the normal cell plate architecture. Both the intrahepatic angiogenesis and following restoration of original plate architecture are inhibited by antiangiogenic treatment (Drixler *et al*., 2002), suggesting that these processes can be achieved when there is a precise coordination among hepatocytes, NPCs including HSCs and SECs, and the extracellular environment such as ECM.

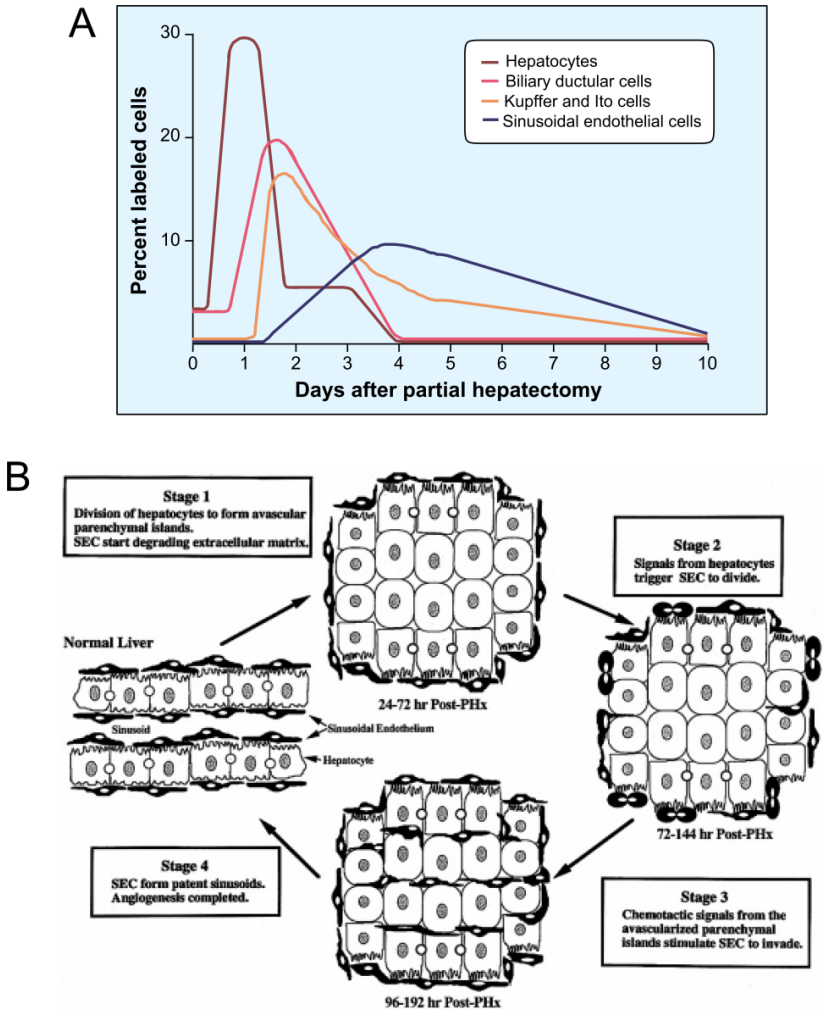

Figure 2-4. Sequential events during liver regeneration. ***A*)** Time kinetics of DNA synthesis in different liver cell types during the liver regeneration after PHx (Image A adapted from Michalopoulos, 1997). The major types of liver cells, such as hepatocytes, biliary ductular cells, Kupffer cells, HSCs and SECs, start to proliferate about 24 hours after PHx undergo DNA synthesis at different times. The DNA synthesis of the hepatocytes is first started and peaks at 24 hours, whereas the other cell types proliferate later. ***B*)** The timing and stages of angiogenic events during liver regeneration (Image B adapted from Ross *et al*., 2001).

2-4. Small hepatocytes

Although a variety of different culturing methods have been developed to induce the proliferation of primary hepatocytes *in vitro*, the proliferation efficiency of adult rat hepatocytes could not be sufficiently improved, which led to the conclusion that primary hepatocytes cannot proliferate *in vitro*. Mitaka *et al*. (1992a) identified small mono-nucleate cells as proliferating cells within primary hepatocytes cultured in serum-free medium supplemented with 10 mM nicotinamide and 10 ng/ml epidermal growth factor (EGF). Immunocytochemistry for hepatocyte-markers showed that the small cells were positive for albumin, transferrin, cytokeratins (CK) 8 and 18. Transmission electron microscopy (TEM) revealed that the cells had abundant mitochondria, peroxisomes with crystalline nucleoids in their cytoplasm (Mitaka *et al*., 1992b). These results suggest that the newly developed cells have typical characteristics of mature hepatocytes (MHs). These mono-nucleate cells are different in size from MHs; SHs are about 17 μm in diameter while MHs are about 24 μm in diameter (Tateno *et al*., 2000). Therefore, these cells are termed SHs.

When a simple technique of low-speed centrifugation was used to isolate SHs from mix population of liver cells, they can be isolated with NPCs such as HSCs, liver epithelial cells (LECs), Kupffer cells, and SECs (Mitaka *et al*., 1995; Mitaka *et al*., 1999). A single SH clonally proliferate to form a colony consisting of several hundred cells (Mitaka *et al*., 1995). SHs also have a capability to reconstruct hepatic organoids with NPCs including HSCs (Mitaka *et al*., 1999). SHs start to proliferate by day 3 and form colonies within 10 days (Fig. 2-5). While most SECs disappear within one week, HSCs and LECs proliferate and surrounded the SH colonies. Thereafter, the NPCs invade under the colonies and accumulate ECM to form a basement membrane-like structure. The besement membrane-like structure is mainly comprised of laminin, type IV collagen and fibronectin. The accumulation of ECM may induce the alteration of

SHs from small and flat to large and thick. With the change of cell morphology, they obtain some hepatic differentiated functions. They express liver-enriched transcription factors (LETFs) such as hepatic nuclear factor (HNF) 4α, HNF-6, and CCAAT/enhancer binding proteins α (C/EBPα) as well as tryptophan 2,3-dioxygenase (TO) and serine dehydratase (SDH), which are considered to be markers of hepatic maturation (Sugimoto *et al*., 2002). In addition, these differentiated hepatocytes form BC between adjacent cells. Anastomoses of BC to each other and their networks are reconstructed in the colony. BC proteins such as ectoATPase, 5'-nucleotidase, dipeptidylpeptidase IV (DPPIV), and multidrug-resistance associated protein 2 (MRP2), were localized in luminal spaceof BC. Tight junction-associated protein zona occludens-1 (ZO-1) was also expressed along the BC. Bilirubin added to the medium were secreted into BC and accumulated without leakage (Sudo *et al*., 2004). Furthermore, these BCs also can synchronize their contraction to make bile flow in a certain direction (Sudo *et al*., 2005). These results revealed that BC reconstructed by SHs is functional with membrane polarity, secretory ability, and motility. Thus, SHs can form functional hepatic tissues with NPCs including HSCs.

SHs can be found in adult human livers as well as in rats (Hino *et al*., 1999) Recently, SHs were successfully isolated also from adult human livers (Sasaki *et al*., 2008). When the cells cultured on hyaluronic acid (HA)-coated dishes in serum-free 1:1 Mixture of Dulbecco's Modified Eagle's Medium and Ham's F-12 (DMEM/F12) including nicotinamide, EGF, and hepatocyte growth factor (HGF), they proliferated to form colonies and many colonies continued growing for more than 3 weeks. Immunocytochemistry showed that the cells forming a colony were positive for albumin, transferrin, CK 8, and CD44. The results of reverse transcription polymerase chain reaction (RT-PCR) showed that colony-forming cells expressed albumin (*Alb*), transferrin, alpha1-antitrypsin, fibrinogen, glutamine synthetase, many cytochrome

P450s, and liver-enriched transcription factors. Furthermore, the cells expressed not only the genes of hepatic differentiated functions but also those of both hepatic stem cell marker and SH marker. Albumin secretion into culture medium was also observed. Thus, human SHs may be a useful source for cell transplantation as well as pharmaceutical and toxicological investigations.

Although the functional hepatic tissues are successfully reconstructed in a two-dimensional (2D) culture, the actual liver tissues exhibit a 3D configuration. A precise manipulation of SHs needs to be developed to expand the hepatic organoids into a 3D configuration. To address this issue, a 3D culture method was developed by stacking up the 2D tissues of SHs (Sudo *et al*., 2005). Pairs of polycarbonate membranes were prepared and SHs are separately cultured on each membrane. After SHs expand to form large colonies, one membrane is inverted on the top of the other to form an SH bilayer. In this condition, SHs of the upper and lower layers adhere to one another and form 3D stacked-up structures. Hepatic differentiated functions increase in the cells and functional BCs are formed between adhering surfaces of the cells.

Besides developing various culture methods for reconstructing functional hepatic tissues using SHs, the cryopreservation technique of SHs was reported (Ikeda *et al*., 2002). SHs were cultured for 12–15 days and SHs colonies were collected using two solutions: Hank's balanced salt solution supplemented with 0.02% ethylene diamine tetraacetic acid (EDTA); cell dissociation solution which is commercially available from Sigma-Aldrich. The collected colonies were then stored at -80°C for more than 6 months. Even after thawing, the cells retain high attachment efficiency (~60%), and the cryopreserved colonies attached on cell culture dishes and then proliferate. The proliferating cells maintained differentiated hepatocyte functions including albumin secretion, transferrin production, and TO expression.

Considering above, SHs is a plausible cell source of hepatocytes to reconstruct functional liver tissues *in vitro*.

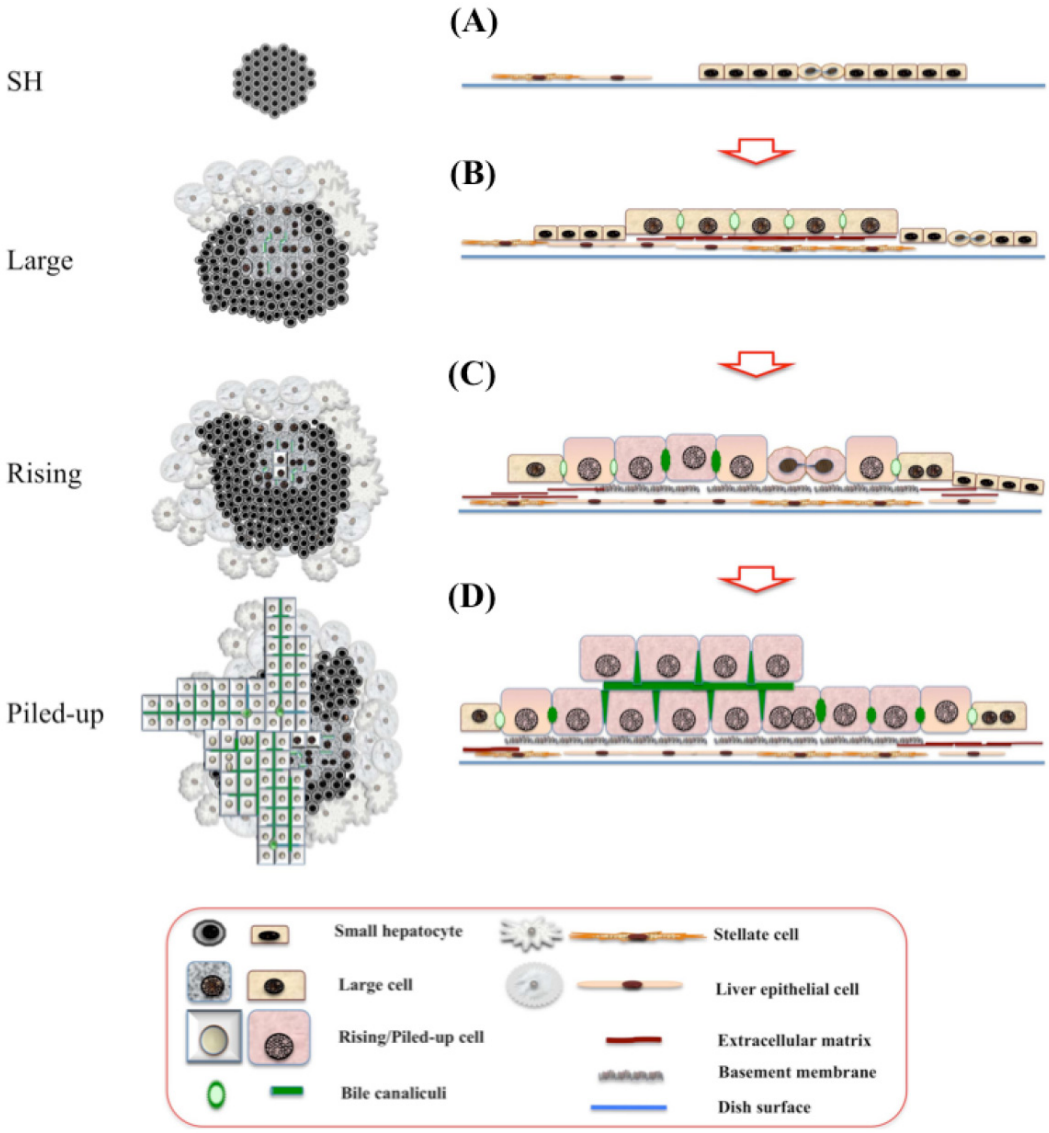

Figure 2-5. Illustration of SH maturation and hepatic organoid formation (The image adapted from Mitaka and Ooe, 2010). For detail description of the morphogenesis process, see section 2-4: small hepatocytes.

2-5. State-of-the-art co-culture methods for the liver sinusoid reconstruction *in vitro*

In order to reconstruct the liver sinusoidal structures, different liver cell co-culture models have been developed. Bader *et al*. (1996) described the first development of a 3D co-culture model of hepatocytes and liver NPCs which aimed to recapture the sinusoidal microenvironment *in vivo*. Hepatocytes were sandwiched with collagen gel and NPCs were cultured on the top of the gel, resulting in layered structure of hepatocytes and NPCs. Considering that previous hepatocyte-NPC co-culture models relied on simply mixing the cells in a 2D configuration (Bojar *et al*., 1976; Billiar *et al*., 1990a; Billiar *et al*., 1990b; Villafuerte *et al*., 1994), this model in part reflects the *in vivo* 3D configuration. However, thick collagen gel between the hepatocytes and the NPCs (>150 μm) prevents their close proximity, interrupting their active interactions. For example, although it has been widely reported that the generation of phase I and phase II metabolites of the cytochrome P-450 1A1 substrate ethoxyresorufin was affected by the presence of co-cultured NPCs (Khetani and Bhatia, 2010; Ohno *et al*., 2008), the one in the model was independent from the presence of co-cultured NPCs. To overcome this problem, several kinds of cell sheet engineering technique have been applied for co-culture of hepatocytes and endothelial cells (Harimoto *et al*., 2002; Ohno *et al*., 2008; Ohno *et al*., 2009; Kim *et al*., 2010; Kim and Rajagopalan, 2010). These techniques enabled the intimate association between layers of hepatocytes and NPCs. In layered co-culture of HepG2 and ECs, maturation of the ECM and the cell adhesion molecules between the layers was observed in addition to an increase in the liver-specific functions (Harimoto *et al*., 2002; Ohno *et al*., 2008; Ohno *et al*., 2009), suggesting that the close association of hepatocytes with NPCs is essential to promote heterotypic cell–cell interactions. However, any further 3D tissue morphogenesis from the layer-by-layer structures, *i.e.*, capillary formation of ECs, was not achieved in these co-culture models.

As mentioned before, the sinusoidal architectures arise from active heterotypic cell–cell interactions and subsequent self-organizing processes of different types of cell. Although the heterotypic interactions between hepatocytes and NPCs were promoted in the above co-culture models, self-organization of the cells into the sinusoidal structures could not be induced. To induce the cellular self-organization toward the sinusoidal reconstruction *in vitro*, a hepatocyte-NPC co-culture in a 3D perfused microreactor (Hwa *et al*., 2007) was established. In this co-culture, culture medium was perfused through mixed cell suspension of hepatocytes and NPCs in the microfabricated wells. The cells reassembled into the tightly-packed cell aggregates including vessel-like formations, suggesting that the medium perfusion promoted the cellular self-organization. Nahmias *et al*. developed a co-culture model of hepatocytes and NPCs using Matrigel (Nahmias *et al*., 2006; Soto-Gutierrez *et al*., 2010). The design of this co-culture model is inspired by the organization processes of the liver sinusoids during development. Hepatocytes migrated toward and adhered to the EC vascular structures which were preformed on Matrigel, resulting in the formation of the hepatocyte-decorated endothelial vascular structures. Although both of these co-culture models partially promoted the self-organization of the cells, the elaborate sinusoidal architectures such as the HSC's incorporation into the EC capillary structures were not recaptured.

The liver sinusoids *in vivo* arise through the heterotypic cell–cell interactions, and these interactions are spatio-temporally controlled by microenvironment which cells create by themselves (section 2-3). Considering the complexity of its organogenesis processes, it appears to be difficult to reconstruct the well-assembled sinusoidal tissues spontaneously. Therefore, appropriate manipulation of the cells is necessary to induce the cellular self-organizing capability and facilitate their organization. As mentioned before (section 1-1 and 2-3), the significance of the HSC's role in the sinusoidal

organization has been increasingly recognized, suggesting that appropriate manipulation of HSCs might promoted the cellular self-organization for the reconstruction of the sinusoidal tissues *in vitro*. This concept motivated this dissertation to focus on the elucidation of HSC's role in the sinusoidal reconstruction.

Reference

Bader A, Knop E, Kern A, Böker K, Frühauf N, Crome O, Esselmann H, Pape C, Kempka G, Sewing KF. 1996, 3-D coculture of hepatic sinusoidal cells with primary hepatocytes-design of an organotypical model, *Exp Cell Res*, **226**: 223–233.

Bedossa P, Paradis V. 2003, Liver extracellular matrix in health and disease, *J Pathol*, **200**: 504–515.

Billiar TR, Curran RD, Ferrari FK, Williams DL, Simmons RL. 1990a, Kupffer cell:hepatocyte cocultures release nitric oxide in response to bacterial endotoxin, *J Surg Res*, **48**: 349–353.

Billiar TR, Lysz TW, Curran RD, Bentz BG, Machiedo GW, Simmons RL. 1990b, Hepatocyte modulation of Kupffer cell prostaglandin E_2 production *in vitro*. *J Leukoc Biol*, **47**: 305–311.

Blomhoff R, Green MH, Berg T, Norum KR. 1990, Transport and storage of vitamin A, *Science*, **250**: 399–404.

Bojar H, Basler M, Fuchs F, Dreyfürst R, Staib W, Broelsch C. 1976, Preparation of parenchymal and non-parenchymal cells from adult human liver--morphological and biochemical characteristics, *J Clin Chem Clin Biochem*, **14**: 527–532.

Braet F, De Zanger R, Sasaoki T, Baekeland M, Janssens P, Smedsrod B, Wisse E. 1994, Assessment of a method of isolation, purification, and cultivation of rat liver sinusoidal endothelial cells, *Lab Invest*, **70**: 944–952.

Braet F, Wisse E. 2002, Structural and functional aspects of liver sinusoidal endothelial cell fenestrae: a review, *Comp Hepatol*, **1**: 1.

D'amore PA and Herman IM. 2001, Molecular and cellular control of angiogenesis' in *The Liver Biology and Pathobiology*, eds. Arias IM, Boyer JL, Chisari, FV, Fausto N, Schachter D, Shafritz DA, Lippincott Williams & Wilkins, Philadelphia, PA, USA; 987–993.

DeLeve LD, Wang X, Hu L, McCuskey MK, McCuskey RS. 2004, Rat liver sinusoidal endothelial cell phenotype is maintained by paracrine and autocrine regulation, *Am J Physiol Gastrointest Liver Physiol*. **287**: G757–G763.

Drixler TA, Vogten MJ, Ritchie ED, van Vroonhoven TJ, Gebbink MF, Voest EE, Borel Rinkes IH. 2002, Liver regeneration is an angiogenesis- associated phenomenon, Ann Surg. **236**: 703–712.

Edwards S, Lalor PF, Nash GB, Rainger GE, Adams DH. 2005, Lymphocyte traffic through sinusoidal endothelial cells is regulated by hepatocytes. *Hepatology*, **41**: 451–459.

Fausto N. 2001, 'Liver regeneration' in *The Liver Biology and Pathobiology*, eds. Arias IM, Boyer JL, Chisari, FV, Fausto N, Schachter D, Shafritz DA, Lippincott Williams & Wilkins, Philadelphia, PA, USA; 591–610.

Friedman SL, Wei S, Blaner WS. 1993, Retinol release by activated rat hepatic lipocytes: regulation by Kupffer cell-conditioned medium and PDGF, *Am J Physiol*, **264(5 Pt 1)**: G947–952.

Friedman SL, Arthur MJP. 2002, Reversing hepatic fibrosis, *Science & Medicine*, **8**: 194–205

Geerts A. 2001, History, heterogeneity, developmental biology, and functions of quiescent hepatic stellate cells, *Semin Liver Dis*, **3**: 311–335.

Goda N, Suzuki K, Naito M, Takeoka S, Tsuchida E, Ishimura Y, Tamatani T, Suematsu M. 1998, Distribution of heme oxygenase isoforms in rat liver. Topographic basis for carbon monoxide-mediated microvascular relaxation, *J Clin Invest*, **101**:604–612.

Harimoto M, Yamato M, Hirose M, Takahashi C, Isoi Y, Kikuchi A, Okano T. 2002, Novel approach for achieving double-layered cell sheets co-culture: overlaying endothelial cell sheets onto monolayer hepatocytes utilizing temperature-responsive culture dishes, *J Biomed Mater Res*, **62**: 464–470.

Hino H, Tateno C, Sato H, Yamasaki C, Katayama S, Kohashi T, Aratani A, Asahara T, Dohi K, Yoshizato K. 1999, A long-term culture of human hepatocytes which show a high growth potential and express their differentiated phenotypes, *Biochem Biophys Res Commun*, **256**: 184–191.

Hwa AJ, Fry RC, Sivaraman A, So PT, Samson LD, Stolz DB, Griffith LG. 2007, Rat liver sinusoidal endothelial cells survive without exogenous VEGF in 3D perfused co-cultures with hepatocytes. *FASEB J*, **21**: 2564–2579.

Ikeda S, Mitaka T, Harada K, Sugimoto S, Hirata K, Mochizuki Y. 2002, Proliferation of rat small hepatocytes after long-term cryopreservation, *J Hepatol*, **37**: 7–14.

Khetani SR, Bhatia SN. 2008, Microscale culture of human liver cells for drug development, *Nat Biotechnol*, **26**:120–126.

Kim Y, Larkin AL, Davis RM, Rajagopalan P. 2010, The design of *in vitro* liver sinusoid mimics using chitosan-hyaluronic acid polyelectrolyte multilayers, *Tissue Eng Part A*, **16**: 2731–2741.

Kim Y, Rajagopalan P. 2010, 3D hepatic cultures simultaneously maintain primary hepatocyte and liver sinusoidal endothelial cell phenotypes, *PLoS One*, **5**: e15456.

Krause P, Markus PM, Schwartz P, Unthan-Fechner K, Pestel S, Fandrey J, Probst I. 2000, Hepatocyte-supported serum-free culture of rat liver sinusoidal endothelial cells, *J Hepatol,* **32**: 718–726.

March S, Hui EE, Underhill GH, Khetani S, Bhatia SN. 2009, Microenvironmental regulation of the sinusoidal endothelial cell phenotype *in vitro*, *Hepatology*, **50**: 920–928.

Martinez-Hernandez A, Amenta PS. 1993, The hepatic extracellular matrix. I. Components and distribution in normal liver. *Virchows Arch A Pathol Anat Histopathol*, **423**: 1–11.

Martinez-Hernandez A, Amenta PS. 1995, The extracellular matrix in hepatic regeneration, *FASEB J*, **19**: 1401–1410.

Mescher AM. 2010, 'Organs Associated with the Digestive Tract' in *Junqueira's Basic Histology: Text & Atlas, 12th Edition*, ed. Mescher AM, McGraw-Hill, New York, NY, USA; 333, Fig 16-11.

Michalopoulos GK. 2007, Liver Regeneration, *J Cell Physiol*, 213: 286–300.

Michalopoulos GK, DeFrances MC. 1997, Liver regeneration, *Science*, **276**: 60–66.

Mitaka T, Kojima T, Mizuguchi T, Mochizuki Y. 1995, Growth and maturation of small hepatocytes isolated from adult rat liver, *Biochem Biophys Res Commun*, **214**: 310–317.

Mitaka T, Mikami M, Sattler GL, Pitot HC, Mochizuki Y. 1992, Small cell colonies appear in the primary culture of adult rat hepatocytes in the presence of nicotinamide and epidermal growth factor, *Hepatology*, **16**: 440–447.

Mitaka T, Sato F, Mizuguchi T, Yokono T, Mochizuki Y. 1999, Reconstruction of hepatic organoid by rat small hepatocytes and hepatic nonparenchymal cells, *Hepatology*, **29**: 111–125.

Mitaka T, Sattler GL, Pitot HC, Mochizuki Y. 1992, Characteristics of small cell colonies developing in primary cultures of adult rat hepatocytes, *Virchows Arch B Cell Pathol Incl Mol Pathol*, **62**: 329–35.

Nahmias Y, Schwartz RE, Hu WS, Verfaillie CM, Odde DJ. 2006, Endothelium-mediated hepatocyte recruitment in the establishment of liver-like tissue *in vitro*. *Tissue Eng*, **12**: 1627–1638.

Naito M, Hasegawa G, Ebe Y, Yamamoto T. 2004, Differentiation and function of Kupffer cells, *Med Electron Microsc*, **37**: 16–28.

Nakatani K, Kaneda K, Seki S, Nakajima Y. 2004, Pit cells as liver-associated natural killer cells: morphology and function, *Med Electron Microsc*, **37**: 29–36.

Ohi N, Nishikawa Y, Tokairin T, Yamamoto Y, Doi Y, Omori Y, Enomoto K. 2006, Maintenance of bad phosphorylation prevents apoptosis of rat hepatic sinusoidal endothelial cells *in vitro* and *in vivo*, *Am J Pathol*, **168**: 1097–1106.

Ohno M, Motojima K, Okano T, Taniguchi A. 2008, Up-regulation of drug-metabolizing enzyme genes in layered co-culture of a human liver cell line and endothelial cells, *Tissue Eng Part A*, **14**: 1861–1869.

Ohno M, Motojima K, Okano T, Taniguchi A. 2009, Maturation of the extracellular matrix and cell adhesion molecules in layered co-cultures of HepG2 and endothelial cells, *J Biochem*, **145**: 591–597.

Ross MH, Kaye GI, Pawlina W. 2003, 'Digestive System III: Liver, Gallbladder, and Pancreas' in *Histology a text and atlas, 4th edition*, Lippincott Williams & Wilkins, Philadelphia, PA, USA; 532–563.

Sasaki K, Kon J, Mizuguchi T, Chen Q, Ooe H, Oshima H, Hirata K, Mitaka T. 2008, Proliferation of hepatocyte progenitor cells isolated from adult human livers in serum-free medium, *Cell Transplant*, **17**: 1221–1230.

Soto-Gutierrez A, Navarro-Alvarez N, Yagi H, Nahmias Y, Yarmush ML, Kobayashi N. 2010, Engineering of an hepatic organoid to develop liver assist devices, *Cell Transplant*, **19**: 815–822.

Sudo R, Ikeda S, Sugimoto S, Harada K, Hirata K, Tanishita K, Mochizuki Y, Mitaka T. 2004, Bile canalicular formation in hepatic organoid reconstructed by rat small hepatocytes and nonparenchymal cells, *J Cell Physiol*, **199**: 252–261.

Sudo R, Kohara H, Mitaka T, Ikeda M, Tanishita K. 2005, Coordinated movement of bile canalicular networks reconstructed by rat small hepatocytes, *Ann Biomed Eng*, **33**: 696–708.

Sudo R, Mitaka T, Ikeda M, Tanishita K. 2005, Reconstruction of 3D stacked-up structures by rat small hepatocytes on microporous membranes, *FASEB J*, **19**: 1695–1697.

Suematsu M. 1999, Recent developments in hepatic circulatory physiology, *Hepatogastroenterology*, **46**: 1406–1408.

Suematsu M, Aiso S. 2001, Professor Toshio Ito: a clairvoyant in pericyte biology, *Keio*

journal of medicine, **50**: 66–71.

Sugimoto S, Mitaka T, Ikeda S, Harada K, Ikai I, Yamaoka Y, Mochizuki Y. 2002, Morphological changes induced by extracellular matrix are correlated with maturation of rat small hepatocytes, *J Cell Biochem*, **87**: 16–28.

Takahashi, T., Shibuya, M. 2001, The overexpression of PKCdelta is involved in vascular endothelial growth factor-resistant apoptosis in cultured primary sinusoidal endothelial cells. *Biochem Biophys Res Commun*, **280**: 415–420.

Tateno C, Takai-Kajihara K, Yamasaki C, Sato H, Yoshizato K. 2000, Heterogeneity of growth potential of adult rat hepatocytes *in vitro*, *Hepatology*, **31**: 65–74.

Tsukamoto H, Cheng S, Blaner WS. 1996, Effects of dietary polyunsaturated fat on ethanol-induced Ito cell activation, *Am J Physiol*, **270(4 Pt 1)**: G581–586.

Villafuerte BC, Koop BL, Pao CI, Gu L, Birdsong GG, Phillips LS. 1994, Coculture of primary rat hepatocytes and nonparenchymal cells permits expression of insulin-like growth factor binding protein-3 *in vitro*. *Endocrinology*, **134**: 2044–2050.

Wake K. 1971, “Sternzellen” in the liver: perisinuosoidal cells with special reference to storage of vitamin A, *Am J Anat*, **132**: 429–462.

Wake K. 2006, Hepatic stellate cells: three-dimensional structures, localization, heterogeneity and development, *Proc Jpn Acad Ser B*, **82**: 155–164.

Wisse E. 1974a, Kupffer cell reactions in rat liver under various conditions as observed in the electron microscope. *J Ultrastruct Res*, **46**: 499–520.

Wisse E. 1974b, Observations on the fine structure and peroxidase cytochemistry of normal rat liver Kupffer cells, *J Ultrastruct Res*, **46**: 393–426.

Wynne HA, Cope LH, Mutch E, Rawlins MD, Woodhouse KW, James OF. 1989, The effect of age upon liver volume and apparent liver blood flow in healthy man. *Hepatology*, **9**: 297–301.

Chapter 3. Materials and methods

3-1. PET microporous membranes (chapter 4 and 5)*

PET microporous membrane from a 12-well cell culture insert (thickness, 20 μm; pore diameter, 0.4, 1.0, 3.0, or 8.0 μm; BD Biosciences, Bedford, MA, USA) were used to construct HSC-mediated three-dimensional tri-culture model of hepatocytes and endothelial cells. Both sides of a PET microporous membrane were initially coated with rat tail collagen (50 μg of dried tendon/0.1% acetic acid). The membranes with 1.0-μm pores were used for the tri-culture if not otherwise specified.

3-2. PLGA microporous membranes (chapter 6)

3-2-1. Fabrication of PLGA microporous membranes

Membranes were fabricated using the dioxane-water phase separation method (Kasuya *et al*., 2011). Briefly, 50/50 PLGA (Corefront, Tokyo, Japan) was dissolved in dioxane (Wako Pure Chemical, Tokyo, Japan) at 50 mg/mL with 0–10% water content. The diameter of the pore can be controlled by adjusting the water content of the solution. Then, 400 μL of the solution above was mounted on a polyethylene sheet (High-tech, Tokyo, Japan) and spin-coated at 2,000 rpm for 1 sec using a spin coater (Mikasa, Tokyo, Japan). The sheets were dried under vacuum conditions for 48 hours. Membranes were peeled off from the sheets with tweezers and cut into 0.5 cm squares.

* Relevant chapters

3-2-2. Scanning electron microscopy (SEM) of PLGA microporous membranes

PLGA membranes were placed in 35-mm cell-culture dishes (Corning Glass Works, Corning, NY) and coated with rat-tail collagen (50 μg of dried tendon/0.1% acetic acid). The membranes were then coated with osmium gas and examined with by scanning electron microscopy (FE-SEM S-4700; Hitachi High-Technologies, Tokyo, Japan).

3-2-3. Membrane thickness measurement

Membrane thicknesses were measured using a color 3D laser scanning microscope (VK-9710; Keyence, Osaka, Japan).

3-3. Cell isolation and culture

3-3-1. Isolation of a SH-enriched fraction containing HSCs (chapter 4, 5, and 6)

Cells were isolated from male Sprague-Dawley rats (SD rats) (250–450 g; Nippon Bio-Supp. Center, Tokyo, Japan) and male transgenic SD rats carrying the enhanced green fluorescent protein (EGFP) transgene (EGFP rats; Japan SLC, Shizuoka, Japan), using the two-step liver-perfusion method (Mitaka *et al*., 1999) with some modifications. Details of the isolation have been described previously (Mitaka *et al*., 1999). MHs were removed from a collagenase-digested liver cell suspension by centrifugation at 50 × *g* for 1 min, and the supernatant was centrifuged at 50 × *g* for 5 min. The supernatant from this centrifugation was retained for HSC isolation. The pellet was suspended in L-15 medium (Invitrogen, Carlsbad, CA, USA) supplemented with 20 mM 4-(2-hydroxyethyl)-1-piperazineethanesulfonic acid (HEPES) (Dojindo, Kumamoto, Japan), 1.1 g/l galactose (Katayama Chemical, Osaka, Japan), 30 mg/l L-proline, 0.5 mg/l insulin (Sigma-Aldrich, St. Louis, MO, USA), 10^{-7} M dexamethasone (Wako Pure Chemical), and antibiotics. The resuspended pellet was again centrifuged at 50 × *g* for 5

min, after which the pellet was again suspended in supplemented L-15 medium and then centrifuged at 150 × *g* for 5 min. This procedure was repeated, and the pellet was suspended in supplemented L-15 medium and centrifuged at 50 × *g* for 5 min. Finally, the pellet was suspended in Dulbecco's modified Eagle's medium (DMEM) with high glucose (Sigma-Aldrich) supplemented with 20 mM HEPES, 25 mM $NaHCO_3$, 30 mg/l L-proline, 0.5 mg/l insulin, 10^{-7} M dexamethasone, 10% fetal bovine serum (FBS), 10 mM nicotinamide (Sigma-Aldrich), 1 mM ascorbic acid 2-phosphate (Wako Pure Chemical), 10 ng/ml EGF (BD Biosciences), and antibiotics, yielding a SH-enriched fraction that contained HSCs. About 5×10^7 SHs were isolated from an adult rat. The percentage of HSCs contained in this fraction has been reported to be ~11% (Mitaka *et al*., 1999). The number of viable SHs was counted using trypan blue exclusion test.

3-3-2. Isolation of HSCs (chapter 4 and 5)

The HSC-enriched fraction for use in the following experiments: "*Quantitative analysis of EC morphology in the HSC-mediated 3D tri-culture model* (section 3-5-3)," "*Quantitative analysis of HSC activation* (section 3-5-4)" and "*EC capillary formation assay* (section 3-5-5)." The supernatants from the centrifugation steps performed to prepare SHs, as described above, were combined and used to isolate HSCs according to the method described by Riccalton-Banks (Riccalton-Banks *et al*., 2003). The supernatant was repeatedly centrifuged at 50 × *g* for 5 min until no pellet was formed. The supernatant was centrifuged at 200 × *g* for 10 min, and the pellet, which contained the HSCs, was suspended in 10 ml of DMEM (Invitrogen) supplemented with 10% FBS, 15 mM HEPES, and antibiotics. After further centrifugation at 200 × *g* for 10 min, the final pellet was suspended in the supplemented DMEM. The number of viable cells was counted by trypan blue exclusion test. The cells were positively identified by immunofluorescence staining with anti-desmin antibody (details of

immunofluorescence staining are described below). The purity of the HSC preparation was >95%, as calculated by the proportion of desmin-positive cells in the total cell population.

3-3-3. Culture of ECs (chapter 4, 5, and 6)

Liver SECs do not adapt well to *in vitro* culture because of their poor survival (Takahashi *et al*., 2001). Therefore, bovine pulmonary microvascular endothelial cells (BPMECs) were used in this study. The cells were obtained commercially from Cell Systems (Kirkland, WA, USA) at the third passage. The cells were cultured in DMEM (Invitrogen) supplemented with 10% FBS, 15 mM HEPES, and antibiotics in a humidified atmosphere of 5% CO_2/95% air at 37°C before tri-culture. The medium was replaced every other day. When confluent, the cells were detached by trypsinization (0.05% trypsin, 0.53 mM EDTA·4Na), resuspended in medium, and split for subculture. Cells were subcultured until the eighth passage and were used for tri-culture between the fifth and eighth passages.

3-3-4. Tri-culture of SHs, HSCs, and ECs using PET microporous membranes (chapter 4 and 5)

The cell culture insert with the PET membrane was inverted, and 115 μl of the SH-rich fraction, which was 6.0×10^5 cells/ml, was mounted on the bottom surface with an area of 0.9 cm^2, resulting in 7.7×10^4 cells/cm^2. As the SH-rich fraction contained HSCs at a rate of ~11% as describe above, corresponding HSC density was 8.4×10^3 cell/cm^2. The samples were then incubated in a humidified atmosphere of 5% CO_2/95% at 37°C (Fig. 3-1A, Step 1). At 2 hours after inoculation, the cell culture insert was turned back over in the holding well, and the medium was exchanged to remove dead cells (Fig. 3-1A, Step 1). Subsequently, the medium was replaced every other day. After

4 days (96 hours after plating), dimethyl sulfoxide (DMSO) (Sigma-Aldrich) was added to the culture medium at a concentration of 1%.

The SHs containing HSCs were allowed to grow on the bottom surface of the microporous membrane for ~14 days (Fig. 3-1A, Step 2). Four hundred microliter of the EC suspension, which was 6.0×10^5 cells/ml, was mounted on the top surface with an area of 0.9 cm^2, resulting in 2.7×10^5 cells/cm^2. The samples were then incubated in a humidified atmosphere of 5% CO_2/95% air at 37°C (Fig. 3-1A, Step 3). The medium was exchanged 3 hours after inoculation to remove dead cells, and every other subsequent day. Modified DMEM supplemented with 1% DMSO was used, which was applied to the co-culture of SHs and HSCs, and to the tri-culture.

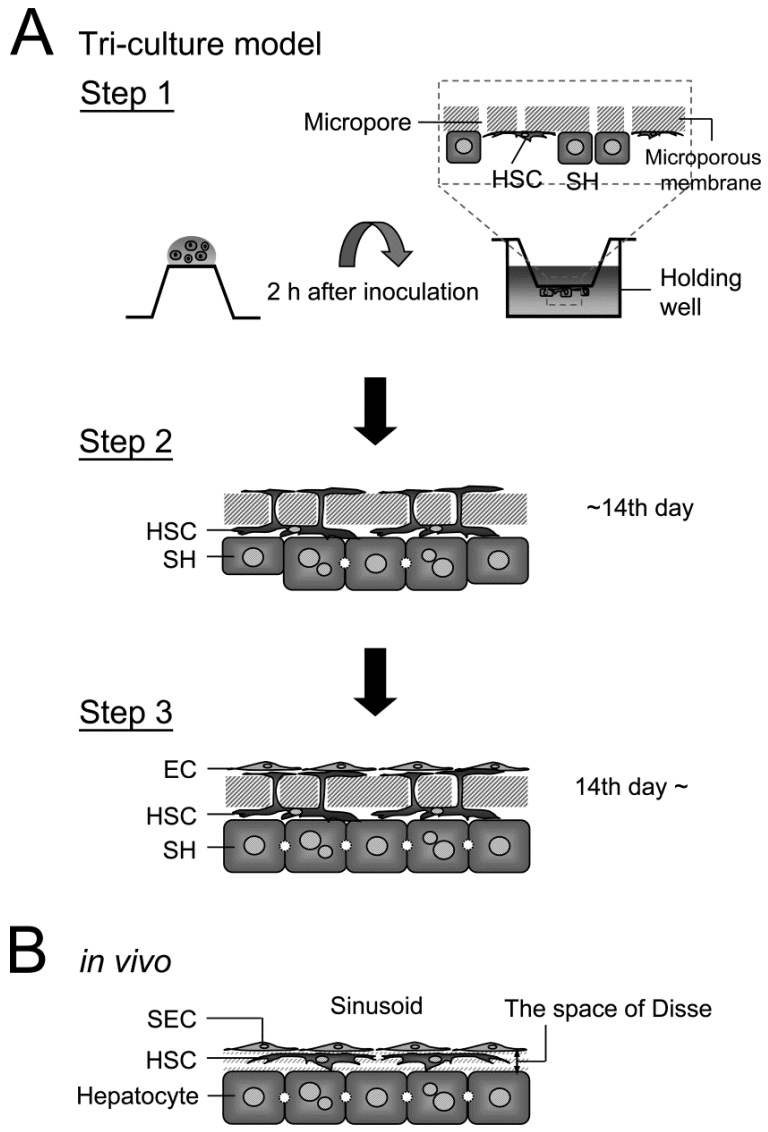

Figure 3-1. Conceptual diagram of the hepatic stellate cell (HSC)-mediated three-dimensional tri-culture model of hepatocytes and endothelial cells (ECs). ***A*)** Initially, small hepatocytes (SHs) and HSCs were inoculated onto the bottom surface of a microporous membrane. After 2 hours, the membrane was turned over in the holding well *(Step 1)*. Within 14 days after inoculation, the SHs had formed colonies, with HSCs located between the SH colonies and the membrane. HSCs also penetrated the pores and were distributed to the top surface of the membrane *(Step 2)*. On day 14, ECs were inoculated onto the top surface of the membrane; after incubation, the HSC-mediated layered architecture of SHs and ECs was observed *(Step 3)*. ***B*)** In the liver, HSCs in the space of Disse are located between the layers of hepatocytes and sinusoidal endothelial cells.

3-3-5. Tri-culture of SHs, HSCs, and EC capillary-like structures PLGA microporous membranes (chapter 6)

The formation of EC capillary-like structures was induced on a PLGA microporous membrane (Matrigel angiogenesis assay; Fig. 3-2). Initially, each side of the membrane was coated with rat tail collagen (50 μg of dried tendon/0.1% acetic acid) and growth factor-reduced Matrigel (GFR Matrigel; BD Biosciences) diluted 1:1 with phosphate-buffered saline (PBS), respectively. The cells were then stained with CellTracker CM-DiI (Invitrogen) according to the manufacturer's instructions and plated on the GFR Matrigel-coated side of the membrane (0.5×10^5 cells/cm^2) to allow for cell attachment to the membrane in a humidified atmosphere of 5% CO_2/95% air at 37°C. At 1 hour after inoculation, unattached cells were removed and fresh culture medium was supplemented with 10% GFR Matrigel. After 24 hours, the formation of EC capillary-like structures was confirmed using a confocal laser scanning microscope (LSM 700; Carl Zeiss, Hallbergmoos, Germany).

SHs containing HSCs were also cultured for ~10 days to allow for proliferation and formation of hepatic organoids, as previously described (Mitaka *et al*., 1999). EC capillary-like structures on the membrane (Matrigel angiogenesis assay; Fig. 3-2) were then stacked on top of the hepatic organoids (SH-HSC co-culture; Fig. 3-2), resulting in a 3D stacked-up tri-culture of SHs, HSCs, and EC capillary-like structures (3D stacked-up structure; Fig. 3-2). DMEM supplemented with 1% DMSO was applied to the co-culture of SHs and HSCs, and to the tri-culture.

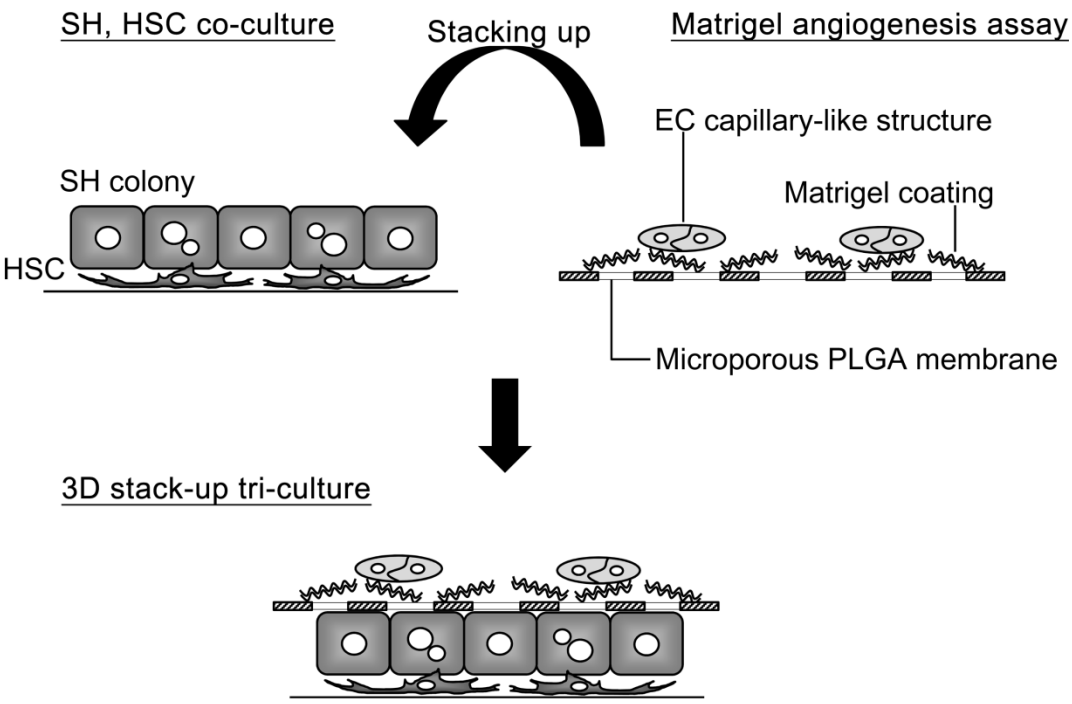

Figure 3-2. The schematic diagram of 3D stacked-up tri-culture using PLGA microporous membranes. SHs and HSCs were cultured on a dish for 6 days to allow them to proliferate and form colonies. On the other hand, ECs were cultured on a Matrigel-coated PLGA microporous membrane to allow them to form capillary-like structures. Thereafter, the membrane was stacked on the top of SHs colonies, resulting in the construction of 3D stacked-up tri-culture.

3-4. Cell imaging

3-4-1. Immunofluorescence staining of cultured cells (chapter 4, 5, and 6)

The cells were fixed in 4% paraformaldehyde (PFA) for 15 min and treated with 0.1% Triton X-100 for 20 min at room temperature (RT). After rinsing with PBS, the cells were incubated with Block Ace (Dainippon Pharma, Tokyo, Japan) at RT for 1 hour. Thereafter, the cells were incubated at RT for 2 hours with primary antibody: rabbit anti-CK wide (DAKO, Copenhagen, Denmark) and mouse anti-CK8 (Progen, Queensland, Australia) for SHs; rabbit anti-desmin (Lab Vision, Fremont, CA, USA) and mouse anti-desmin (ScyTek Laboratories, West Logan, UT, USA) for HSCs; mouse anti-α-smooth muscle actin (α-SMA) (Sigma-Aldrich) for activated HSCs; rabbit anti-vascular endothelial-cadherin (VE-cadherin; Alexis, Lausen, Switzerland) for ECs; rabbit anti-fibronectin (LSL, Tokyo, Japan), rabbit anti-collagen type I (LSL), rabbit anti-collagen type IV (LSL), or rabbit anti-laminin (LSL) antibody, mouse anti-bromodeoxyuridine (BrdU; DAKO) antibody for proliferating cells, and rabbit anti-platelet-derived growth factor (PDGF) β (Thermo scientific, IL, USA). After three rinses with PBS, the cells were incubated at RT for 2 hours with a secondary antibody [Alexa Fluor 430/488/594-conjugated anti-mouse or anti-rabbit IgG (Invitrogen)]. Thereafter, the nuclei were counterstained with 4',6-diamidino-2-phenylindole (DAPI; Sigma-Aldrich) or propidium iodide (PI; Invitrogen). The z-axis series of the fluorescence images were obtained with a confocal laser scanning microscope (LSM5 Pascal or LSM 700; Carl Zeiss) and three-dimensionally reconstructed using Imaris software (Bitplane AG, Zurich, Switzerland).

3-4-2. Fluorescent staining of ECs (chapter 4, 5, and 6)

To visualize the ECs in the tri-culture model, the cells were incubated with low-density lipoprotein acetylated DiI complex (DiI-acLDL; Invitrogen) for 1 h

(chapter 3 and chapter 4) or CellTracker CM-DiI (Invitrogen) for 2h (chapter 5) in a humidified atmosphere of 5% CO_2/95% air at 37°C. After three rinses with PBS, the fluorescence images of the cells were obtained by confocal laser-scanning microscopy.

3-4-3. Frozen section procedure for imaging of heterotypic cell configuration in the HSC-mediated 3D tri-culture model (chapter 4)

To prepare transverse sections, tri-cultured cells were fixed in 4% PFA and double immunofluorescent stainings for CK8 and desmin were performed on day 3 of tri-culture, as described above. The cells were then immersed in 30% sucrose overnight, frozen in OCT compound (Sakura Finetek Japan, Tokyo, Japan), sliced into sections 12 μm-thick with a cryostat (Microme Cryostat HM525; Carl Zeiss), and mounted in 90% glycerol containing 1 g/l *p*-phenylenediamine and 1 mg/l DAPI for assessment by fluorescence microscopy (Carl Zeiss).

3-4-4. TEM of vertical sections of the HSC-mediated 3D tri-culture model (chapter 4)

On day 2 of tri-culture, the cells were fixed with 2.5% glutaraldehyde and 2% PFA in 0.1 M cacodylate buffer (pH 7.4) overnight at 4°C. The remaining process was performed by Chobikeitai Laboratory (Yokohama, Japan). The cells were postfixed in 2% OsO_4 for 2 hours, dehydrated through a graded ethanol series (70%–100%), and embedded in Epon-812 (Shell Chemicals, San Francisco, CA, USA). Semi-thin (1 μm) and ultra-thin (100 nm) sections were cut perpendicular to the base of the membrane, using an LKB ultramicrotome. The semi-thin sections were stained with 0.1% methylene blue and examined under a light microscope. The ultra-thin sections were stained with uranyl acetate followed by lead citrate and examined under a JEM-100S transmission electron microscope (JEOL, Tokyo, Japan) at 80 kV.

3-5. Quantitative analysis of cell morphology and behavior

3-5-1. Quantitative analysis of HSC migration and process extension to the top surface of the PET membrane (chapter 4)

HSCs contained in the SH-enriched fraction were allowed to grow on the bottom surface of the microporous membrane (pore diameter, 0.4, 1.0, 3.0, or 8.0 μm) for 14 days. To quantify the number of migrated HSCs on the top surface of the membrane, the cells isolated from the wild-type rats were fixed on day 14 and immunocytochemically stained for desmin, as described above. Thereafter, the nuclei were counterstained with PI. The number of migrated HSCs on the top surface of the membrane was counted.

To quantify the coverage ratio of HSCs on the top surface of the membrane, the cells isolated from the EGFP rats were fixed on day 14. A field occupied by SH colonies on the bottom surface of a membrane was chosen at a magnification of ×200 under a confocal laser scanning microscope, and the fluorescence image of the corresponding field on the top surface of the membrane was obtained. Six fields were randomly chosen and imaged for each specimen. At least three experiments were performed. The HSC coverage was calculated as follows:

HSC coverage (%) = (area of GFP-labeled cells on top membrane surface / top membrane surface area) × 100.

3-5-2. Quantitative analysis of EC coverage on the top surface of the PET membrane (chapter 4)

The EC coverage ratio on the top surface of microporous membranes with different pore-sizes were analyzed quantitatively. At 24 hours and day 6 after seeding of ECs, the cells were visualized by DiI-acLDL and fixed, as described above. The EC coverage, defined as the area covered by DiI-acLDL-positive cells as a proportion of the top surface area of the membrane, was calculated as follows:

EC coverage (%) = (area of DiI-acLDL-positive cells on top membrane surface / top membrane surface area) × 100.

Six fields were chosen randomly and imaged for each specimen. At least three experiments were performed.

3-5-3. Quantitative analysis of EC morphology in the HSC-mediated 3D tri-culture model (chapter 4)

The effects of heterotypic cellular communication on EC morphology in the tri-culture model were analyzed quantitatively. On day 20 (day 6 of tri-culture), the cells were fixed in 4% PFA and double immunofluorescently stained for VE-cadherin and desmin, as described above. Five images from each experiment were captured using a confocal laser scanning microscope, and 10 random cells per image were traced using ImageJ (version 1.36; National Institutes of Health, Bethesda, MD, USA). At least three experiments were performed. The circularity was calculated from the area and perimeter of the traced EC using the formula:

$$Circularity = 4\pi (Area/Perimeter^2)$$

A circularity of 1.0 indicates a perfect circle. As the circularity approaches 0.0, the shape becomes an increasingly elongated ellipse.

Analysis was performed for four different culture conditions: (1) tri-culture of SHs, HSCs, and ECs using a 1.0-μm porous membrane, as described above (tri-culture); (2) co-culture of SHs, HSCs, and ECs using a 0.4-μm porous membrane (0.4-μm pore co-culture); (3) co-culture of HSCs and ECs on each side of a 1.0-μm porous membrane (HSC+EC co-culture); and (4) monoculture of ECs (monoculture).

3-5-4. Quantitative analysis of HSC activation (chapter 4)

To investigate the effects of SHs on the HSC phenotype, HSCs from two different

cultures were used: the HSCs contained in the SH-enriched fraction and primary monocultured HSCs. On day 14 of culture, the HSCs were fixed, double immunostained for α-SMA and desmin, and stained with DAPI. Five images from each experiment were captured using 3D deconvolution microscopy (Carl Zeiss). The proportion of α-SMA-positive cells as a percentage of desmin-positive cells, which was called the α-SMA(+) cell ratio, was calculated as follows:

α-SMA(+) cell ratio (%) = (number of α-SMA-positive cells/number of desmin-positive cells) × 100

Three independent experiments were performed.

3-5-5. EC capillary formation assay (chapter 5)

To induce capillary formation by ECs in the tri-culture, the Matrigel overlay method described by Connolly *et al*. (Connolly *et al*., 2002) was used. At 24 hours after starting the tri-culture, the medium was aspirated and the ECs, which had reached confluency, were overlaid with 200 μL Matrigel (BD Biosciences). Matrigel was allowed to polymerize for 1 hour in a humidified, 5% CO_2 / 95% air incubator at 37°C before the addition of medium. On day 6 after the Matrigel overlay, capillary formation was assessed using a confocal laser scanning microscope (LSM 700). Images were acquired and processed using the ImageJ software. Five fields were chosen randomly and imaged for each specimen. At least three experiments were performed. The capillary morphogenesis index (CMI), defined as the area covered by CM-DiI–positive ECs as a proportion of the top surface area of the membrane, was calculated as follows:

Capillary Morphogenesis Index (CMI; %) = (area of CM-DiI–positive ECs on top membrane surface / top membrane surface area) × 100.

The analysis was performed for four different culture conditions: (1) tri-culture of SHs, HSCs, and ECs using a 1.0-μm porous membrane, as described above [tri-culture

(contact+)], (2) tri-culture of SHs, HSCs, and ECs using a 0.4-μm porous membrane, in which the contact between HSCs and ECs was inhibited [tri-culture (contact-)], (3) co-culture of activated HSCs and ECs on each side of a 1.0-μm porous membrane, in which the HSCs and the ECs had contact with each other (co-culture with activated HSC), and (4) monoculture of ECs (monoculture).

3-5-6. Quantitative analysis of the time course of HSC coverage on the top surface of the PET membrane (chapter 5)

To quantify the time course of the coverage ratio of HSCs on the top surface of the membrane, SHs containing HSCs isolated from the EGFP rats were allowed to grow on the bottom surface of the 1.0-μm membrane and were photographed at days 2, 4, 6, 8, 10, 12, and 14. A field occupied by SH colonies on the bottom surface of a membrane was chosen at magnification (×200) under a confocal laser scanning microscope, and the fluorescence image of the corresponding field on the top surface of the membrane was obtained. Six fields were randomly chosen and imaged for each specimen. At least three experiments were performed. HSC coverage was calculated as follows:

HSC coverage (%) = (area of EGFP-labeled cells on top membrane surface / top membrane surface area) × 100.

3-5-7. Quantitative analysis of HSC recruitment by EC capillary formation (chapter 5)

HSC recruitment by EC capillary formation was analyzed quantitatively. For this analysis, the SH-enriched fraction isolated from the EGFP rats was used. A 50-μM solution of Tyrphostin AG 1295 (Enzo Life Sciences Inc., Farmingdale, NY, USA) was used to selectively block autophosphorylation of tyrosine kinase in PDGF-receptor β. The cells were fixed in 4% PFA for 15 min at RT. The distribution of EC capillary formation and HSCs on the top surface of the membrane was then assessed using

confocal laser scanning microscopy. Images were acquired and processed using the ImageJ software. HSC coverage, as defined above, was calculated for both the tri-culture and the culture of SHs containing HSCs, the top surface of which was covered with Matrigel on day 2 after the inoculation.

Additionally, to quantify the localized distribution between EC capillary formation and HSCs on the top surface of the membrane in the tri-culture, the HSC in the region of interest (ROI) was calculated as follows:

HSC in ROI (%) = (area of EGFP-labeled cells in ROI on top membrane surface / area of ROI on top membrane surface) ×100.

Nine fields were chosen randomly and imaged for each specimen. At least three experiments were performed.

3-6. Measurement of SH growth activity (chapter 5)

Growth activity of SHs was measured. Cells were cultured for 24 hours in the medium containing 40 μM BrdU (Sigma-Aldrich) to investigate cell-proliferation activity. The cells were fixed and treated with 2 N hydrochloric acid (HCl) for 30 min. Thereafter, double immunofluorescent staining was performed for BrdU and CK wide as described above. The cells were counterstained with PI. Samples were analyzed by confocal laser scanning microscopy, and the mean number and standard deviation (SD) of SHs with BrdU incorporation were calculated.

3-7. Hepatocyte functional assays (chapter 5 and 6)

Albumin secretion from SHs every 48 hours was measured using a rat albumin enzyme-linked immunosorbent assay (ELISA) quantitation kit (Bethyl laboratories inc., Montgomery, TX) according to the manufacturer's instructions. The urea production of SHs incubated with 1 mM ammonium chloride (NH_4Cl) for 24 hours was measured

using the QuantiChrom urea assay kit (BioAssay systems, Hayward, CA, USA) according to the manufacturer's instructions.

3-8. Ribonucleic acid (RNA) isolation and quantitative real-time polymerase chain reaction (QPCR) analysis for hepatic differentiation markers (chapter 5 and 6)

QPCR analysis was performed to identify messenger ribonucleic acid (mRNA) transcription in the cells in the tri-culture after the induction of capillary formation by ECs. Total RNA was isolated using the RNeasy RNA isolation kit (Qiagen, Hilden, Germany). Reverse transcription was performed using the SuperScript VILO cDNA synthesis kit (Invitrogen). The gene-specific primers used were designed using Primer3 software; most primers were designed to amplify a region spanning the splice site of an exon. The gene-specific primers for albumin (*Alb*), tyrosine aminotransferase (Tat), tryptophan 2,3-dioxygenase (To), hepatic nuclear factor 4α (*Hnf4a*), CCAAT/enhancer binding protein α (*Cebpa*), multidrug-resistance associated protein 2 (*Mrp2*), and bile salt export pump (*Bsep*) are listed in Table 3-1. The mRNA expression of glyceraldehyde-3-phosphate-dehydrogenase (*Gapdh*) was used for normalization. For the QPCR analysis, EXPRESS SYBR GreenER qPCR SuperMix (Invitrogen) was used. Real-time PCR was performed using the Mx3000P real-time PCR system (Stratagene, La Jolla, CA, USA).

3-9. Statistical analyses (chapter 4, 5, and 6)

Data are presented as means ± SD. A Student's *t*-test was used to test for differences, which were considered statistically significant at error levels of $p < 0.05$, $p < 0.01$, and $p < 0.001$.

Table 3-1. Sequences of QPCR primers.

Gene name	Sequence
Alb	5'-TCAACAAGGAGTGCTGTCACG-3'
	5'-CAGCTATTGAGGGCAGATCG-3'
Tat	5'-AGCTTCCTCAAGTCCAATGC-3'
	5'-ACGTTGCTGGGAGACAGTC-3'
To	5'-GAACGACGACTGTCATACCG-3'
	5'-CACCTTGTACCTGTCGCTCA-3'
Hnf4a	5'-CTGCAGGCTCAAGAAGTGC-3'
	5'-GGGAGGTGATCTGCTGAGAC-3'
Cebpa	5'-GCCGAGATAAAGCCAAACAG-3'
	5'-CCTTGACCAAGGAGCTCTCAG-3'
Mrp2	5'-ACCTTCCACGTAGTGATCCT-3'
	5'-ACTGTAGGCTCTGGGAAATC-3'
Bsep	5'-CTGGCATTTGTTGGAAGCAG-3'
	5'-CTGGCTCCTGGGAGACAATC-3'
Gapdh	5'-ATCAACGGGAAACCCATCAC-3'
	5'-TCTCGTGGTTCACACCCATC-3'

References

Connolly JO, Simpson N, Hewlett L, Hall A. 2002, Rac regulates endothelial morphogenesis and capillary assembly, *Mol Biol Cell*, **13**: 2474–2485.

Mitaka T, Sato F, Mizuguchi T, Yokono T, Mochizuki Y. 1999, Reconstruction of hepatic organoid by rat small hepatocytes and hepatic nonparenchymal cells, *Hepatology*, **29**: 111–125.

Riccalton-Banks L, Bhandari R, Fry J, Shakesheff KM. 2003, A simple method for the simultaneous isolation of stellate cells and hepatocytes from rat liver tissue, *Mol Cell Biochem*, **248**: 97–102.

Takahashi, T., Shibuya, M. 2001, The overexpression of PKCdelta is involved in vascular endothelial growth factor-resistant apoptosis in cultured primary sinusoidal endothelial cells. *Biochem Biophys Res Commun*, **280**: 415–420.

Chapter 4. Hepatic stellate cell-mediated three-dimensional hepatocyte and endothelial cell tri-culture model

4-1. Introduction

The liver is an important target of *in vitro* tissue engineering (Griffith and Naughton, 2002). Orthotopic liver transplantation is currently the only clinically accepted therapy for most patients suffering from severe liver failure. However, a worldwide shortage of donor organs seriously limits this option. *In vitro* reconstruction of liver tissues is urgently needed to enable the transplantation of tissue-engineered organs (Sundback and Vacanti, 2000). In addition, there is increasing demand for *in vitro* models that capture complex physiological and pathological events occurring in the liver (Griffith and Swartz, 2006). These models would be useful for understanding the mechanisms of liver diseases and for developing new drugs. As the liver is composed of heterotypic cells, physiological and pathological events depend on active communication among these cell types. Therefore, it is necessary to establish an *in vitro* culture model that captures the heterotypic cellular communication present in the liver.

HSCs form a physiological complex with SECs and hepatocytes to play a pivotal role in cell–cell communication in the liver. As liver-specific pericytes, HSCs closely adhere to SECs, which line the hepatic sinusoids (Wake, 2006). HSCs also directly face hepatocytes, being interposed by a sparse ECM. In addition to the physical contacts, close physiological relationships have been reported for HSCs in *in vitro* culture models. HSCs communicate with hepatocytes *via* gap junctional complexes, possibly maintaining the diverse functions of the liver (Rojkind *et al*., 1995), and are thought to communicate with SECs *via* N-cadherin in a spheroidal co-culture model (Wirz *et al*., 2008). HSCs appear to actively exchange molecules with these neighboring cell types.

For example, the retinol-binding protein complex released from hepatocytes is transported to HSCs (Bloomhoff *et al*., 1982). In addition, endothelin/nitric oxide released from SECs induces contraction/relaxation of HSCs to regulate blood microcirculation in hepatic sinusoids (Kawada *et al*., 1993). Thus, HSCs facilitate and integrate cell–cell communications between SECs and hepatocytes (Wake, 2006; Wirz *et al*., 2008). However, due to the lack of *in vitro* models, little is known about the mechanisms by which HSCs facilitate and integrate communications in the hepatocyte–HSC–SEC complex.

Various co-culture models have been developed to reproduce the elaborate 3D architecture of the liver microenvironment. These include EC or hepatic NPC culture on collagen gel containing hepatocytes (Bader *et al*., 1996; Jindal *et al*., 2009), hepatocyte and NPC culture in a 3D perfused microreactor (Hwa *et al*., 2007), and double-layered culture of an EC sheet and a hepatocyte sheet (Harimoto *et al*., 2002). These culture models have been used to investigate some heterotypic cell interactions. For example, co-culture of ECs on collagen-embedded hepatocytes promotes secretion of albumin and fibrinogen from the hepatocytes during the first week of co-culture, as compared with culture of hepatocytes alone (Jindal *et al*., 2009). Co-culture in a 3D perfused microreactor supports long-term SEC viability (Hwa *et al*., 2007). However, these models lack the intimate associations among HSCs and neighboring cell types such as hepatocytes and SECs.

Here, a novel tri-culture model with hepatocytes, HSCs, and ECs, which are the main cell types occupying the space of Disse in the liver, was established. Microporous membranes with different pore sizes were used to control HSC behavior. Under optimized conditions, the three cell types reassembled into an *in vivo*-like structure, in which HSCs were intercalated between layers of hepatocytes and ECs. It was confirmed that HSCs mediated cell–cell interactions in the tri-culture model. This HSC-mediated 3D tri-culture model is useful for investigating complex heterotypic cellular

communications *in vitro*.

4-2. Results

4-2-1. SHs and HSCs form hepatic organoids on a microporous membrane

Previously, Mitaka *et al*. reported that mixed populations of SHs and HSCs proliferated and formed hepatic organoids when cultured in culture dishes (1999). Sudo *et al*. have also demonstrated that the cells proliferated and formed organoids even when cultured on microporous membranes (2005). Similarly, in the present study, SHs and HSCs proliferated and formed hepatic organoids within 14 days on the bottom surface of microporous membranes. This growth of SHs and HSCs was independent of the pore size of the membrane (data not shown). Immunostainings for CK8 and desmin revealed CK8-positive SH colonies and desmin-positive HSCs with dendritic morphology located between the SH colonies and the membrane (Figs. 4-1A and B). When cultured on a 1.0-μm porous membrane, the HSCs also penetrated the pores and were distributed on the top surface of the membrane (Figs. 4-1C–F).

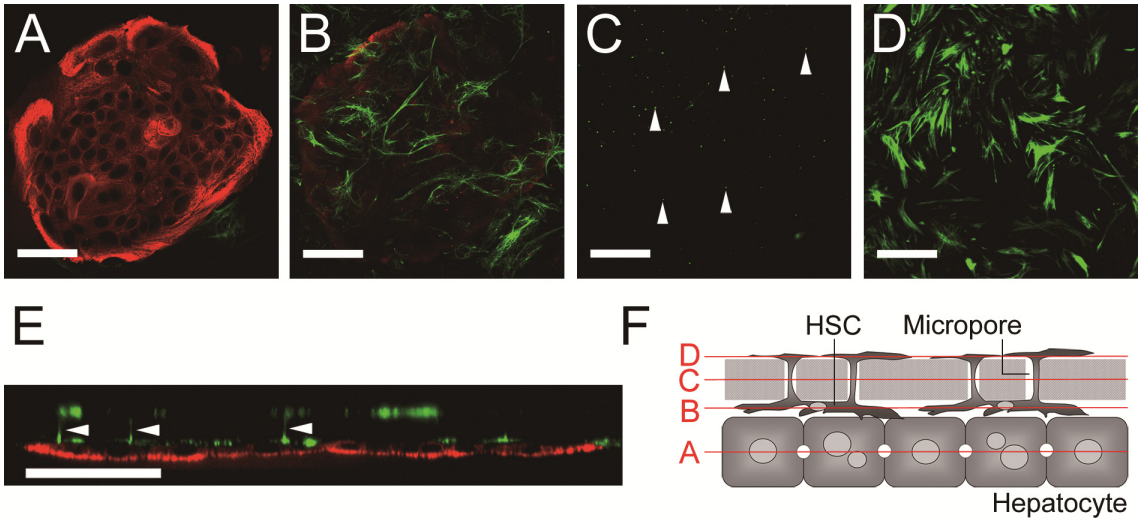

Figure 4-1. Three-dimensional distribution of small hepatocytes (SHs) and hepatic stellate cells (HSCs) cultured on a 1.0-μm porous membrane. The cells were fixed on day 14 and double immunostained for CK8 (red) and desmin (green). The cells were photographed using confocal microscopy. ***A–E***) Images were three-dimensionally reconstructed by calculating 88 planes at 0.675-μm intervals: the 32nd (*A*), 40th (*B*), 45th (*C*), and 66th (*D*) planes are shown. The *x*-*z* axes in the three-dimensional image are shown (*E*). Arrowheads show HSC processes penetrating the micropores. Scale bar in *A*–*E*: 50 μm. Original magnifications: ×400 (*A*–*D*). ***F***) Schematic representation of a vertical section of the culture system. The Z-sections (A, B, C, and D) correspond to each image shown in *A*–*D*.

4-2-2. HSC migration is controlled by the membrane pore size

HSC migration was successfully controlled by using membranes with different pore sizes. HSC migration through the micropores was analyzed quantitatively to clarify the effect of pore size. Cells were cultured for 14 days on membranes with 0.4-, 1.0-, 3.0-, or 8.0-μm pores, and the number of migrated HSCs on the top surface and their coverage were calculated. On the membrane with 0.4-μm pores, the HSCs neither migrated nor extended cytoplasmic processes through the micropores onto the top surface (Figs. 4-2A–D). However, the HSCs remained on the bottom surface of the 1.0-μm porous membrane and extended cytoplasmic processes through the micropores. In contrast, on membranes with pore sizes >3.0 μm, the HSCs migrated through the micropores onto the top surface. The translocation of HSCs from the bottom to the top surface of the membrane was demonstrated by detection of their nuclei on the top surface. The coverage of HSCs on the top surfaces of 0.4-, 1.0-, 3.0-, and 8.0-μm pore size membranes on day 14 were 0% ± 0%, 63.6% ± 11.6%, 75.9% ± 10.8%, and 81.4% ± 4.3%, respectively (Fig. 4-2D). Cell migration through the micropores was specific to HSCs, as SHs neither migrated nor extended cytoplasmic processes through the micropores regardless of pore size (data not shown).

4-2-3. ECs form a distinct confluent distribution in intimate association with HSCs on 1.0-μm porous membranes

On day 14, cultured HSCs covered the top surfaces of the 1.0-, 3.0-, and 8.0-μm porous membranes (Figs. 4-2A–D). ECs were then added to the top surface of each membrane to reconstruct the hepatocyte-HSC-EC complex. After 24 hours, the ECs that had attached to the top surface were stained with DiI-acLDL. The ECs exhibited a uniform distribution on the 1.0-μm porous membrane, forming a confluent layer (Fig. 4-2E), and maintained a uniform distribution for as long as 40 days in tri-culture.

However, few ECs attached to the 3.0- or 8.0-μm porous membrane (Fig. 4-2E), and the cells failed to distribute uniformly even after 7 days in tri-culture (data not shown). The coverage of ECs on the top surfaces of 1.0-, 3.0-, and 8.0-μm pore size membranes at 24 hours of tri-culture were 100% ± 0%, 45.3% ± 14.1%, and 52.3% ± 27.0%, respectively (Fig. 4-2F), whereas those on day 6 of tri-culture were 100% ± 0%, 44.7% ± 17.1%, and 34.0% ± 10.2%, respectively (Fig. 4-2F). Thus, as the 1.0-μm porous membrane was best for establishing the complex, it was used for the 3D tri-culture model.

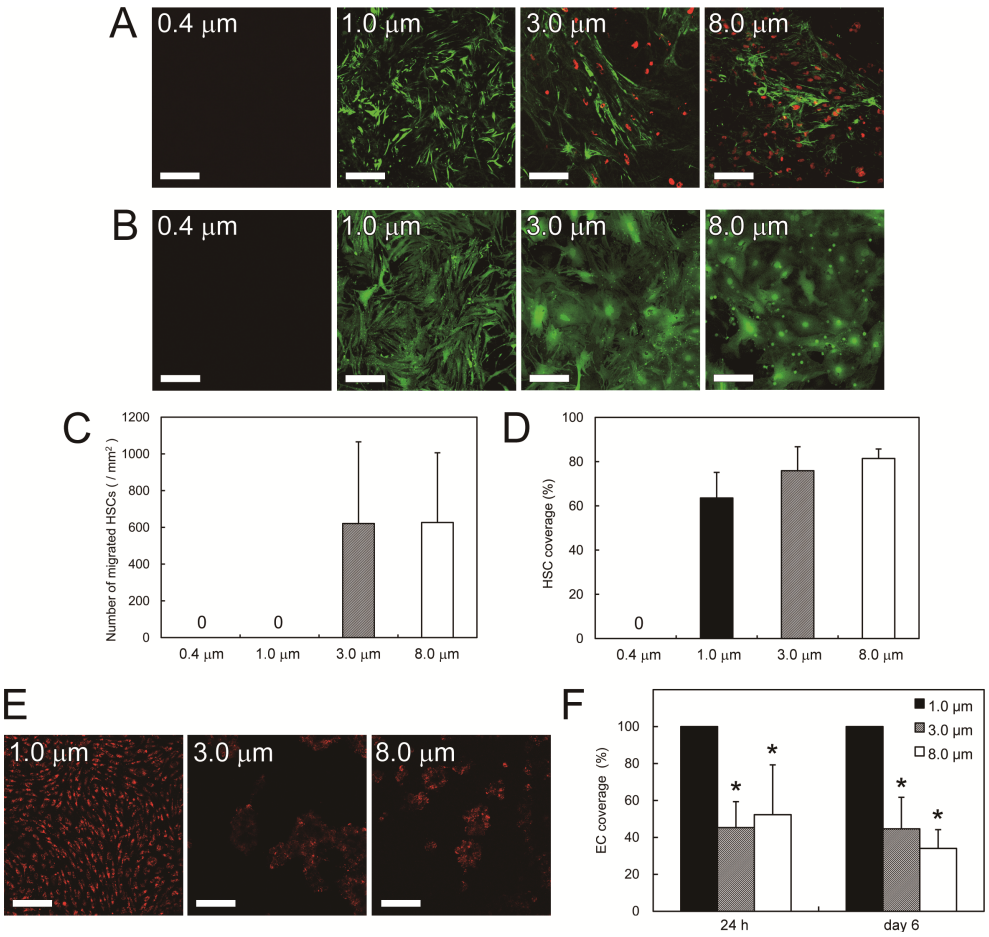

Figure 4-2. Effects of pore size on hepatic stellate cell (HSC) migration, extension of cellular processes through the micropores (*A–D*), and attachment of endothelial cells (ECs) on the top surface of the membrane (*E and F*). ***A*)** Migrated HSCs onto the top surface of a microporous membrane with micropores of various sizes. On day 14 after inoculation, the cells were immunostained for desmin (green) and the nuclei were stained with propidium iodide (red). Scale bar: 100 μm. Original magnification: ×200. ***B*)** Distribution of GFP-labeled HSCs on the top surface of a microporous membrane with micropores of various sizes. On day 14 after inoculation, the GFP-labeled HSCs were fixed and the fluorescence image of the top surface of the membrane was obtained. Scale bar: 100 μm. Original magnification: ×200. ***C*)** Number of migrated HSCs onto the top surface of the membrane. ***D*)** Coverage of the top surface of the membrane by HSCs. ***E*)** Fluorescence micrographs of ECs on the top surface of each kind of microporous membrane. ECs were stained with DiI-acLDL at 24 hours after inoculation and photographed using confocal microscopy. ECs attached to and were uniformly distributed on the 1.0-μm porous membrane. In contrast, few ECs attached to the 3.0- or 8.0-μm porous membranes. Scale bar: 100 μm. Original magnification: ×200. ***F*)** Coverage of the top surface of the membrane by ECs at 24 hours and day 6 after inoculation of EC. * p <0.05 compared with the 1.0-μm porous membrane.

4-2-4. HSCs are physically connected with SHs and ECs through the membrane micropores

When cultured on the bottom surface of a 1.0-μm porous membrane, SHs formed colonies and HSCs extended cytoplasmic processes onto the membrane's top surface (Fig. 3-1A, Step 2). On day 14, ECs were added to the top surface and allowed to form a confluent distribution, which resulted in establishment of the hepatocyte-HSC-EC complex (Fig. 3-1A, Step 3).

The heterotypic cellular configuration of the 3D tri-culture model was analyzed. An immunostained vertical section of the model showed HSCs physically connected with SHs and ECs through the membrane micropores (Fig. 4-3A). TEM images revealed that the HSCs were physically connected with the SHs and ECs on each side of the membrane by cytoplasmic processes extending from the HSCs and through the micropores (Figs. 4-3B1–4). ECM-like substances accumulated between HSCs and ECs were often observed (Fig. 4-3B3 and 3B4). In addition, electron-dense materials that were suspected to be junction-like structures were occasionally present where the HSCs and ECs made close contact (Figs. 4-3B4–6).

4-2-5. Distribution analysis of basement membrane components in the 3D tri-culture model

Basement membrane components are intercalated in the space of Disse *in vivo* (Martinez-Hernandez and Amenta, 1993). To clarify the types of ECM accumulated between the HSCs and ECs in the tri-culture model, immunofluorescent stainings were performed for basement membrane components, such as type IV collagen, laminin, and fibronectin. These proteins showed a continuous distribution along the gaps between the HSCs and ECs on the top surface of the 1.0-μm porous membrane (Fig. 4-3C).

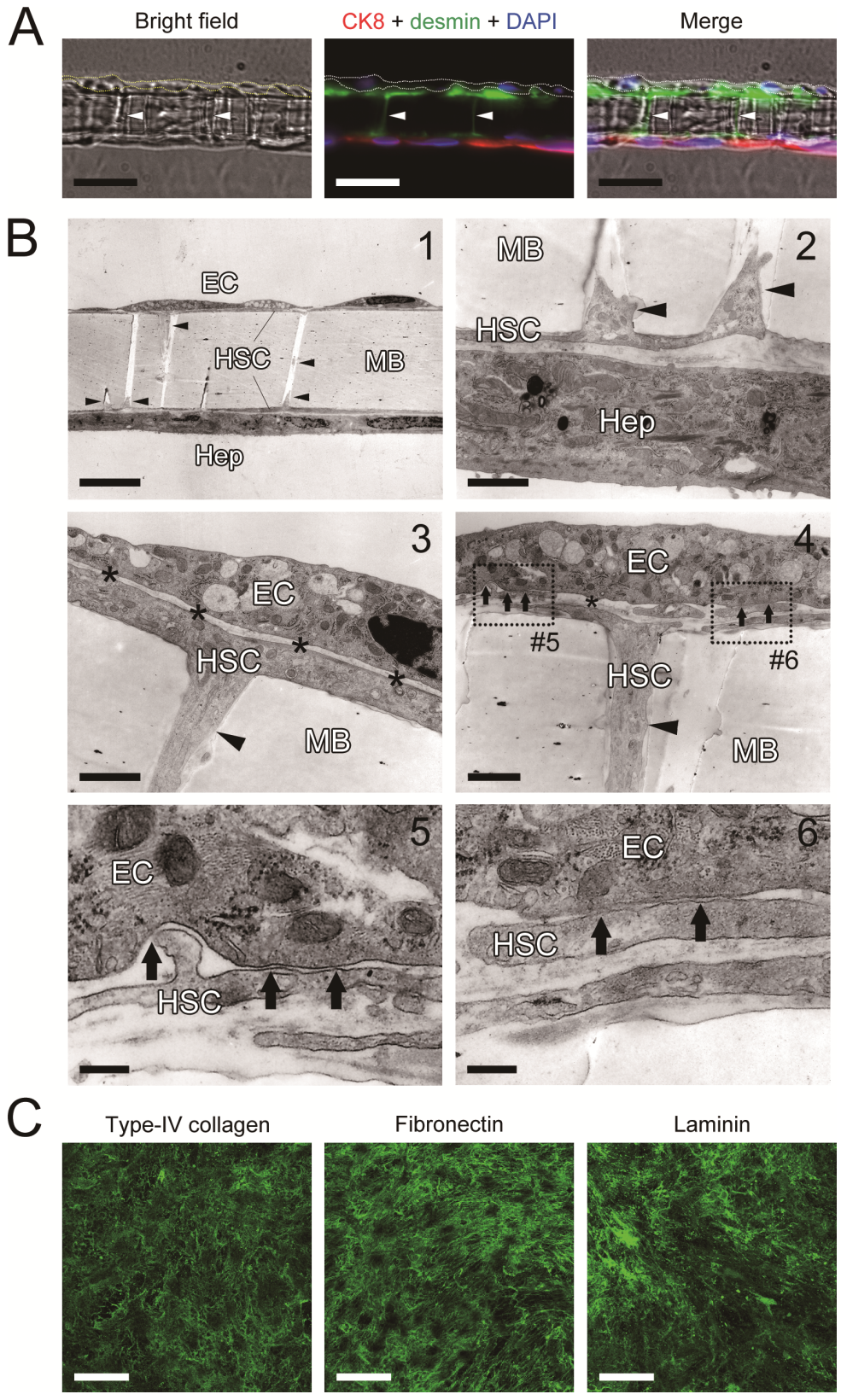

Figure 4-3. *Note that figure captions are in next page.

Figure 4-3. Vertical section of the hepatic stellate cell (HSC)-mediated three-dimensional tri-culture model (*A*, *B*) and the distribution of basement membrane components in the gap between the HSCs and endothelial cells (ECs) on the top surface of the membrane (*C*). ***A*)** Cells after 3 days in tri-culture were stained for CK8 (red) and desmin (green), and with DAPI (blue). A bright field image, a corresponding fluorescence image, and a merged image are shown. Dotted lines: outlines of the EC layer. Arrowheads: HSC processes penetrating the micropores. Scale bars: 20 μm. Original magnification: ×400. ***B*)** Electron micrographs of model vertical sections. Cells were fixed on day 2 of tri-culture. *1*) Hepatocytes (Heps) on the bottom surface and ECs on the top surface of the membrane (MB) were interconnected by underlying HSCs. Arrowheads: cytoplasmic processes of the HSCs in micropores. *2*) HSC between Heps and the bottom surface of the membrane extended their cytoplasmic processes into the micropores (arrowheads). *3*) Extracellular matrix-like substances (asterisk) accumulated between the HSC processes and the EC confluent layer. Arrowhead: a cytoplasmic process penetrating a micropore. *4–6*) Junction-like structures (arrows) were occasionally present where the cytoplasmic processes of HSCs and the ECs made close contact. Magnified images of the numbered rectangles in (*4*) are shown in (*5*) and (*6*), respectively. Arrowhead: a cytoplasmic process of HSC penetrating a micropore. Asterisk: extracellular matrix-like substances. Scale bars: 10 μm (*1*), 1 μm (*2–4*) and 200 nm (*5, 6*). Original magnification: ×1000 (*1*), ×10000 (*2–4*). ***C*)** Distribution of basement membrane components in the gaps between HSCs and ECs on the top surface of the membrane. Cells were fixed on day 6 of tri-culture and immunostained for basement membrane components (type IV collagen, laminin, and fibronectin). Fluorescent micrographs show the *x-y* plane between the HSC processes and ECs. Scale bars: 50 μm. Original magnification: ×400.

4-2-6. HSC-mediated heterotypic interactions induce EC morphological changes in the 3D tri-culture model

To confirm heterotypic cellular communication, quantitative analysis of EC morphology was performed in the presence and absence of HSCs (Fig. 4-4). The ECs in the 3D tri-culture model were more elongated than ECs in monoculture, based on circularity (0.71 ± 0.12 *vs*. 0.40 ± 0.12, respectively).

To investigate whether an intimate association with HSCs is essential for EC elongation, a tri-culture using a membrane with 0.4-μm pores was set up, which were too small to allow HSC processes to pass through (Fig. 4-2A–D). Only soluble factors could be exchanged between the ECs and HSCs. Under these conditions, the ECs showed typical cobblestone-like morphology, as seen in monoculture (Fig. 4-4A). To investigate whether SHs are needed for EC elongation in tri-culture, a 3D co-culture model was constructed with HSCs and ECs, but without SHs. In this case, the ECs exhibited a cobblestone-like morphology, even though they made close associations with HSCs (Fig. 4-4A).

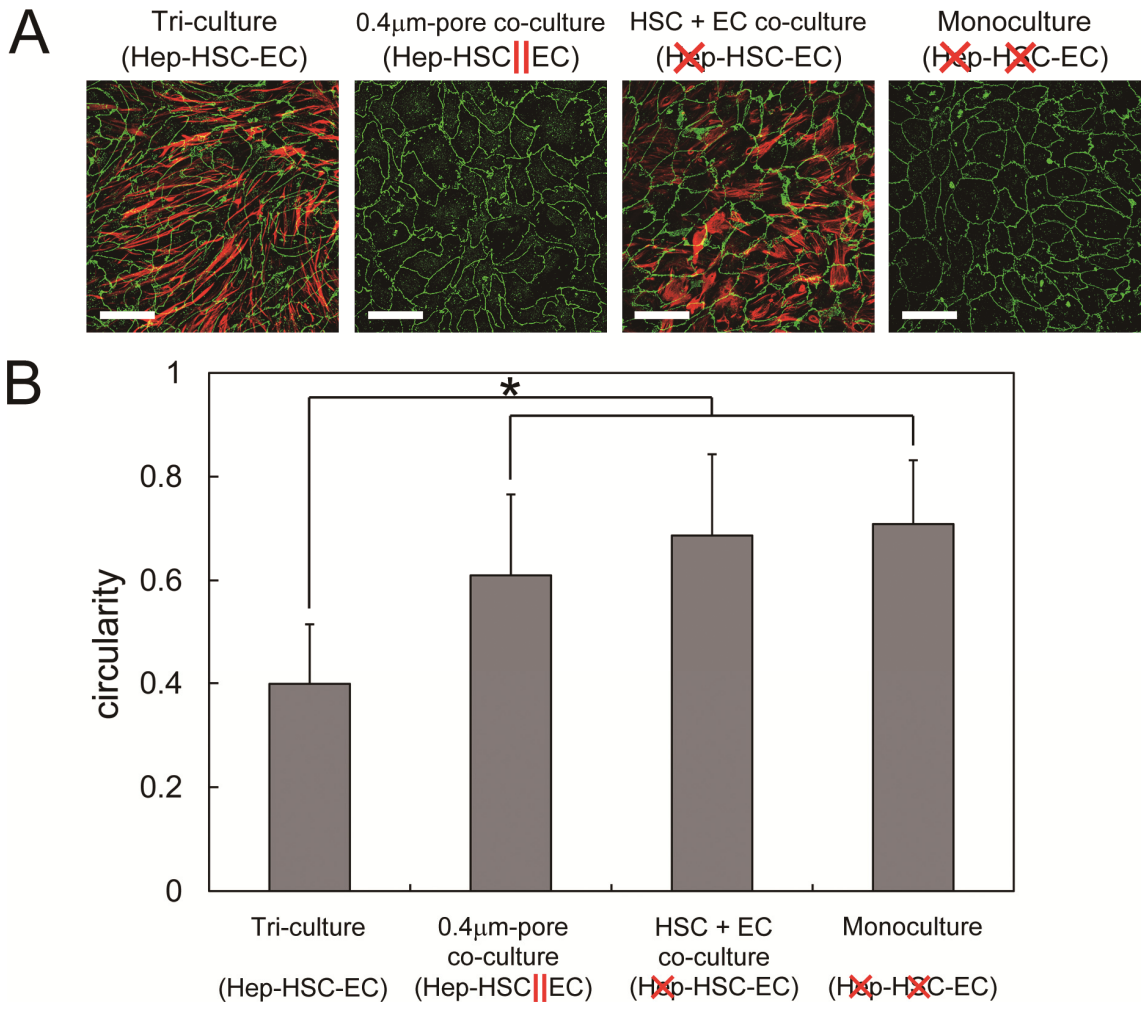

Figure 4-4. Hepatic stellate cell (HSC)-mediated heterotypic interactions of hepatocytes induced a morphological change in the endothelial cells (ECs). ***A*)** EC and HSC distributions on the top surface of the membrane. Cells were fixed on day 6 of tri-culture, double immunostained for VE-cadherin (green) and desmin (red), and photographed using confocal microscopy. Scale bars: 50 μm. Original magnification: ×400. ***B*)** Quantitative analysis of EC circularity. * p <0.05 compared with the tri-culture.

4-2-7. SHs prevent HSC activation

To clarify the effects of SHs on the HSC phenotype in this tri-culture model, immunofluorescence staining of α-SMA was performed to detect activated HSCs, in both co-culture with SHs and monoculture. Only 12.6% ± 14.9% of the HSCs expressed α-SMA in co-culture, whereas 94.2% ± 9.9% of the HSCs expressed α-SMA in monoculture (Fig. 4-5), indicating that SHs significantly prevented the activation of HSCs in co-culture.

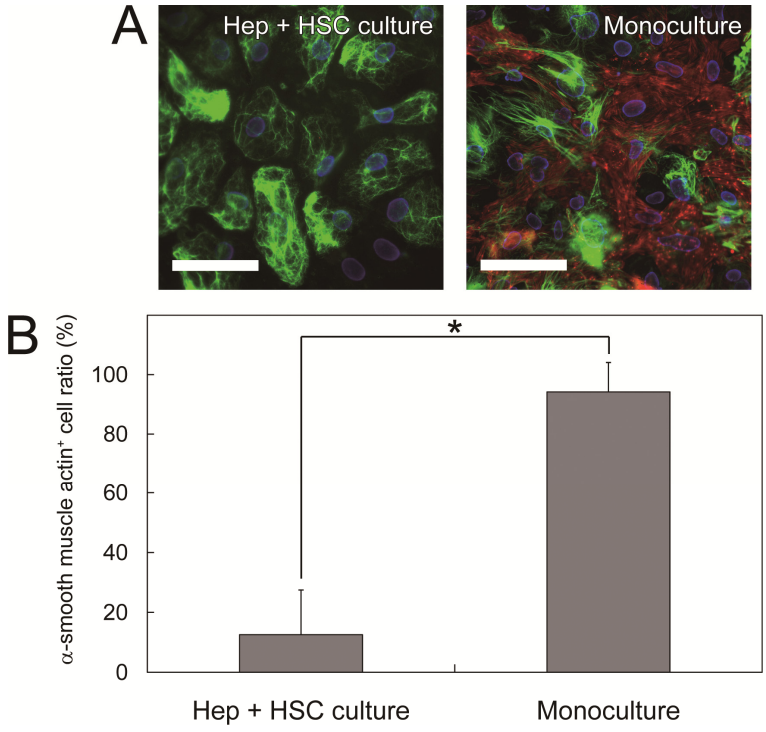

Figure 4-5. Effects of co-culture with small hepatocytes (SHs) on hepatic stellate cell (HSC) phenotype. ***A)*** HSC distribution on the top surface of the membrane. Cells were fixed on day 14, immunostained for desmin (green) and α-smooth muscle actin (α-SMA, red), and stained with DAPI (blue). Fluorescence micrographs of the HSCs co-cultured with SHs and in monoculture. Scale bars: 50 μm. Original magnification: ×400. ***B)*** Quantitative analysis of α-SMA-positive cell ratio. * p <0.05 compared with monoculture.

4-3. Discussion

In this chapter, a novel 3D tri-culture model in which HSCs were intercalated between SHs and ECs was developed. The layered architecture formed in the tri-culture model mimics the *in vivo* heterotypic cellular configuration. Regulating HSC behavior was the most important factor to obtain this configuration. As HSCs tend to migrate through membrane micropores (Sudo *et al*., 2005), membranes with different pore sizes was used to control HSC behavior. When cultured on membranes with >3.0-μm pores, the HSCs passed through the pores and migrated onto the top surface of the membrane. Under these conditions, ECs failed to attach to the top of the HSC layer. When cultured on a 1.0-μm porous membrane, the HSCs extended cytoplasmic processes through the pores to cover the top surface, although the HSC nuclei remained on the bottom surface of the membrane (Figs. 4-2A–D). ECs attached to the top of the HSC layer only under these conditions, suggesting that it is essential for the layered architecture. HSC migration was limited with a reduced pore size, resulting in contact between SHs on the bottom surface and ECs on the top surface of the membranes (Fig. 4-3A). Consequently, HSCs can mediate heterotypic cellular communication between the SH and EC layers in the tri-culture model. These results suggest that the spatial configuration of hepatocytes, HSCs, and ECs must be considered to create a functional unit of these cell types. In addition, each HSC cultured on the 1.0-μm pore size membrane bridged between hepatocytes on the bottom surface and ECs on the top surface of the membrane. *In vivo*, single HSC bridges between hepatocytes and ECs (Wake, 2006) in the same manner as those cultured on the 1.0-μm pore size membranes. Such continuous hepatocyte–HSC–EC connections may lead to effective signal transfer among these cell types.

In the tri-culture model, only the HSCs intruded into 1.0-μm pores of the membrane by extending long cytoplasmic processes. It is possible that the characteristic HSC morphology enabled specific intrusion into the pores. *In vivo*, HSCs extend long

cytoplasmic processes that spread three-dimensionally into two, three, and sometimes more neighboring sinusoids (Wake, 2006), whereas hepatocytes show cuboidal morphology. Although the membranes used here (thickness, 20 μm) were much thicker than the space of Disse (thickness, <1.0 μm) (Martinez-Hernandez and Amenta, 1993), HSCs extended cytoplasmic processes that were long enough to connect the different cell types on each side of the membrane. This HSC-specific behavior can be explained by differential expression of integrins, which are migration-promoting receptors (Ridley *et al*., 2003). Both HSCs and hepatocytes express α1β1, α2β1, and α6β4 integrins. However, only HSCs express α8β1, αvβ1, and αvβ3 integrins, and only hepatocytes express α3β1, α5β1, and α9β1 integrins (Languino *et al*., 2001; Friedman, 2008). Cell type-specific behaviors in response to microporous membranes have also been reported in previous studies. When ECs were co-cultured with mural cells separated by a microporous membrane, the mural cells specifically intruded into the membrane pores to make physical contact with the ECs (Saunders and D'amore, 1992; Fillinger *et al*., 1997).

Using the tri-culture model, the interactions among HSCs, ECs, and SHs were investigated. In monoculture or co-culture, ECs showed typical cobblestone-like morphology, whereas ECs in the tri-culture model exhibited significantly elongated morphology (Fig. 4-4). When the intimate association between HSCs and ECs was inhibited by using a membrane with 0.4-μm pores, the elongated EC morphology was no longer observed, indicating that intimate associations between HSCs and ECs are required for EC elongation in the 3D tri-culture model. Furthermore, the elongated EC morphology did not occur in the absence of SHs, even though ECs were intimately associated with HSCs, indicating that SHs affected EC morphology *via* HSCs. Taken together, the SH–HSC–EC configuration appears to be essential for EC morphogenesis. The intercalated HSCs may mediate heterotypic cellular communication. There is evidence that HSCs may directly communicate with ECs *in vivo via* physical contacts,

such as N-cadherin, to modulate SEC phenotypes and functions (Wirz *et al*., 2008). Junction-like structures were occasionally observed between HSCs and ECs in this tri-culture model (Fig. 4-3B), and this intimate association between HSCs and ECs seemed to induce a morphological change in the ECs. The accumulation of ECM is also important for mediating signals. Accumulation of basement membrane components between HSCs and ECs was often observed in the tri-culture model (Figs. 4-3B and C). Accumulated ECM may play an important role in establishing the SH–HSC–EC configuration and elongated EC morphology. The elongated EC morphology tended to orient parallel to the underlying cytoplasmic processes of quiescent HSCs. To determine whether the morphological changes in ECs in the tri-culture model were affected by ECM synthesized by quiescent HSCs, immunofluorescent stainings of basement membrane components, such as type IV collagen, laminin, and fibronectin on the top surface of the 1.0-μm pore size membrane were performed immediately before the addition of ECs. The basement membrane components synthesized by the HSCs were detected on the top surface. In particular, fibronectin, which is the most abundant ECM component in the space of Disse (Martinez-Hernandez and Amenta, 1993), was expressed on the cytoplasmic processes of HSCs (data not shown). Thus, the elongated morphology of the ECs may be due to the oriented fibronectin deposited on the surface of the cytoplasmic processes of the quiescent HSCs. Furthermore, at least one previous study indicated a similar interaction between ECs and smooth muscle cells (SMCs); when ECs were seeded on top of SMCs, the ECs spread along the native fibrillar form of fibronectin synthesized by the underlying SMCs (Wallace *et al*., 2007). *In vivo*, HSCs are the main ECM producers in the space of Disse, and the basement membrane proteins help to maintain homeostasis of the subendothelial extracellular environment (Friedman, 2008). This culture model may be made to mimic the *in vivo* environment.

HSCs were maintained in a quiescent phenotype when cultured with SHs, whereas HSCs in monoculture became activated into myofibroblast-like cells (Fig. 4-5).

This suggests that heterotypic interactions with SHs are important for maintaining the quiescent phenotype in HSCs. The suppression of the HSCs' activation may be explained by the deposited ECM between SHs and HSCs. Previously, Mitaka *et al*. reported that a basement membrane-like substrate was deposited between the SH colonies and the underlying HSCs when they were co-cultured (1999). The results of electron microscopic and immunohistochemical analyses in the present study also confirmed that a basement membrane-like substrate was deposited between SHs and HSCs (data not shown). It is well known that culturing HSCs on a laminin-rich gel that mimics a basement membrane preserves the quiescent phenotype (Friedman, 2008). This may have implications for the pathogenesis of cirrhosis. The migration of resident HSCs within the space of Disse and potentially in other compartments is considered important for the progression of liver fibrosis, ultimately leading to cirrhosis. Basement membrane matrices in the space of Disse play an important role in anchoring HSCs and preventing them from spreading within the space of Disse and potentially elsewhere in the liver (Yang *et al*., 2003). In addition, alteration of the HSC phenotype is closely linked with the biological properties of ECs. For example, HSC activation and the morphological alteration of SECs are considered pivotal events leading to fibrosis (Friedman, 2008; Mori *et al*., 1993). In the present study, quiescent HSCs induced morphological changes in the tri-cultured ECs, whereas activated HSCs had no effect on EC morphology. ECM secretion and membrane binding protein expression by HSCs differ qualitatively and quantitatively between the quiescent and activated phenotypes (Friedman, 2008). Such differences in HSC properties may lead to different morphological changes in the ECs.

The concept of a hepatocyte-HSC-EC complex that functions as a unit for transduction between the bloodstream and hepatic parenchyma was proposed based on *in vivo* observations (Wake, 2006). However, no culture models have been developed that can reproduce a hepatocyte-HSC-EC complex. In the present chapter, the

hepatocyte-HSC-EC complex as a tri-culture model, in which HSCs maintain their quiescent phenotype and interact with hepatocytes (Fig. 4-6) was reconstructed. The quiescent HSCs extended cytoplasmic processes into 1.0-μm pores as a bridge between hepatocytes and ECs *via* basement membrane components and/or junction-like structures, and induced morphological changes in the ECs, suggesting that HSCs act as transducers by mediating cellular communication between hepatocytes and ECs. Intercalated HSCs may mediate the SH-HSC-EC complex both structurally and functionally.

In conclusion, the hepatocyte-HSC-EC complex was reconstructed in a tri-culture model, in which HSC-mediated heterotypic cellular communication occurred. The 3D tri-culture model described here reproduces the complexity of the liver microenvironment and will enable investigations of more complex and physiological cell–cell communications.

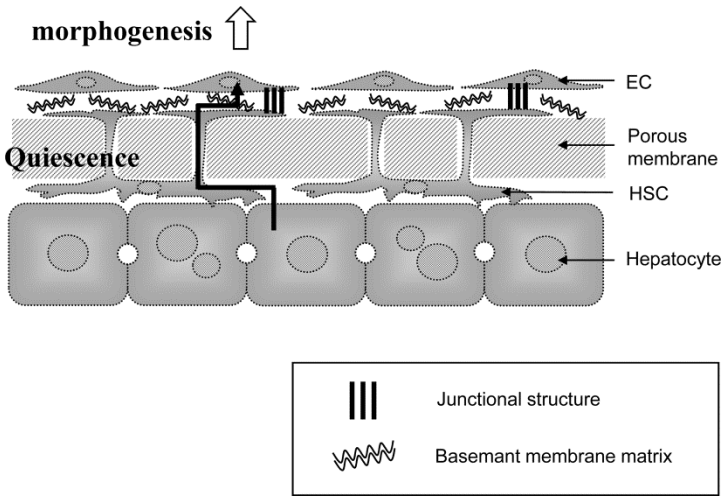

Figure 4-6. Schematic of the proposed mechanism of hepatic stellate cell (HSC)-mediated communication between hepatocytes and endothelial cells (ECs) in the three-dimensional tri-culture model. HSCs maintain a quiescent phenotype through a heterotypic interaction with hepatocytes. Quiescent HSCs extend cytoplasmic processes into the top surface of the membrane and intimately associate with ECs *via* basement membrane components and/or junction-like structures, to induce morphological changes in the ECs.

4-4. Summary

HSCs form a functional unit with endothelia and hepatocytes in the liver to play a pivotal role in heterotypic cellular communication. To investigate this role of HSCs, it is of great benefit to establish a tri-culture model that forms the functional unit from proximal layers of hepatocytes, HSCs, and ECs. Here, we established a 3D tri-culture model, using a microporous membrane to create the functional unit. HSC behavior was controlled by the membrane pore size, which was critical for achieving proximal cell layers. With a specific pore size, the HSCs intercalated between layers of hepatocytes and ECs, due to the limitation on HSC behavior. When only cytoplasmic processes of quiescent HSCs were adjacent to ECs, while the HSC bodies remained on the side of the hepatocytes, the ECs changed morphologically and were capable of long-term survival. We confirmed that HSCs mediated the communication between hepatocytes and ECs in terms of EC morphogenesis. This tri-culture model allows us to investigate the roles of HSCs as both facilitators and integrators of cell–cell communication between hepatocytes and ECs, and is useful for investigating heterotypic cellular communication *in vitro*.

References

Bader A, Knop E, Kern A, Böker K, Frühauf N, Crome O, Esselmann H, Pape C, Kempka G, Sewing KF. 1996, 3-D coculture of hepatic sinusoidal cells with primary hepatocytes-design of an organotypical model, *Exp Cell Res*, **226**: 223–233.

Blomhoff R, Helgerud P, Rasmussen M, Berg T, Norum KR. 1982, In vivo uptake of chylomicron [3H]retinyl ester by rat liver: evidence for retinol transfer from parenchymal to nonparenchymal cells, *Proc Natl Acad Sci USA*, **79**: 7326–7330.

Fillinger MF, Sampson LN, Cronenwett JL, Powell RJ, Wagner RJ. 1997, Coculture of endothelial cells and smooth muscle cells in bilayer and conditioned media models. *J Surg Res*, **67**: 169–178.

Friedman SL. 2008, Hepatic stellate cells: protean, multifunctional, and enigmatic cells of the liver, *Physiol Rev*, **88**: 125–172.

Griffith LG, Naughton G. 2002, Tissue engineering—current challenges and expanding opportunities. *Science*, **295**: 1009–1014.

Griffith LG, Swartz MA. 2006, Capturing complex 3D tissue physiology in vitro, *Nat Rev Mol Cell Biol*, **7**: 211–224.

Harimoto M, Yamato M, Hirose M, Takahashi C, Isoi Y, Kikuchi A, Okano T. 2002, Novel approach for achieving double-layered cell sheets co-culture: overlaying endothelial cell sheets onto monolayer hepatocytes utilizing temperature-responsive culture dishes, *J Biomed Mater Res*, **62**: 464–470.

Hwa AJ, Fry RC, Sivaraman A, So PT, Samson LD, Stolz DB, Griffith LG. 2007, Rat liver sinusoidal endothelial cells survive without exogenous VEGF in 3D perfused co-cultures with hepatocytes. *FASEB J*, **21**: 2564–2579.

Jindal R, Nahmias Y, Tilles AW, Berthiaume F, Yarmush ML. 2009, Amino acid-mediated heterotypic interaction governs performance of a hepatic tissue model. *FASEB J*, **23**: 2288–2298.

Kawada N, Tran-Thi TA, Klein H, Decker K. 1993, The contraction of hepatic stellate (Ito) cells stimulated with vasoactive substances. Possible involvement of endothelin 1 and nitric oxide in the regulation of the sinusoidal tonus, *Eur J Biochem*, **15**: 815–823.

Languino LR, Wells RG. 2001, 'Integrins' in *The Liver Biology and Pathobiology fourth edition*, eds. Arias JM, Boyer JL, Chisari F, Fausto N, Schachter D, Shafritz DA, Lippincott Williams & Wilkins, Philadelphia, PA, USA; 475–482.

Martinez-Hernandez A, Amenta PS. 1993, The hepatic extracellular matrix. I. Components and distribution in normal liver, *Virchows Arch A Pathol Anat Histopathol*, **423**: 1–11.

Mitaka T, Sato F, Mizuguchi T, Yokono T, Mochizuki Y. 1999, Reconstruction of hepatic organoid by rat small hepatocytes and hepatic nonparenchymal cells, *Hepatology*, **29**: 111–125.

Mori T, Okanoue T, Sawa Y, Hori N, Ohta M, Kagawa K. 1993, Defenestration of the sinusoidal endothelial cell in a rat model of cirrhosis, *Hepatology*, **17**: 891–897.

Ridley AJ, Schwartz MA, Burridge K, Firtel RA, Ginsberg MH, Borisy G, Parsons JT, Horwitz AR. 2003, Cell migration: integrating signals from front to back, *Science*, **302**: 1704–1709.

Rojkind M, Novikoff PM, Greenwel P, Rubin J, Rojas-Valencia L, de Carvalho AC, Stockert R, Spray D, Hertzberg EL, Wolkoff AW. 1995, Characterization and functional studies on rat liver fat-storing cell line and freshly isolated hepatocyte coculture system, *Am J Pathol*, **146**: 1508–1520.

Saunders KB, D'Amore PA. 1992, An in vitro model for cell–cell interactions, *In vitro Cell Dev Biol*, **28A**: 521–528.

Sudo R, Mitaka T, Ikeda M, Tanishita K. 2005, Reconstruction of 3D stacked-up structures by rat small hepatocytes on microporous membranes, *FASEB J*, **19**: 1695–1697.

Sundback CA, Vacanti JP. 2000, Alternatives to liver transplantation: from hepatocyte transplantation to tissue-engineered organs, *Gastroenterology*, **118**: 438–442.

Wake K. 2006, Hepatic stellate cells: three-dimensional structures, localization, heterogeneity and development, *Proc Jpn Acad Ser B*, **82**: 155–164.

Wallace CS, Champion JC, Truskey GA. 2007, Adhesion and function of human endothelial cells co-cultured on smooth muscle cells, *Ann Biomed Eng*, **35**: 375–386.

Wirz W, Antoine M, Tag CG, Gressner AM, Korff T, Hellerbrand C, Kiefer P. 2008, Hepatic stellate cells display a functional vascular smooth muscle cell phenotype in a three-dimensional co-culture model with endothelial cells, *Differentiation*, **76**: 784–794.

Yang C, Zeisberg M, Mosterman B, Sudhakar A, Yerramalla U, Holthaus K, Xu L, Eng F, Afdhal N, Kalluri R. 2003, Liver fibrosis: insights into migration of hepatic stellate cells in response to extracellular matrix and growth factors, *Gastroenterology*, **124**: 147–159.

Chapter 5. Spatio-temporal control of hepatic stellate cell–endothelial cell interactions for reconstruction of liver sinusoids *in vitro*

5-1. Introduction

Vascularization of engineered tissues *in vitro* remains a major challenge in liver tissue engineering (Griffith and Naughton, 2002). In the liver, hepatocytes have abundant blood supplies from liver microvessels, termed liver sinusoids, enabling the highly differentiated functions of hepatocytes. To reconstruct functional liver tissues *in vitro*, various culture models have been developed. These include hepatocyte spheroid culture (Evenou *et al*., 2010; Takahashi and Shibuya, 2010), multi-layered culture of hepatocyte sheets (Sudo *et al*., 2005; Ohashi *et al*., 2007), and co-culture with NPCs (Hui and Bahtia, 2007; Riccalton-Banks *et al*., 2003; Jindal *et al*., 2009). In these culture models, hepatic functions were partially promoted, compared with conventional 2D culture models. However, because these culture models depend on diffusion for the supply of oxygen and nutrients, as well as the removal of cellular by-products and waste, the hepatic functions are still insufficient and 3D growth of the reconstructed tissues is restricted due to the diffusional limitations of oxygen and nutrients.

Liver sinusoids consist of three major cell types: hepatocytes, HSCs, and SECs. Hepatocytes form layered structures called hepatic cords. SECs form liver-specific microvessels and are closely situated to the hepatic cords, being interposed by a sparse ECM. HSCs reside between the hepatic cords and SECs and bridge the three cell types by direct contacts. These HSC-intercalated sinusoidal structures enable HSCs to mediate communication between hepatocytes and SECs (chapter 4). It is thus necessary in the reconstruction of such highly specialized liver structures to form a model of

induced capillary morphogenesis of ECs. The previously established tri-culture model consisting of hepatocytes, HSC, and ECs (chapter 4) may be suitable for examining this issue.

The effects of heterotypic cell–cell interactions on EC capillary morphogenesis have been documented previously using various co-culture models of ECs and differing cell types (Hurley *et al*., 2010; Nehls *et al*., 1998; Duffy *et al*., 2009; Sudo *et al*., 2009). Dermal fibroblasts in biocompatible nanofibers mediate an angiogenic process by direct regulation of capillary morphogenesis via the expression of angiogenic factors, and by indirect regulation through the alteration of the mechanical microenvironment via matrix disruption, deposition, and remodeling (Hurley *et al*., 2010). Cardiac fibroblasts in 3D fibrin gels *in vitro* inhibit EC angiogenesis in a contact-dependent manner (Nehls *et al*., 1998). Bone marrow–derived mesenchymal stem cells on Matrigel promote angiogenic processes in a time- and dose-dependent manner (Duffy *et al*., 2009). Hepatocytes in a microfluidic platform promote the formation of capillary-like structures by microvascular ECs (Sudo *et al*., 2009). The findings of these studies have indicated that the effects of heterotypic cell–cell interactions are important for the successful induction of EC capillary morphogenesis. However, less is known about this type of cellular effect in the context of *in vitro* sinusoidal reconstruction.

The role of direct contacts between ECs and HSCs in capillary morphogenesis has been increasingly recognized. In a co-culture spheroid model of ECs and HSCs, HSCs inhibited vascular sprout formation by direct contact with each other (Wirz *et al*., 2008). Co-culture of ECs and HSCs on Matrigel led to the formation of vascular networks, where ECs made direct contact with cellular processes of HSCs (Semela *et al*., 2008). These vascular networks remained more durable than those in EC monoculture, suggesting that direct contact with HSCs regulates EC capillary morphogenesis. However, this hypothetical role of the direct HSC–EC contacts on capillary morphogenesis has not been elucidated in a hepatocyte-HSC-EC tri-culture.

In the present chapter, the effects of direct HSC–EC contacts on EC capillary morphogenesis was first determined using the hepatocyte-HSC-EC tri-culture model in which HSC behaviors were controlled spatially to achieve HSC-mediated proximal layers of hepatocytes and ECs (chapter 4). Capillary morphogenesis was induced by overlaying Matrigel on an EC layer. Direct HSC–EC contacts inhibited EC capillary morphogenesis, suggesting that they were important in capillary formation. I next tested the hypothesis that, in addition to spatial control, temporal control of HSC behavior is also important in achieving capillary morphogenesis. ECs responded to the induction of capillary morphogenesis before the formation of direct HSC–EC contacts, while the ECs remained in monolayers when capillary morphogenesis was induced after HSC–EC contacts had been established. When capillary morphogenesis was successfully achieved in the tri-culture, HSCs tended to preferably localize near the pre-formed capillary-like structures, resulting in the reconstruction of liver sinusoidal structures. In these structures, hepatocyte maturation was induced. These findings indicate that control, both spatial and temporal, of HSC behavior is a key engineering strategy for the vascularization of engineered liver tissue *in vitro*.

5-2. Results

5-2-1. HSC–EC direct contacts inhibited EC capillary morphogenesis in the tri-culture

To determine the effects of HSC–EC direct contacts on EC capillary morphogenesis in the hepatocyte-HSC-EC tri-culture, capillary morphogenesis was induced by overlaying Matrigel on a confluent EC monolayer (Fig. 5-1A). ECs cultured alone (monoculture) formed capillary-like formations within a few days after induction (CMI 21.8 ± 3.2%; Figs. 5-1B and C), as reported previously (Connolly *et al*., 2002). In contrast, ECs in the tri-culture [tri-culture (contact+)], in which the cells were in direct contact with the underlying HSCs (HSC coverage 63.6 ± 11.6%) exhibited no capillary

morphogenesis (CMI 73.2 ± 5.8%; Fig. 5-1).

To investigate whether HSC–EC direct contacts were responsible for EC resistance to capillary formation, HSC–EC direct contacts were inhibited in the tri-culture. HSC behaviors were controlled spatially by a 0.4-μm pore membrane, where HSCs were unable to extend their cytoplasmic processes onto the upper surface of the membrane, and only soluble factors could be exchanged between the HSCs and ECs (Semela *et al*., 2008). In this condition, ECs formed capillary-like formations after induction (CMI 38.8 ± 5.3%), which is similar to that in EC monoculture [tri-culture (contact-); Fig. 5-1]. It was also investigated whether hepatocytes were necessary for the inhibitory effects of HSC–EC direct contact on capillary morphogenesis in tri-culture. When ECs were cultured with HSCs, which are known to exhibit activated phenotypes (section 4-2-7), the ECs exhibited capillary-like formation (CMI 23.6 ± 6.7%) even though they made direct contacts with the HSCs (co-culture with activated HSC; Fig. 5-1).

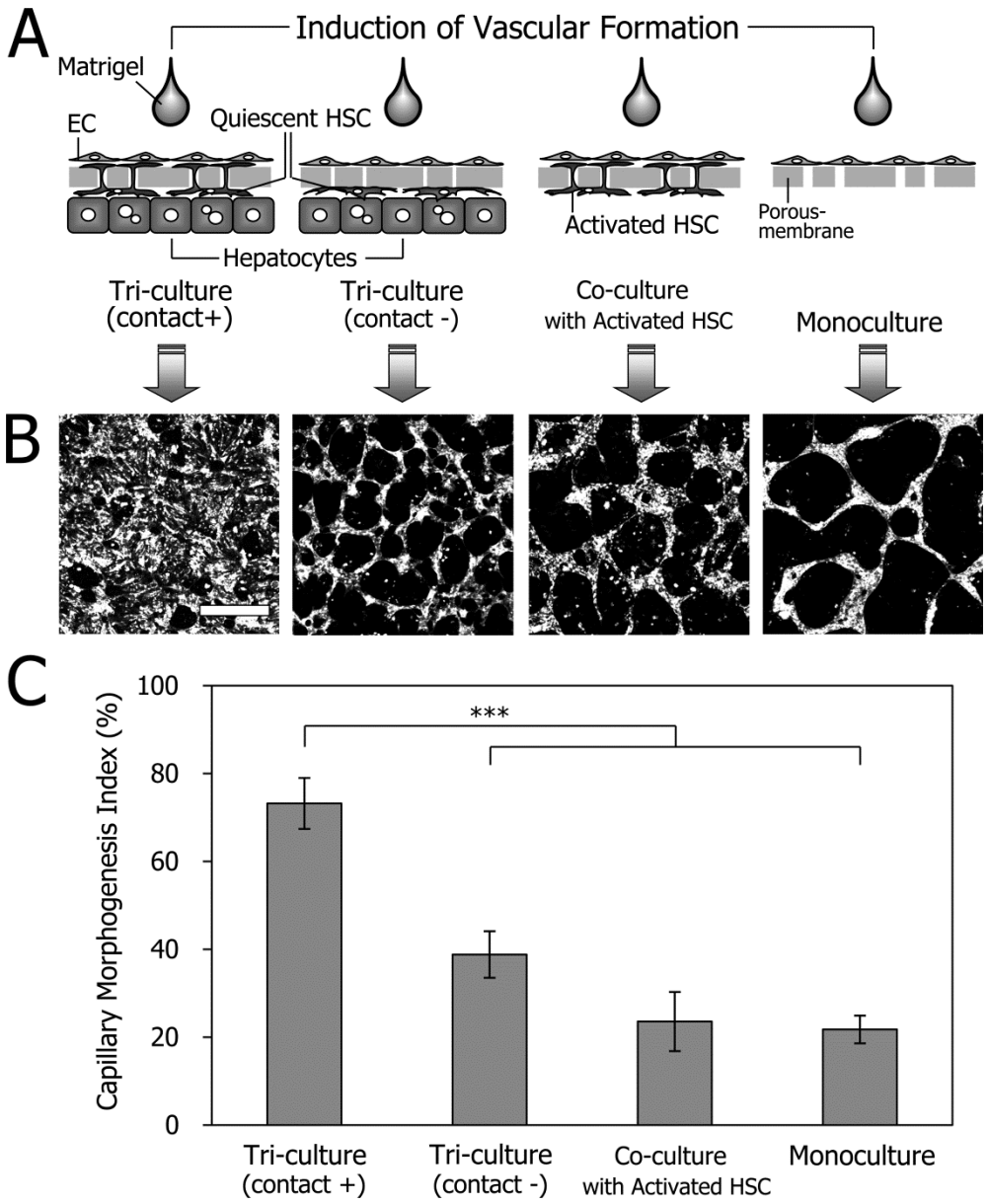

Figure 5-1. Effects of heterotypic cell–cell interactions on Matrigel-induced EC capillary morphogenesis. ***A)*** Schematic diagram of a vertical section of the culture system. Membranes with 1.0-μm pores and 0.4-μm pores were used for Tri-culture (contacts +) and Tri-culture (contacts -), respectively. ***B)*** Fluorescent micrographs of ECs on the top side of each culture system. On day 10 after the induction of capillary morphogenesis, ECs stained with CM-DiI were photographed by confocal microscopy. Scale bar: 200 μm. ***C)*** Quantitative analysis of capillary morphogenesis. *** indicates p <0.001.

5-2-2. HSCs in the tri-culture inhibited EC capillary morphogenesis in a contact area–dependent manner

Because HSC behavior is a key factor in the regulation of EC capillary morphogenesis, the time course of the HSC distribution on the top surface of the membrane was analyzed quantitatively in hepatocyte-HSC co-culture using a 1.0-μm pore membrane. Cells inoculated on the bottom surface of the membrane extended their cytoplasmic processes through the micropores and increasingly covered the top surface of the membrane in a time-dependent manner (Fig. 5-2A). The coverages on days 2, 8, and 14 were 0.4 ± 1.4%, 29.2 ± 6.8%, and 62.1 ± 10.4%, respectively (Fig. 5-2B).

The effect of the HSC–EC contact area on EC capillary morphogenesis was then investigated. Capillary morphogenesis was induced at three different time points: days 2, 8, and 14. When capillary morphogenesis was induced at day 2, when the HSC coverage was only 0.4%, ECs exhibited capillary-like formation (+Matrigel day 2; Fig. 5-3). On the other hand, when capillary morphogenesis was induced at day 8, when the HSC coverage was 29.2%, some ECs exhibited capillary-like formation (+Matrigel day 8; Fig. 5-3). This capillary morphogenesis was diminished when the induction was performed at day 14, when the HSC coverage was 62.1% (+Matrigel day 14; Fig. 5-3). A quantitative analysis of the CMI revealed that capillary-like formation was diminished with increasing HSC–EC contact area (25.5 ± 3.6%, 34.5 ± 6.5%, and 59.6 ± 5.3% on days 2, 8, and 14, respectively; Fig. 5-3).

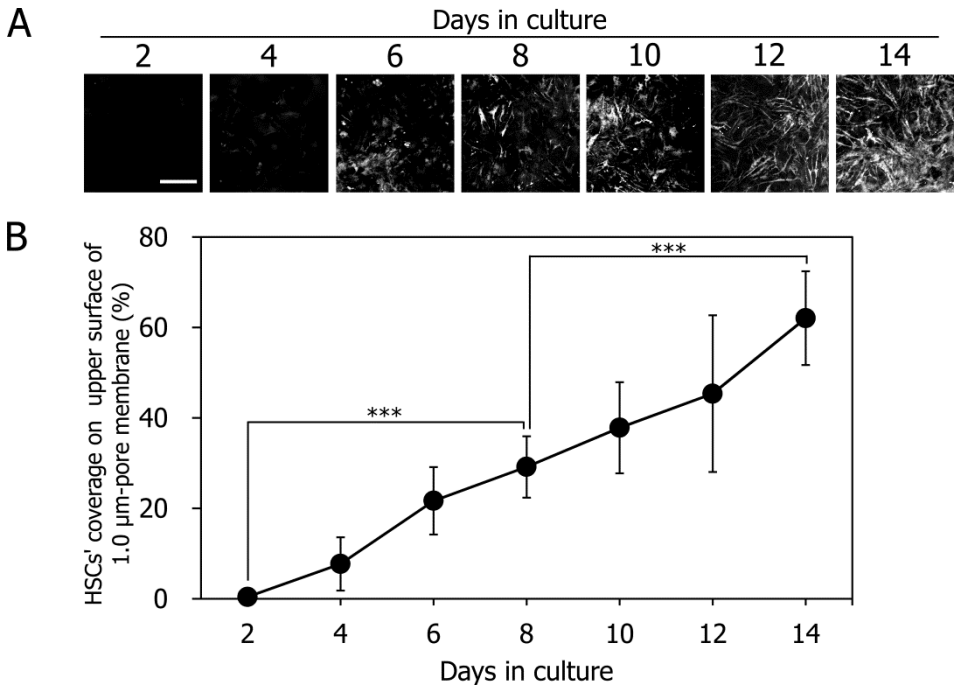

Figure 5-2. Time-dependent increase in HSC coverage on the upper surface of the membrane in the SH, HSC co-culture. ***A*)** Fluorescent micrographs of EGFP-positive HSC cytoplasmic processes on the upper surface of the membrane on different culture days. Scale bar: 200 μm. ***B*)** Quantitative analysis of EGFP-positive HSC coverage on the upper surface of the membrane. *** indicates p <0.001.

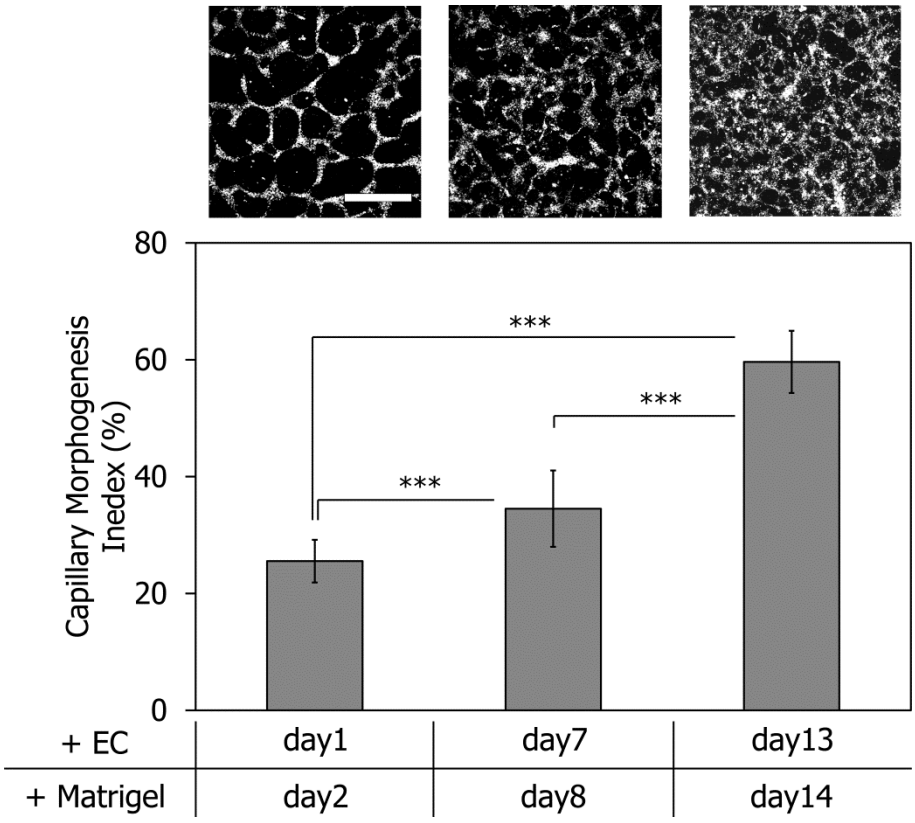

Figure 5-3. Effect of quantitative differences in HSC–EC contact area on Matrigel-induced EC capillary morphogenesis. On day 10 after the induction of EC capillary morphogenesis with Matrigel, ECs stained with CM-DiI were photographed using confocal microscopy and capillary morphogenesis was analyzed quantitatively. Scale bar: 400 μm. *** indicates p <0.001.

5-2-3. Temporal regulation of HSC behavior was essential for the reconstruction of liver sinusoid–like structures

I next tested the hypothesis that stepwise induction of EC capillary morphogenesis and subsequent HSC–EC direct contact formation was essential for the reconstruction of liver sinusoid–like structures. First, hepatocytes and HSCs were inoculated on the bottom surface of a 1.0-μm pore membrane. On the following day, ECs were inoculated on the top surface and capillary morphogenesis was induced. On day 10, the cellular configuration of the tri-culture was analyzed immunohistochemically. An immunostained vertical section of the tri-culture showed that HSCs physically connected both with hepatocyte colonies and EC capillary-like structures through the membrane micropores (Fig. 5-4D). In this tri-culture, HSC cytoplasmic processes and capillary-like structures were well co-localized (Fig. 5-4E). HSCs *in vivo* are thought to be recruited by ECs in developmental and pathological angiogenic events (Lee *et al*., 2007). It was hypothesized that the capillary-like structures in the tri-culture recruited HSCs. To test this hypothesis, a culture including hepatocytes and HSCs was set up and the top surface of the membrane was covered with Matrigel (Fig. 5-4F). In this condition, HSCs did not extend their cytoplasmic processes on the top surface of the membrane at all (SH, HSC co-culture; Fig. 5-4G). In addition, the recruitment of HSCs to the pre-formed capillary-like structures was totally inhibited by administrating the tyrosine kinase inhibitor of PDGF-receptor β (tri-culture + AG 1295; Fig. 5-4G).

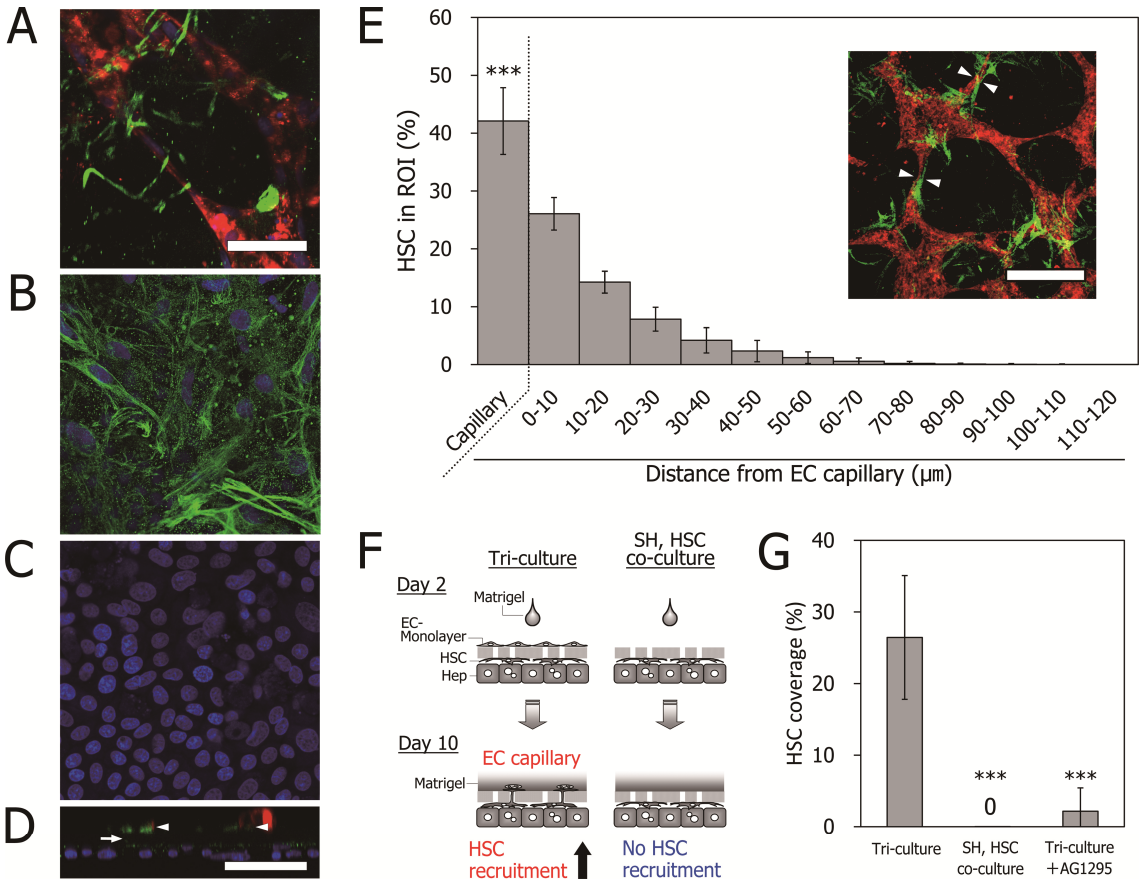

Figure 5-4. *Note that figure captions are in next page.

Figure 5-4. Liver sinusoidal structures in the hepatocyte-HSC-EC tri-culture (A-D), and HSC recruitment by EC capillary-like structures in the sinusoidal structures (E-G). ***A-D*)** Three-dimensional configuration of liver sinusoidal structures in the hepatocyte-HSC-EC tri-culture. Cells were fixed on day 10 post-EC capillary morphogenesis induction and stained with CM-DiI (red) for ECs, with desmin (green) for HSCs, and DAPI (blue) for nuclei. The cells were photographed using confocal microscopy. Images were three-dimensionally reconstructed by calculating 85 planes at 0.47-μm intervals: the 27^{th} (A), 52^{nd} (B), and 62^{nd} (C) planes are shown. A vertical section in the three-dimensional image is shown (D). HSCs (B) physically connected both with hepatocyte colonies (C) and EC capillary-like structures (A) through the membrane micropores. The arrow in (D) indicates HSC cytoplasmic processes penetrating the micropores. Arrowheads in (D) show direct contacts between the HSC cytoplasmic processes and the EC capillary-like structures. Scale bar (A–D): 50 μm. ***E*)** Quantitative analysis of co-localization between EC capillary-like structures and HSC on the upper surface of the membrane. *** indicates $p < 0.001$, compared with HSCs in the area outside of the EC capillary-like structures. A fluorescent micrograph of the distribution of EGFP-labeled HSC cytoplasmic processes (green) and CM-DiI stained EC capillary-like structures (red) on the upper surface of the membrane is shown in the inset. Scale bar: 200 μm. ***F, G*)** HSC recruitment onto the upper surface of the membranes by the EC capillary-like structures. Because the HSC cytoplasmic processes and the EC capillary-like structures were well colocalized in the liver sinusoidal structures, it was hypothesized that EC capillary-like structures in the tri-culture recruited HSCs. To test this, a culture including hepatocytes and HSCs was set up and the top surface of the membrane was covered with Matrigel (SH, HSC co-culture; F) In addition, a tri-culture supplemented with the tyrosine kinase inhibitor of PDGF-receptor β, AG1295 was set up. Quantitative analysis of HSC recruitment on the upper surface of the membranes by the EC capillary-like structures on day 10 (G). *** indicates $p < 0.001$ compared with tri-culture.

5-2-4. Effect of HSC–EC contacts on the maintenance of EC capillary-like structures

To investigate the effect of HSC–EC contacts on the maintenance of EC capillary-like structures, capillary morphogenesis was analyzed in the tri-culture with and without HSC–EC contacts. In the tri-culture, where ECs directly contacted the underlying HSC cytoplasmic processes (tri-culture HSC–EC contact +; Fig. 5-5A), ECs maintained capillary-like structures even after 14 days in culture. On the other hand, ECs in the tri-culture without the HSC–EC direct contacts (tri-culture HSC–EC contact -; Fig. 5-5A) failed to maintain capillary-like structures after 14 days in culture. Quantitative analysis of the CMI revealed that the EC capillary-like structures with the HSC–EC direct contacts were much more durable than those without HSC–EC direct contacts (26.2 ± 4.9%, 19.2 ± 3.7%, and 16.1 ± 2.9% in the tri-culture with HSC–EC contacts and 22.8 ± 7.1%, 12.8 ± 2.7%, and 8.4 ± 3.9% in the tri-culture without HSC–EC contacts, on days 2, 8, and 14, respectively; Fig. 5-5B).

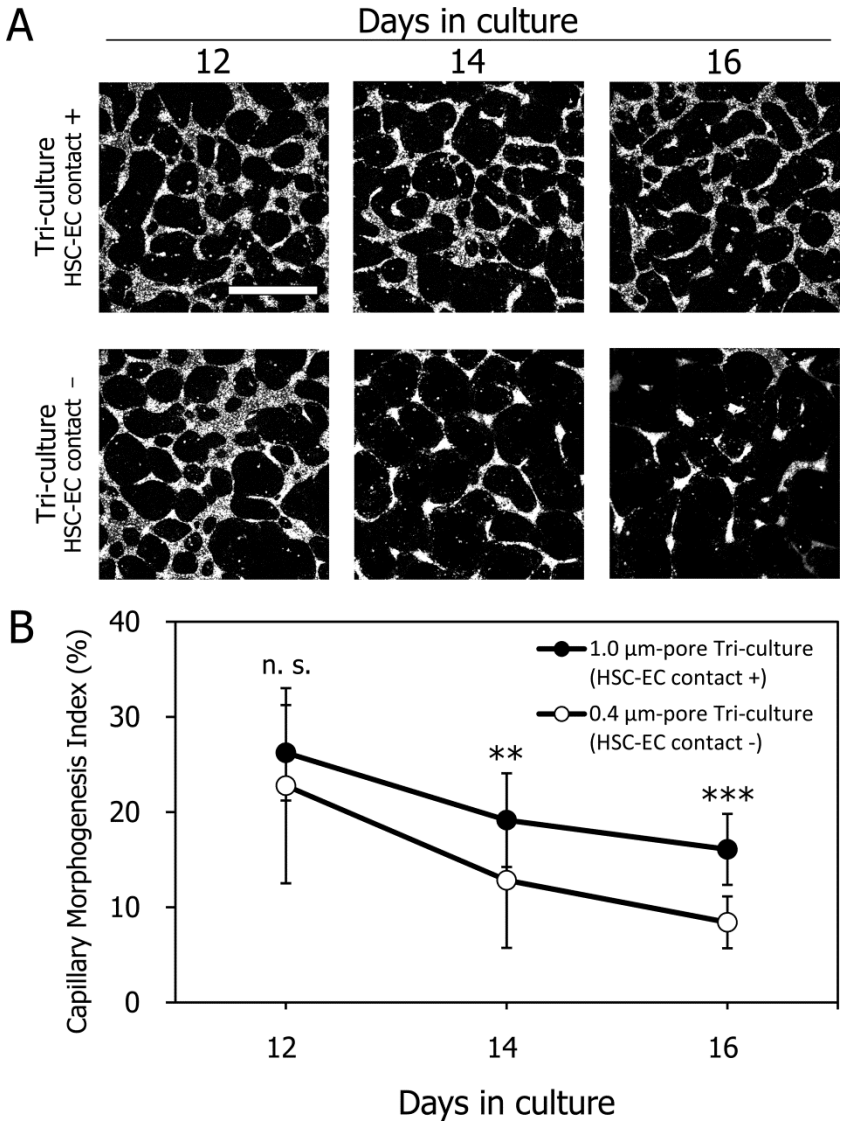

Figure 5-5. Maintenance of EC capillary-like structures in liver sinusoidal structures by HSC–EC direct contacts. ***A*)** Time-sequence fluorescent micrographs of the EC capillary structures in the hepatocyte-HSC-EC tri-culture with or without HSC-EC direct contacts. ECs were stained with CM-DiI. Scale bar: 500 µm. ***B*)** Quantitative analysis of the maintenance of EC capillary-like structures in the hepatocyte-HSC-EC tri-culture with or without HSC-EC direct contacts. *n.s.* indicates $p > 0.05$ (not significant). ** indicates $p < 0.01$ and *** indicates $p < 0.001$.

5-2-5. Morphology and growth activity of SHs in the liver sinusoidal structures

To examine the morphology of SHs in the liver sinusoidal structures, immunostaining for CK 8 and counterstaining for PI were performed. SH colonies in the sinusoidal structures were constructed using various sizes of cells (Fig. 5-6A), while those in the culture without ECs were constructed mainly using small cells of uniform size (Fig. 5-6B). In addition, SH colonies in the sinusoidal structures contained more binucleated cells (17.4 ± 8.8% of total SHs) than did those in the culture without ECs (1.2 ± 0.9% of total SHs; Fig. 5-6C).

To investigate the growth activity of SHs in the sinusoidal structures, BrdU incorporation was examined in SH colonies. The percentage of BrdU-positive SHs was 30.8 ± 5.5% in the sinusoidal structures, whereas that in the culture without ECs was 41.2 ± 5.7% (Fig. 5-7). Quantitative analysis of the ratio of BrdU-positive SHs revealed that the growth activity of SHs in the sinusoidal structures was lower than that in the culture without ECs.

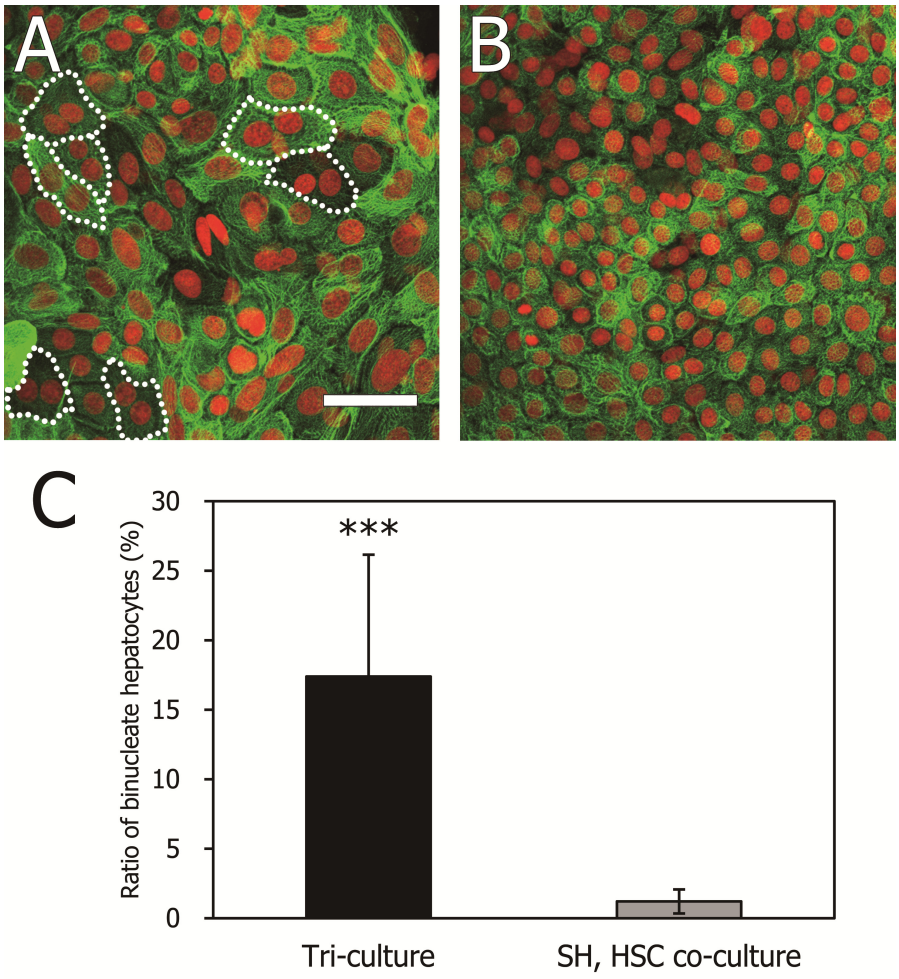

Figure 5-6. Morphology of SHs in the liver sinusoidal structures. ***A and B*)** Fluorescent micrographs of the hepatocytes in the liver sinusoidal structures in the tri-culture (A) and those in the culture including hepatocytes and HSCs (B). The cells were fixed on day 12 and immunostained for CK 8 (green) and nuclei were counterstained with PI (red). Binucleate hepatocytes in the liver sinusoidal structueres were surrounded with dotted lines (C). Scale bar: 50 μm. ***C*)** Quantitative analysis of the ratio of binucleate hepatocytes to total hepatocytes in the liver sinusoidal structures (Tri-culture). As control, the ratio was also calculated in the culture including hepatocytes and HSCs (SH, HSC co-culture). *** indicates p <0.001.

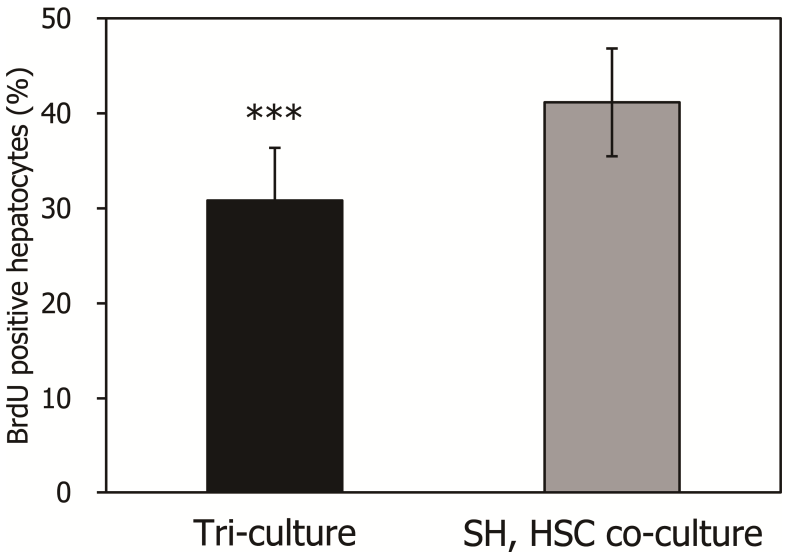

Figure 5-7. Quantitative analysis of the growth activity of SHs in the liver sinusoidal structures. The cells were fixed on day 10 and double immunofluorescent staining was performed for BrdU-incorporated nuclei and CK wide-positive SHs. The cell nuclei were countestained with PI. The BrdU labeling index of the SHs in the liver sinusoidal structures (Tri-culture) was calculated using the staining data of the cells. As control, the index was also calculated in the culture without ECs (SH, HSC co-culture). *** indicates $p < 0.001$.

5-2-6. Upregulation of SH differentiation in the liver sinusoidal structures

To investigate the function of SHs in the liver sinusoidal structures, the amounts of albumin secretion and urea synthesis were measured. No significant differences in these two hepatic functions were observed between the sinusoidal structures and the cultures without ECs (Fig. 5-8).

The mRNA expressions of hepatocyte-differentiation markers were also examined by QPCR analysis. In the sinusoidal structures, the SH differentiation markers (*Tat*, *To*, *Hnf4a*, and *Cebpa*) were significantly upregulated compared with those in the culture without ECs (Figs. 5-9B–E). The expression of *Alb* mRNA by the SHs in the sinusoidal structures was comparable to that in the culture without ECs (Fig. 5-9A).

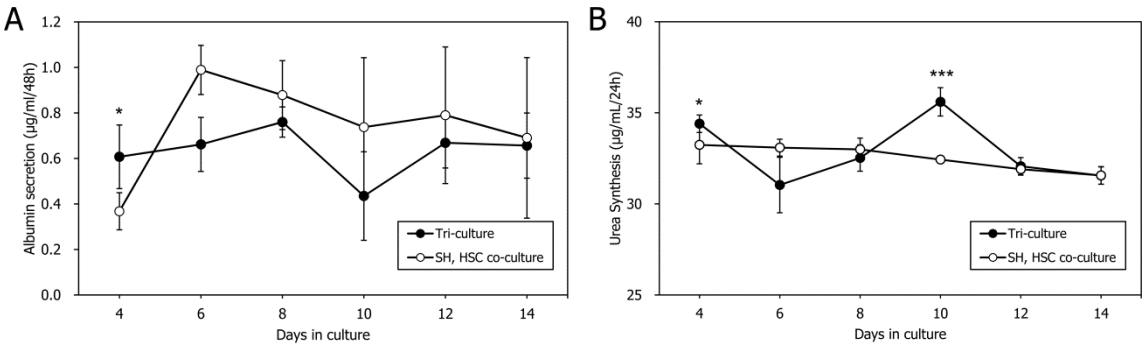

Figure 5-8. Quantitative analysis of hepatic functions in the liver sinusoidal structures in the tri-culture (Tri-culture) (A, albumin secretion; B, urea synthesis). As control, the functions were also analyzed in the culture without ECs (SH, HSC co-culture). No significant differences in these two hepatic functions were observed between the sinusoidal structures and the cultures without ECs. * indicates p <0.05 and *** indicates p <0.001.

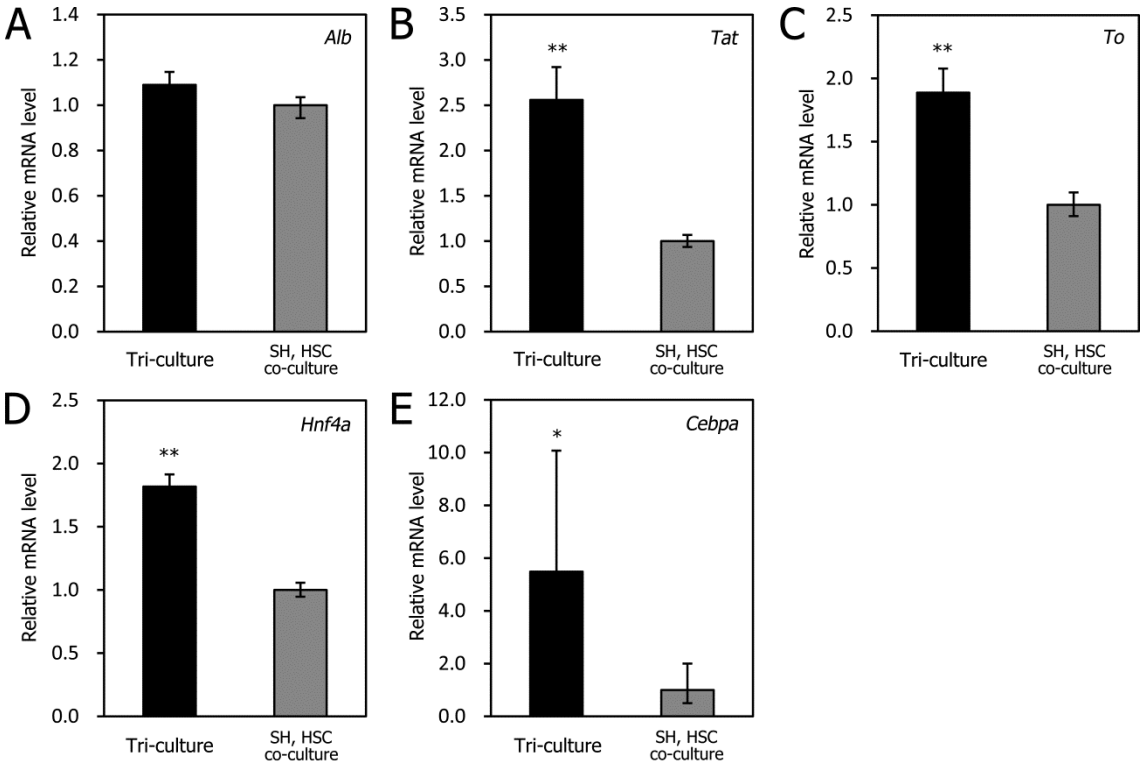

Figure 5-9. QPCR analysis for mRNA expressions of hepatocyte-differentiation markers (A, *Alb*; B, *Tat*; C, *To*; D, *Hnf4a*; E, *Cebpa*). The analysis was performed with total RNA isolated from the cells in the tri-culture after the induction of capillary formation (Tri-culture) and from those cultured without ECs (SH, HSC co-culture) at day 14. The amount of mRNA expressions was normalized with those of SH, HSC co-culture. The SHs in Tri-culture expressed the hepatocyte-differentiation markers stronger than those in SH, HSC co-culture. * indicates p <0.05 and ** indicates p <0.01.

5-3. Discussion

5-3-1. Direct HSC–EC contact inhibited EC capillary morphogenesis in the tri-culture

HSCs directly contact ECs by extending their long cytoplasmic processes in the normal liver where new capillary growth does not occur (Wake, 2006); they thus play a pericytic role in the regulation of capillary stability (Lee *et al*., 2007). In recent studies, the role of direct HSC–EC contacts in EC capillary morphogenesis has been increasingly recognized (Wirz *et al*., 2008; Semela *et al*., 2008). However, the hypothetical role of HSC–EC contacts in morphogenesis remains unclear in hepatocyte-HSC-EC tri-culture. In this chapter, it was shown for the first time that direct HSC–EC contacts play an important role in the regulation of capillary morphogenesis using the hepatocyte-HSC-EC tri-culture. HSCs in the tri-culture appeared to promote EC resistance to the induction of capillary morphogenesis and to stabilize an EC monolayer through direct HSC–EC contacts (Fig. 5-1).

The effect of hepatocytes on direct HSC–EC contacts plays an important role in capillary morphogenesis; HSCs cultured without hepatocytes failed to inhibit capillary morphogenesis, whereas those cultured with hepatocytes inhibited it through direct HSC–EC contacts (Fig. 5-1). HSCs maintained their quiescent phenotype when cultured with hepatocytes, while those in monoculture became activated into myofibroblast-like cells (section 4-2-7). This difference in HSC phenotype, regulated by hepatocytes, appeared to lead to the differing inhibitory effects of the direct HSC–EC contacts on capillary morphogenesis. This finding is consistent with those of the previous study, in which quiescent HSCs cultured with hepatocytes induced an elongated EC morphology, whereas activated HSCs cultured without hepatocytes did not induce EC morphogenesis (section 4-2-6).

The alteration in the HSC phenotype closely relates to capillary morphogenesis *in vivo*. In the regenerating liver, HSC phenotypic alteration, from quiescent to activated, is a prerequisite for capillary morphogenesis to restore the original sinusoid

architectures (Connolly *et al*., 2002; Mabuchi *et al*., 1995). After a two-thirds resection of the liver, activated HSCs migrate into newly replicating avascular islands of hepatocytes, followed by capillary invasion (Díaz-Flores *et al*., 2009). During this HSC phenotypic alteration, the HSCs qualitatively and quantitatively change the expression of ECM and membrane-binding proteins (Friedman, 2008). In the present chapter, it was confirmed that basement membrane components, such as laminin, type-IV collagen, and fibronectin, were deposited less frequently on activated HSC cytoplasmic processes than on quiescent HSC cytoplasmic processes (data not shown). Thus, hepatocytes may indirectly contribute to the inhibitory effect of direct HSC–EC contacts on capillary morphogenesis via maintenance of the HSC quiescent phenotype in the tri-culture.

Matrigel was used to induce capillary morphogenesis. Although Matrigel is known to contain various contaminants, which might have had some effects on the cells, it was used equally in all experiments. For this reason, cell–cell interactions in the tri-culture dominate the effects on cells and outweigh any effects caused by contaminants in the Matrigel.

5-3-2. Temporal control of HSC behavior plays an important role in EC capillary morphogenesis

Based on the finding that HSCs in the tri-culture inhibited capillary morphogenesis by making direct contacts with ECs, it was hypothesized that capillary induction prior to direct HSC–EC contact formation was necessary to achieve capillary morphogenesis in the tri-culture. To test this, capillary morphogenesis was induced at day 2, when direct HSC–EC contacts had not yet formed, resulting in the formation of capillary-like structures in the tri-culture (Fig. 5-3). These structures were maintained even after the HSCs extended their cytoplasmic processes onto the top surface of a membrane and made direct contact with the pre-formed capillary-like structures (Figs. 5-4D and 5-5). Using this method, liver sinusoid-like architectures were successfully formed in the

tri-culture (Figs. 5-4A–D). On the other hand, ECs failed to form the capillary-like structures when capillary morphogenesis was induced *after* direct HSC–EC contacts had formed, even in part (+Matrigel days 8 and 14; Fig. 5-3).

In vivo, pericytes dynamically regulate EC capillary states, from quiescent to angiogenic, through direct contacts (Díaz-Flores *et al*., 2009). In the quiescent stage, the pericytes directly contact capillaries to stabilize them. Once the pericytes depart from capillary walls, capillaries begin to form new vessel lumens. Pericytes are then recruited around the newly formed capillaries and make direct contacts with them, resulting in capillary restabilization. This dynamic process of capillary formation and stabilization *in vivo* is similar to the process in the construction of sinusoidal architecture occurring in the present chapter. This is supported by the results obtained in this chapter, in which ECs maintained their capillary-like structures in the presence of direct HSC–EC contacts in the tri-culture (Fig. 5-5). These results suggest that temporal control of HSC behavior, in addition to spatial control, is necessary to successfully induce capillary morphogenesis in the tri-culture, and to further construct the liver sinusoidal architectures (Fig. 5-10).

5-3-3. HSC–EC interactions and hepatocyte differentiation in liver sinusoidal structures

In the present tri-culture model, SHs, HSCs, and ECs interacted with each other and maintained their composite structures and functions. HSCs extended their cytoplasmic processes preferably to pre-formed capillary-like structures in the tri-culture (Fig. 5-4E). This HSC behavior was not observed without ECs (Figs. 5-4F and G). These results suggest that capillary-like structures recruited HSCs by secreting HSC chemotactic factors and forming a concentration gradient around the cells. Therefore, PDGF signaling, which is the most potent chemotactic signaling in the recruitment of pericytes to newly formed capillaries *in vivo* (Lee *et al*., 2007), was inhibited by administrating a

tyrosine kinase inhibitor of PDGF-receptor β. Under this condition, no HSC recruitment by the capillary-like structures was observed (Fig. 5-4G). The PDGF receptor has also been identified in rat HSCs (Friedman, 2008) and in pericytes (Díaz-Flores *et al*., 2009; Armulik *et al*., 2005). PDGF signaling appeared to be responsible for the selective distribution of HSCs near capillary-like structures in the tri-culture.

Differentiation of SHs was also confirmed in the tri-culture. SH is a hepatic progenitor cell with a single nucleus, although binucleate hepatocytes are commonly observed in the liver. Some SHs differentiated into binucleate mature hepatocytes in the tri-culture (Fig. 5-6). This finding is consistent with the results that showed suppression of SH growth activity (Fig. 5-7), since mature hepatocytes are well known to have less growth activity compared with SHs (Mitaka, *et al*., 1999; Sugimoto *et al*., 2002). In addition, it was confirmed the upregulation of the hepatocyte differentiation markers in the sinusoidal structures (Fig. 5-9). These results indicated that the reconstruction of the sinusoidal structures enhanced the maturation of SHs.

In conclusion, it was demonstrated that temporal control of HSC behavior, in addition to spatial control, is necessary to successfully induce EC capillary morphogenesis in the tri-culture, and to further form liver sinusoid-like architectures. This is the first report to show the importance of temporal control of direct HSC–EC contacts in the construction of liver sinusoidal architectures *in vitro*. The control of HSC behaviors described in the present chapter indicates a key strategy for constructing vascularized liver constructs *in vitro*.

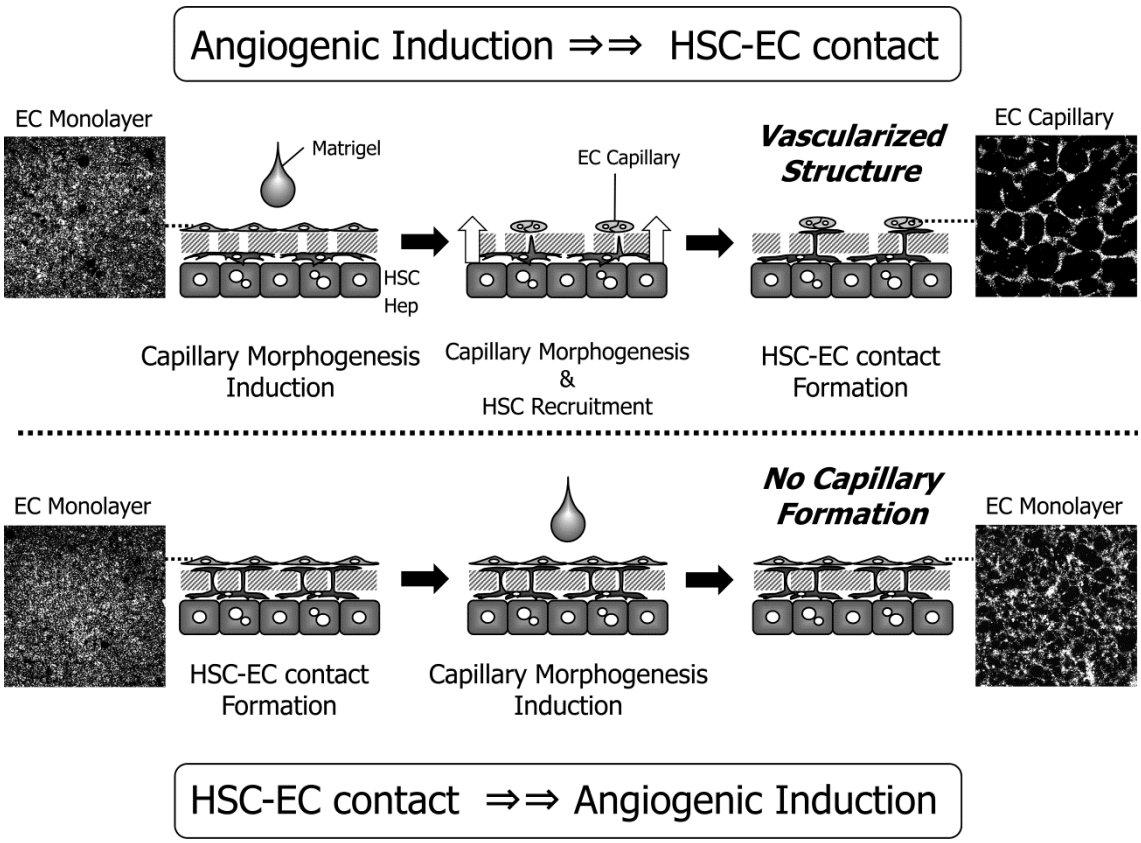

Figure 5-10. Schematic diagrams of proposed engineering strategy for construction of liver sinusoids in the hepatocyte-HSC-EC tri-culture. Spatial and temporal control of HSC behaviors is a key engineering strategy for vascularization of engineered liver tissues *in vitro*.

5-4. Summary

Vascularization of engineered tissues *in vitro* remains a major challenge in liver tissue engineering. Liver microvessels, termed liver sinusoids, have highly specialized structures, and recapturing these sinusoidal structures is essential for reconstruction of functional liver tissue *in vitro*. Liver sinusoids are composed of hepatocytes, HSCs, and ECs. Direct HSC–EC contacts are increasingly recognized for their roles in EC capillary morphogenesis. However, the hypothetical role of HSC–EC contacts in morphogenesis remains unclear in hepatocyte-HSC-EC tri-culture. In the present chapter, the effects of direct HSC–EC contacts on EC capillary morphogenesis was first determined using a hepatocyte-HSC-EC tri-culture model where HSC behavior was spatially controlled to achieve HSC-mediated proximal layers of hepatocytes and ECs. EC capillary morphogenesis was induced by overlaying Matrigel on an EC layer. Direct HSC–EC contacts inhibited EC capillary morphogenesis, suggesting that the HSC–EC contacts may be an important factor in capillary formation. I next tested the hypothesis that, in addition to spatial control, temporal control of HSC behavior is also important in achieving capillary morphogenesis in the tri-culture. ECs responded to the induction of capillary morphogenesis before the formation of direct HSC–EC contacts, while the ECs remained to form monolayers when capillary morphogenesis was induced after the HSC–EC contacts were established. When capillary morphogenesis was successfully achieved in the tri-culture, HSCs tended to preferably localize near the pre-formed capillary-like structures, resulting in the reconstruction of liver sinusoidal structures. In these structures, hepatocyte maturation was induced. These findings indicate that control, both spatial and temporal, of HSC behavior is a key engineering strategy for the vascularization of engineered liver tissue *in vitro*.

References

Armulik A, Abramsson A, Betsholtz C. 2005, Endothelial/pericyte interactions, *Circ Res*, **97**: 512–523.

Connolly JO, Simpson N, Hewlett L, Hall A. 2002, Rac regulates endothelial morphogenesis and capillary assembly, *Mol Biol Cell*, **13**: 2474–2485.

Díaz-Flores L, Gutiérrez R, Madrid JF, Varela H, Valladares F, Acosta E, Martín-Vasallo P, Díaz-Flores L Jr. 2009, Pericytes. Morphofunction, interactions and pathology in a quiescent and activated mesenchymal cell niche, *Histol Histopathol*, **24**: 909–969.

Duffy GP, Ahsan T, O'Brien T, Barry F, Nerem RM. 2009, Bone marrow-derived mesenchymal stem cells promote angiogenic processes in a time- and dose-dependent manner *in vitro*, *Tissue Eng Part A*, **15**: 2459–2470.

Evenou F, Fujii T, Sakai Y. 2010, Spontaneous formation of stably-attached and 3D-organized hepatocyte aggregates on oxygen-permeable polydimethylsiloxane membranes having 3D microstructures, *Biomed Microdevices*, **12**: 465–475.

Friedman SL. 2008, Hepatic stellate cells: protean, multifunctional, and enigmatic cells of the liver, *Physiol Rev*, **88**: 125–172.

Griffith LG, Naughton G. 2002, Tissue engineering.—current challenges and expanding opportunities, *Science*, **295**: 1009–1014.

Hui EE, Bhatia SN. 2007, Micromechanical control of cell–cell interactions. *Proc Natl Acad Sci U S A*, **104**: 5722–5726.

Hurley JR, Balaji S, Narmoneva DA. 2010, Complex temporal regulation of capillary morphogenesis by fibroblasts, *Am J Physiol Cell Physiol*, **299**: C444–453.

Jindal R, Nahmias Y, Tilles AW, Berthiaume F, Yarmush ML. 2009, Amino acid-mediated heterotypic interaction governs performance of a hepatic tissue model, *FASEB J*, **23**: 2288–2298.

Lee JS, Semela D, Iredale J, Shah VH. 2007, Sinusoidal remodeling and angiogenesis: a new function for the liver-specific pericyte?, *Hepatology*, **45**: 817–825.

Mabuchi A, Mullaney I, Sheard PW, Hessian PA, Mallard BL, Tawadrous MN, Zimmermann A, Senoo H, Wheatley AM. 2004, Role of hepatic stellate cell/hepatocyte interaction and activation of hepatic stellate cells in the early phase of liver regeneration in the rat. *J Hepatol*, **40**: 910–916.

Mitaka T, Sato F, Mizuguchi T, Yokono T, Mochizuki Y. 1999, Reconstruction of hepatic organoid by rat small hepatocytes and hepatic nonparenchymal cells, *Hepatology*, **29**: 111–125.

Nehls V, Herrmann R, Hühnken M, Palmetshofer A. 1998, Contact-dependent inhibition of angiogenesis by cardiac fibroblasts in three-dimensional fibrin gels *in vitro*: implications for microvascular network remodeling and coronary collateral formation, *Cell Tissue Res*, **293**: 479–488.

Ohashi K, Yokoyama T, Yamato M, Kuge H, Kanehiro H, Tsutsumi M, Amanuma T, Iwata H, Yang J, Okano T, Nakajima Y. 2007, Engineering functional two- and three-dimensional liver systems *in vivo* using hepatic tissue sheets, *Nat Med*, **13**: 880–885.

Riccalton-Banks L, Liew C, Bhandari R, Fry J, Shakesheff K. 2003, Long-term culture of functional liver tissue: three-dimensional coculture of primary hepatocytes and stellate cells, *Tissue Eng*, **9**: 401–410.

Semela D, Das A, Langer D, Kang N, Leof E, Shah V. 2008, Platelet-derived growth factor signaling through ephrin-b2 regulates hepatic vascular structure and function, *Gastroenterology*, **135**: 671–679.

Sudo R, Chung S, Zervantonakis IK, Vickerman V, Toshimitsu Y, Griffith LG, Kamm RD. 2009, Transport-mediated angiogenesis in 3D epithelial coculture, *FASEB J*, **23**: 2155–2164.

Sudo R, Mitaka T, Ikeda M, Tanishita K. 2005, Reconstruction of 3D stacked-up structures by rat small hepatocytes on microporous membranes, *FASEB J*, **19**; 1695–1697.

Sugimoto S, Mitaka T, Ikeda S, Harada K, Ikai I, Yamaoka Y, Mochizuki Y. 2002, Morphological changes induced by extracellular matrix are correlated with maturation of rat small hepatocytes, *J Cell Biochem*, **87**: 16–28.

Takahashi R, Sonoda H, Tabata Y, Hisada A. 2010, Formation of hepatocyte spheroids with structural polarity and functional bile canaliculi using nanopillar sheets, *Tissue Eng Part A*, **16**: 1983–1995.

Wake K. 2006, Hepatic stellate cells: three-dimensional structure, localization, heterogeneity and development, *Proc Jpn Acad Ser B*, **82**: 155–164.

Wirz W, Antoine M, Tag CG, Gressner AM, Korff T, Hellerbrand C, Kiefer P. 2008, Hepatic stellate cells display a functional vascular smooth muscle cell phenotype in a three-dimensional co-culture model with endothelial cells, *Differentiation*, **76**: 784–794.

Chapter 6. Reconstruction of hepatic stellate cell-incorporated liver sinusoidal structures in small hepatocyte tri-culture using microporous membranes

6-1. Introduction

Recapturing liver sinusoidal structures *in vitro* remains a major challenge in liver tissue engineering and is essential to reconstruct functional liver tissue *in vitro*. In liver sinusoids, hepatocytes form layered structures (termed hepatic cords), while SECs form liver-specific microvessels. HSCs reside in the space between the hepatic cords and microvessels, termed the space of Disse, and extend their long cytoplasmic processes to line the outer surface of the microvessels. These HSC-incorporated sinusoidal structures are responsible for active heterotypic cell–cell interactions and result in highly differentiated liver functions, such as the regulation of vascular tone (Lee *et al*., 2007) and maintenance of ECM environment homeostasis (Sato *et al*., 1998; Friedman, 2008).

Various co-culture methods have been developed to form the HSC-incorporated sinusoidal structures *in vitro*. These include a layered co-culture of hepatocytes and NPCs (Bader *et al*., 1996, Harimoto *et al*., 2002; Ohno *et al*., 2008; Ohno *et al*., 2009), co-culture of hepatocytes and NPCs on Matrigel (Nahmias *et al*., 2006; Soto-Gutierrez *et al*., 2010), and co-culture of hepatocytes and NPCs in a perfusion microbioreactor (Hwa *et al*., 2007). Although heterotypic cell–cell interactions have been observed, these co-cultures did not result in sinusoidal structures. In these studies, cells did not form any tissues when co-culture was initiated, and the sinusoidal tissue organization was dependent on their spontaneous assembly. The organization of HSC-incorporated sinusoidal structures during liver development and regeneration is a highly complex process (Martinez-Hernandez and Amenta, 1993; Martinez-Hernandez and Amenta,

1995). Thus, it might be difficult to reconstruct the HSC-incorporated sinusoidal structures *in vitro* spontaneously.

In chapter 5, spatio-temporal control of HSC behavior was shown to be essential to achieve the EC capillary formation in a hepatocyte-HSC-EC tri-culture using PET microporous membranes. However, the sinusoidal structures did not form since the PET microporous membranes are thick and have low porosity, which may act as a barrier for heterotypic cell–cell interactions. To overcome this problem, microporous membranes with high porosity and reduced thickness are required.

PLGA microporous membranes were recently developed to establish the 3D stacked-up culture, where the membranes were intercalated between the hepatocyte layers (Kasuya *et al*., 2012). These membranes have a subcellular thickness and higher porosity as compared with the PET microporous membranes. In addition, their pore-size and porosity can be configured. In this culture, the membranes allowed hepatocytes to actively interact and subsequently organize into 3D differentiated hepatocyte tissues. Therefore, the PLGA microporous membranes may be applicable as cellular scaffolds to form HSC-incorporated sinusoidal structures *in vitro*. I therefore focused on the effective use of the PLGA microporous membranes in hepatocyte-HSC-EC tri-culture to reconstruct the HSC-incorporated liver sinusoidal structures *in vitro*.

In this chapter, a hepatocyte-HSC-EC tri-culture model where HSCs incorporated EC capillary-like structures on the SH-HSC organoids was proposed. The Matrigel angiogenesis assay and SH-HSC organoids were combined by using PLGA microporous membrane. When the membranes with optimized pore-size and porosity were used, HSCs selectively migrated toward the EC capillary-like structures and firmly incorporated their outer surface. In addition, SHs in the HSC-lines sinusoidal tissues retained higher level of differentiated functions as compared to those without ECs. This model will provide a structural unit for constructing the functional, thick, and vascularized liver tissues *in vitro*.

6-2. Results

6-2-1. Control of pore size and porosity of the PLGA membrane

The pore size and porosity of the PLGA membranes were controlled by changing the water content in the PLGA-dissolved dioxane. At 0% water content, no pore was created in the membranes. At 1–5% water contents, pores were randomly distributed in the membranes. Some of these pores did not completely penetrate the membranes (Figs. 6-1A–C). When the water content was over 6%, pores did not overlap each other (Figs. 5-2D–F). Pore size and porosity became higher with increasing water content (Figs. 6-1A and B). Pore sizes were 4.5 ± 3.5, 5.7 ± 3.5, 7.3 ± 3.6, 8.4 ± 1.7, and 13.7 ± 4.8 μm in membranes with 6%, 7%, 8%, 9%, and 10% water content, respectively (Fig. 6-1G). Porosities were 14.0 ± 3.8%, 31.6 ± 2.5%, 46.6 ± 3.7%, 49.6 ± 2.9%, and 57.3 ± 1.6% in membranes with 6%, 7%, 8%, 9%, and 10% water content, respectively (Fig. 6-1H). The average thickness of the membrane was 2.4 ± 0.1 μm, which was independent of water content. The distribution of pore sizes in a membrane with 10% water content is shown in Figure 6-1I. Membranes fabricated with 10% water content were used in this chapter unless otherwise specified.

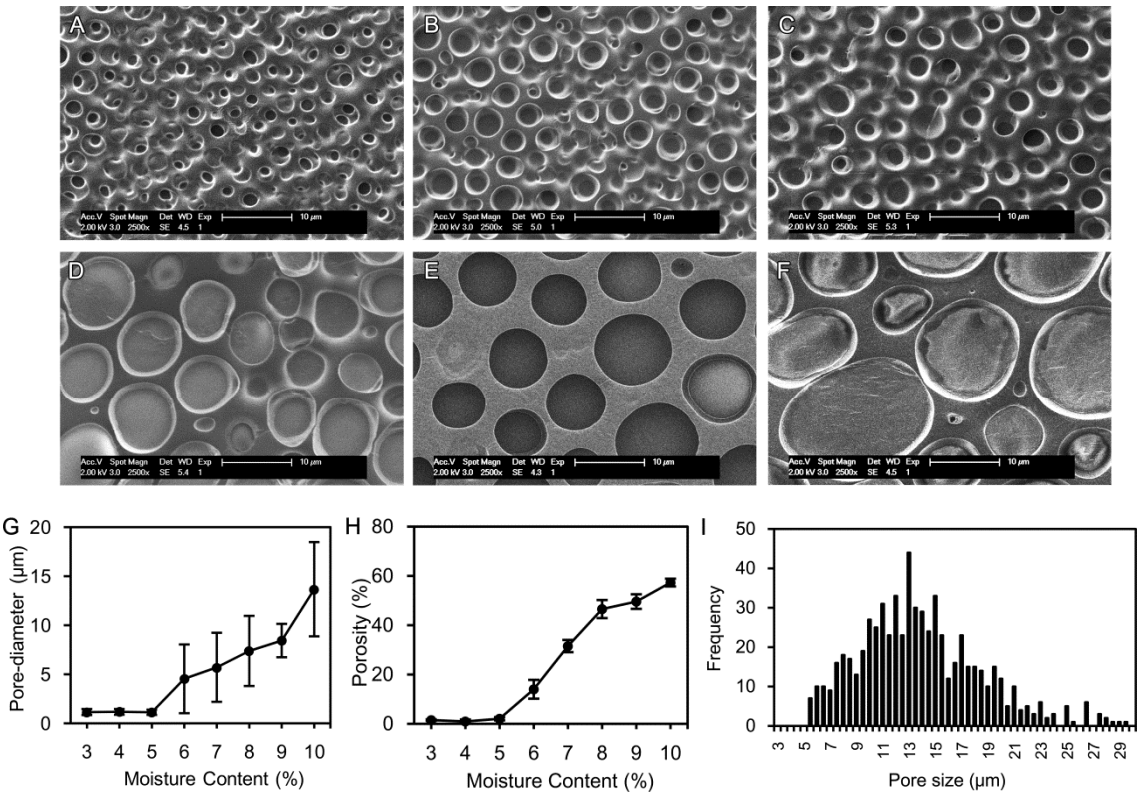

Figure 6-1. Specification of the fabricated PLGA membranes. ***A–F*)** SEM images of the fabricated PLGA membranes with water contents of 3% (A), 4% (B), 5% (C), 7% (D), 8% (E), and 10% (F). All images were taken at the same magnification (×2,500). Pore size of the membranes increased with increasing water content. In the case of 3 5% water content, pores were randomly distributed and they did not penetrate through the membranes, while with 7–10% water content, pores did not overlap each other, and they passed through the membranes. ***G*)** Pore diameter in the fabricated PLGA membranes with a series of water contents. ***H*)** Porosity of the fabricated PLGA membranes with a series of water contents. ***I*)** Distribution of pore diameters of a membrane with 10% water content. n >2000.

6-2-2. Three-dimensional stacked-up configuration

Initial 3D configuration of the stacked-up tri-culture was examined by confocal microscopy on day 1 after stacking. Three-dimensionally reconstructed fluorescent images revealed that EC capillary-like structures on the membranes (40th plane; Fig. 6-2) were successfully stacked on the hepatic organoids composed of SH colonies and the HSCs on a glass-bottom dish surface (7th plane; Fig. 6-2). The distance between the EC capillary-like structures and the hepatic organoids varied from approximately 10 to 30 μm.

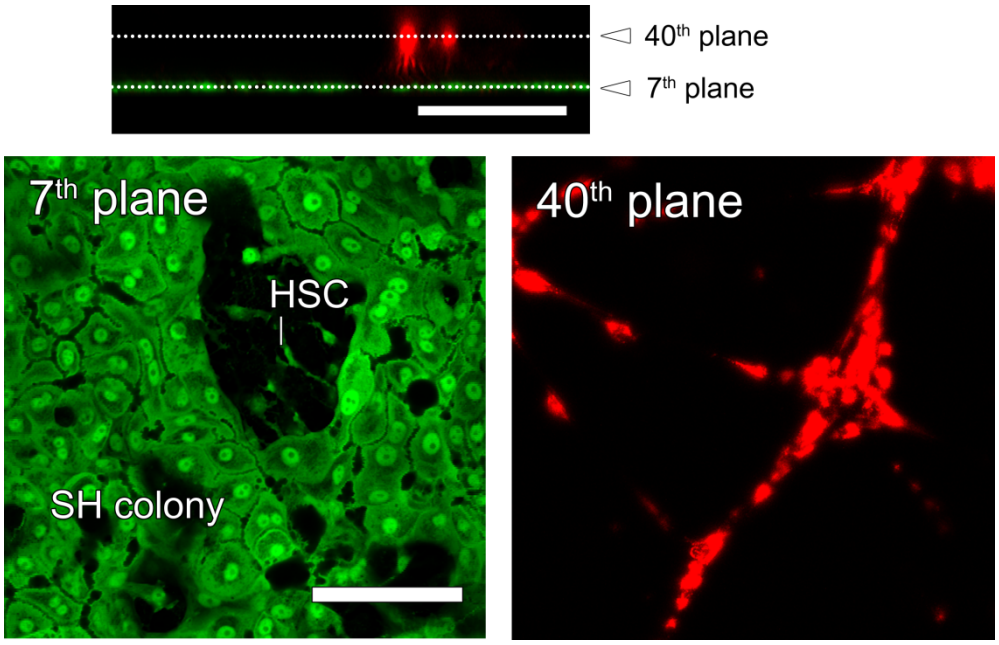

Figure 6-2. Initial 3D configuration of the stacked-up tri-culture. Cells were fixed on day 1 post-stacking and photographed using confocal microscopy. Images were three-dimensionally reconstructed by calculating 62 planes at 0.99-μm intervals: the 7th and 40th planes and a vertical section are shown. EC capillary-like structures stained with CM-DiI (red) were stacked on the EGFP-positive SH colony and HSCs. Scale bars: 100 μm.

6-2-3. Selective migration of HSCs to the EC capillary-like structures

HSC distribution around the EC capillary-like structures was monitored over time by confocal microscopy. Although HSCs were not detected around the EC capillary-like structures until day 4 (Day 4; Fig. 6-3A), cells were detected around the EC capillary-like structures from day 8 and gradually increased their distribution (Day 8, 12, and 16; Fig. 6-3A). These HSCs were firmly attached to the outside of the EC capillary-like structures (arrowheads; Fig. 6-3A). The ratio of EC capillary-like structures to the surrounding HSCs was quantitatively analyzed (Fig. 6-3B). The value reached a plateau by day 16, indicating that over half of the EC capillary-like structures were associated with HSCs at this time.

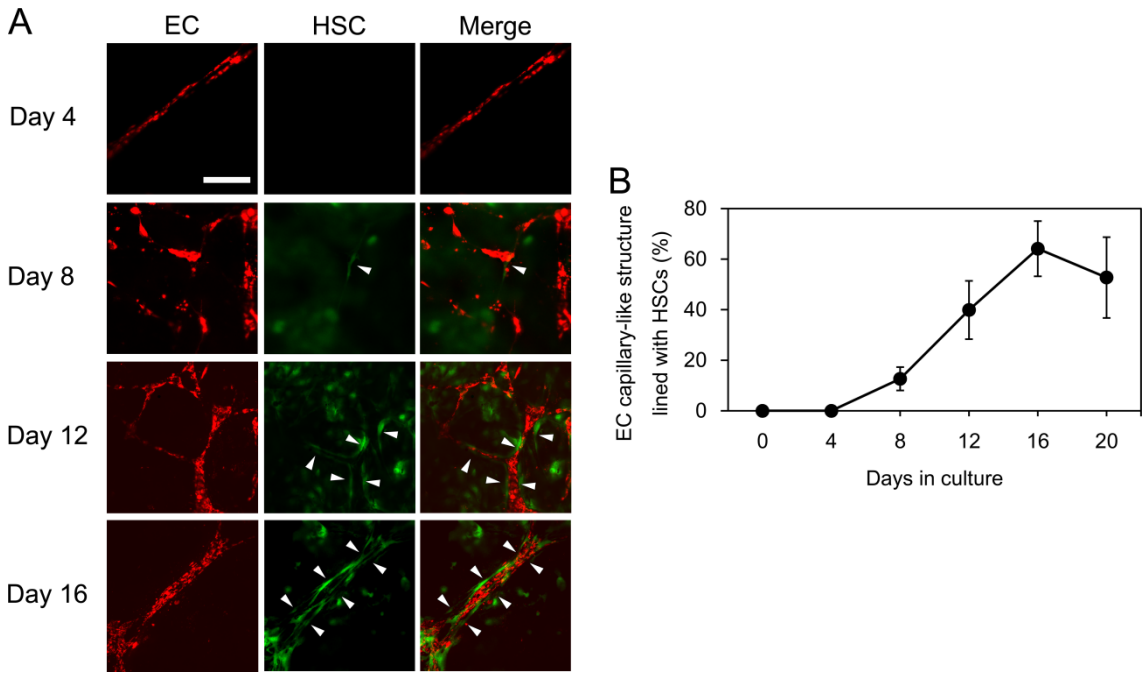

Figure 6-3. HSC recruitment by EC capillary-like structures. ***A)*** Fluorescent micrographs of EGFP-positive HSCs (green) (arrowheads) and EC capillary-like structrues stained with CM-DiI (red). HSCs beneath a PLGA membrane gradually migrated to the EC capillary-like structures over culture time. Scale bars: 100 μm. ***B)*** Quantitative analysis of HSC recruitment by EC capillary-like structures.

6-2-4. PDGF-β and its receptor interactions in the HSC recruitment by EC capillary-like structures

Interactions between PDGF-β and PDGF receptor-β are the most potent chemotactic signals in the recruitment of pericytes to newly formed capillaries *in vivo* (Lee *et al*., 2007). Additionally, PDGF receptor-β has been identified in rat HSCs (Friedman, 2008) in pericytes (Díaz-Flores *et al*., 2009; Armulik *et al*., 2005). Therefore, it was hypothesized that PDGF signaling is responsible for the selective migration of HSCs to the EC capillary-like structures in the 3D stacked-up culture. To test this hypothesis, PDGF-β expression was immunohistochemically analyzed. Strong intracellular expression of PDGF-β was detected in the EC capillary-like structures (EC capillary-like structure; Fig. 6-4A), while little intracellular PDGF-β expression was detected in SHs and HSCs (SH-HSC co-culture; Fig. 6-4A). Quantitative analysis confirmed that the EC capillary-like structures expressed higher levels of PDGF-β than SHs and HSCs (Fig. 6-4B).

Next, PDGF signaling was inhibited in the 3D stack-up culture by a tyrosine kinase inhibitor of the PDGF-receptor β, AG1295. Under this condition, no HSC recruitment by the capillary-like structures was observed (Fig. 6-4C).

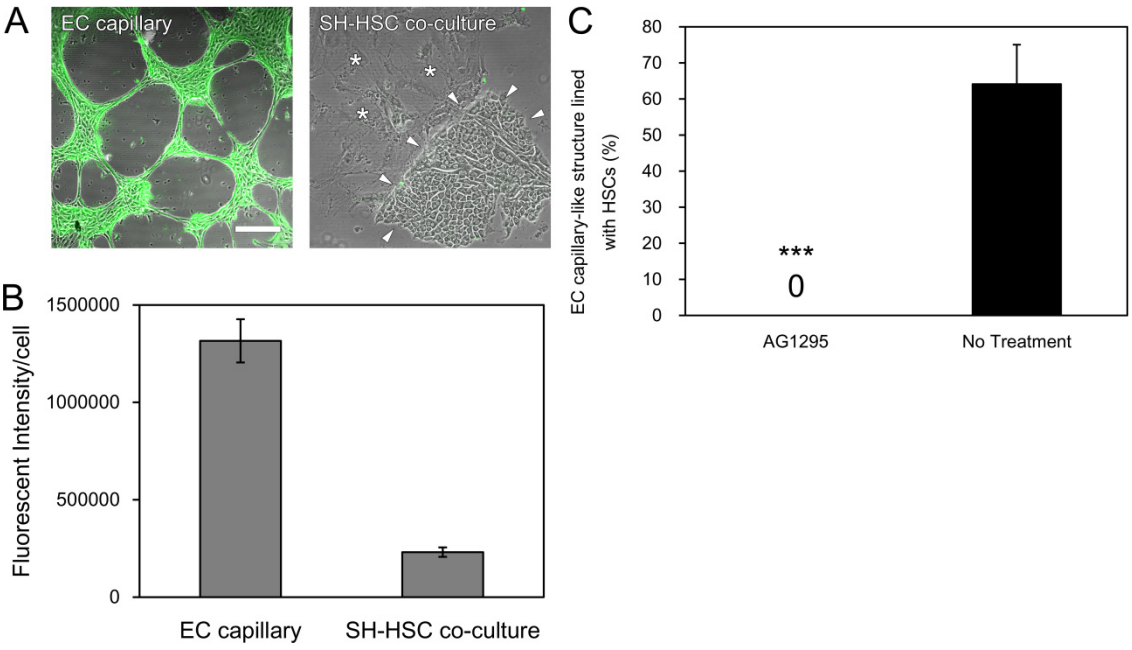

Figure 6-4. PDGF-BB-dependent HSC recruitment by EC capillary-like structures. ***A)*** Intracellular PDGF-BB immunofluorecent staining in EC capillary-like structures 24 h after seeding, SH colonies (arrowheads) and HSCs (asterisks) 14 days after seeding. Scale bars: 100 μm. ***B)*** Quantification of intracellular PDGF-BB expression. ***C)*** The HSC recruitment was significantly inhibited by the addition of the tyrosine kinase inhibitor of PDGF-receptor β, AG1295. *** indicates p <0.001 compared with tri-culture.

6-2-5. Effect of membrane pore-size and porosity on the HSC recruitment to the EC capillary-like structures

The effect of membrane configuration on HSC recruitment to EC capillary-like structures was investigated. Pore-size and porosity of the membranes can be controlled by changing the water content in PLGA-dissolved solvent during fabrication of the membranes (Fig. 6-1). Three types of membranes were used and their configurations are listed in Table. 6-1. Membranes fabricated with 10% water content had 69.2% of the EC-capillary structures incorporated with HSCs, while those fabricated with 4% and 8% water content had no EC-capillary structures lining the HSCs (Table. 6-1).

Table 6-1. Effects of the membrane configurations on HSC recruitment to the EC capillary-like structures.

Moisture content (%)	4	8	10
Pore-size (μm)	1.2 ± 0.3	7.4 ± 3.6	13.7 ± 4.8
Porosity (%)	1.0 ± 0.8	46.6 ± 3.7	57.3 ± 1.6
EC capillary-like structure lined with HSCs (%)	0	0	64.1 ± 10.9

6-2-6. HSC-incorporated liver sinusoidal structures

On day 16, the cellular configuration of the tri-culture was analyzed immunohistochemically. An immunostained fluorescent image showed that EC capillary-like structures were distributed on SH colonies with 10–20 μm gaps between them, and that the EC capillary-like structures were surrounded by HSCs (arrowheads; Fig. 6-5A). To further analyze the distribution of ECs and HSCs in the stacked-up structures, a *z*-axis series of fluorescence images was three-dimensionally reconstructed (Fig. 6-5B). The image revealed that HSCs were firmly attached to the EC capillary-like structures in association with their nuclei (arrowheads; Fig. 6-5B). In addition, HSCs extended their cytoplasmic processes mainly along the long axis direction of the EC capillary-like structures, resulting in formation of HSC-incorporated sinusoidal structures. The presence of HSC-incorporated capillary structures was confirmed by quantitative analysis for both HSC localization around the EC capillary-like structures (Fig. 6-5C) and HSC major axis angle to EC capillary-like structures (Fig. 6-5D).

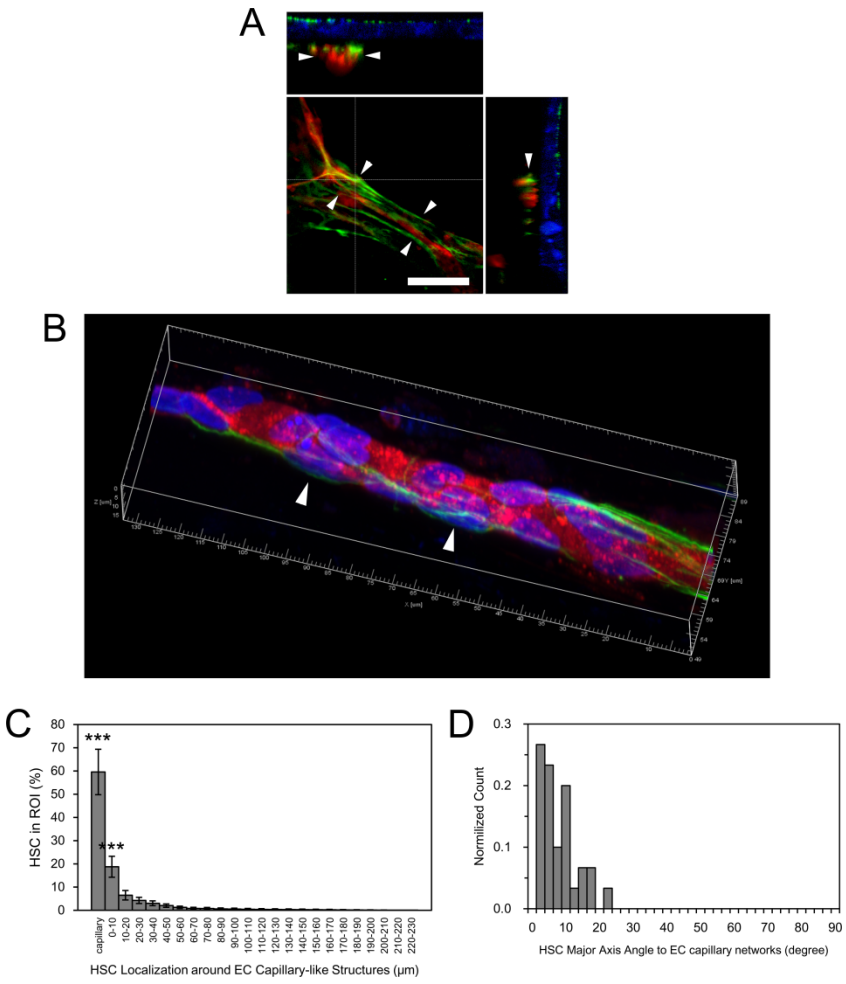

Figure 6-5. Three-dimensional configuration of sinusoidal structures. ***A*)** Fluorescent micrographs of sinusoidal structures. Cells were fixed on day 20 and photographed using confocal microscopy. Images were three-dimensionally reconstructed by calculating 186 x-y planes at 0.36-μm intervals: the 90th x-y plane, and x-z and y-z vertical sections are shown. EC capillary-like structures stained with CM-DiI (red) were stacked on the CK8-positive SH colony (blue) and well colocalized with desmin-positive HSCs (green). Scale bars: 100 μm. ***B*)** Stereoimage of a HSC-wrapped EC capillary-like structure. EC capillary-like structures stained with CM-DiI (red) were tightly wrapped with desmin-positive HSCs (green). Cell nuclei were counterstained with DAPI (blue). Note that HSCs are attached firmly to the EC capillary-like structure with accompanying their nuclei (arrowheads). ***C and D*)** Quantitative analysis of HSC-incorporated EC capillary-like structures. Localization of HSCs around EC capillary-like structures (C) and HSC major axis angle to EC capillary-like structures (D). *** indicates p <0.001, compared with HSCs in the area outside of the EC capillary-like structures and those in the area more than 10 μm away from the EC capillary-like structures.

6-2-7. Upregulation of SH differentiation in the HSC-incorporated liver sinusoidal structures

To investigate the function of SHs in HSC-incorporated liver sinusoidal structures, albumin secretion was measured. From day 4 after tri-culture, significant differences in albumin secretion were observed between the sinusoidal structures and the cultures without ECs, and a high level of albumin secretion was maintained at least until day 20 (Fig. 6-6).

mRNA expression levels of hepatocyte-differentiation markers were also examined by qPCR analysis (Fig. 6-7). In the sinusoidal structures, the hepatocyte-differentiation markers (*Tat*, *To*, and *Bsep*) were significantly upregulated compared to those in culture without ECs. The expression of *Mrp2* mRNA by the SHs in the sinusoidal structures was comparable to that in the culture without ECs.

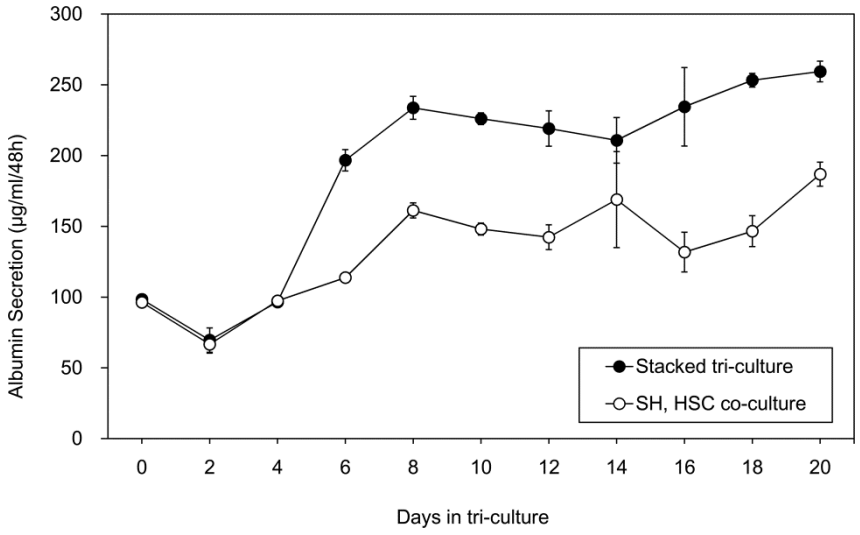

Figure 6-6. Quantitative analysis of albumin secretion into the medium during 48-hour periods. As control, the functions were also analyzed for the cells that were not stacked with EC capillary-like structures.

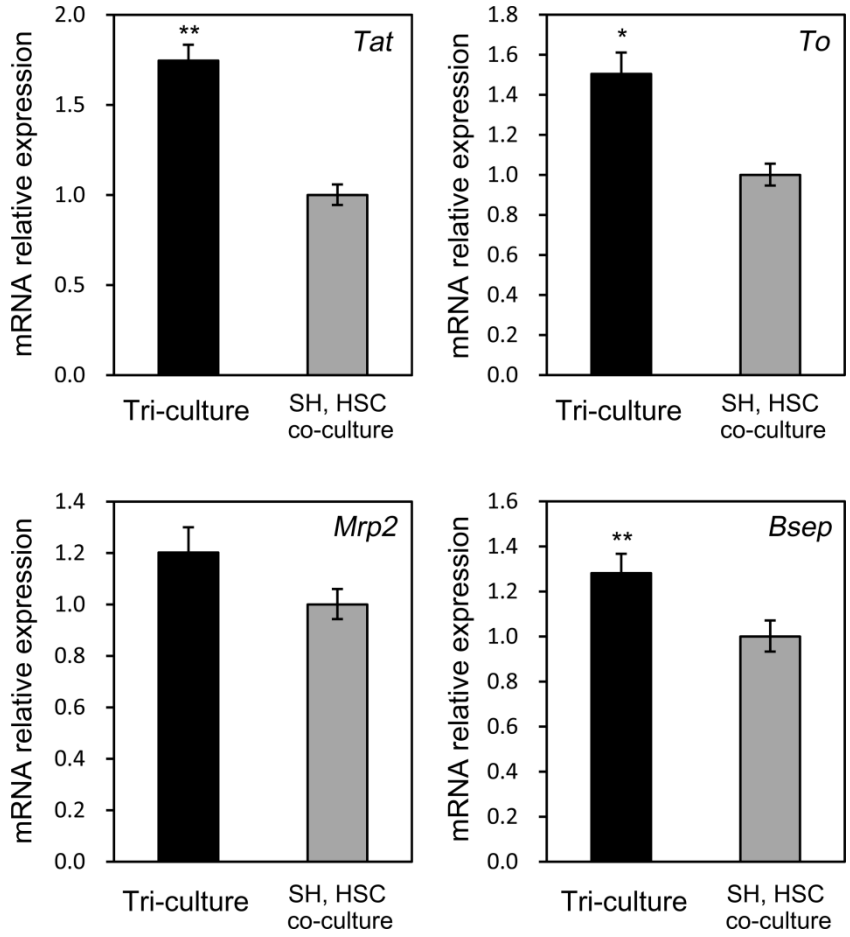

Figure 6-7. QPCR analysis for mRNA expressions of hepatocyte-differentiation markers (*Tat*, *To*, *Mrp2*, *Bsep*). The analysis was performed with total RNA isolated from the cells in the 3D stacked-up tri-culture (Tri-culture) and from those cultured without ECs (SH, HSC co-culture) at day 16. The amount of mRNA expressions was normalized with those of SH, HSC co-culture. The SHs in Tri-culture expressed the hepatocyte-differentiation markers stronger than those in SH, HSC co-culture. * and ** indicate p <0.05 and p <0.01 as compared with SH-HSC co-culture, respectively.

6-3. Discussion

6-3-1. Enhancement of heterotypic cell–cell interactions using PLGA microporous membranes

Miroporous membranes made from polymeric materials, such as polycarbonate and PET, have been widely used for co-culturing different cell types (Edwards *et al*., 2005; Kinard *et al*., 1997) and partially enhanced the heterotypic cell–cell interactions. In chapter 4, PET microporous membranes was used to establish the hepatocyte-HSC-EC tri-culture model. Under these conditions, HSCs were distributed around the EC capillary-like structures. However, the cells did not line the EC capillary-like structures. In contrast, the present chapter demonstrated that the EC capillary-like structures were surrounded by HSCs, which firmly attached the cell body to the capillary-like structures and extend their cytoplasmic processes to wrap the capillary-like structures. These results suggest that the PLGA membranes provide the microenvironment which enhanced the heterotypic cell–cell interactions to recapture the HSC-incorporated sinusoidal structures. There are two possible reasons for the improved heterotypic cell–cell interactions by using the PLGA membranes. Firstly, thickness of the PLGA microporous membrane was 2.4 ± 0.1 μm while that of the PET membrane is 15–20 μm. Secondly, the porosity of the PLGA membranes is 57.3 ± 1.6 %, while that of the PET membranes is under 5 %. A previous study demonstrated that reduction of thickness and increase of porosity in microporous membrane scaffolds improved mass transport via the membranes (Zhang *et al*., 2008). These improvements may have enhanced the heterotypic cell–cell interactions, which are essential for sinusoidal tissue reconstructions.

A previous study demonstrated that kidney-like tissues could be reconstructed from combination of epithelial tissues and mesenchymal tissues (Rosines *et al*., 2010), suggesting that tissue-by-tissue assembly is a plausible strategy for reconstruction of complex 3D tissues from cultured cells *in vitro*. However, no studies have addressed the

potency of tissue-by-tissue assembly in liver sinusoidal tissue reconstruction. In this chapter, a stack-up method using the PLGA membranes enabled combination of Matrigel angiogenesis assay and SH-HSC co-culture. The stack-up culture method using microporous membranes has been previously explored for 3D expansion of engineered hepatocyte tissues (Sudo *et al*., 2005). In contrast to other stack-up culture methods, such as those using temperature-responsive culture dishes (Harimoto *et al*., 2002; Ohno *et al*., 2008; Ohno *et al*., 2009; Ohashi *et al*., 2007), magnetic nanoparticles (Ito *et al*., 2008), and nanometer-sized ECM films (Matsusaki *et al*., 2007), the stack-up culture method using microporous membranes do not need any complex processes, which can prevent cells from being damaged by excessive manipulations. Considering above, the present culture approach is plausible for reconstruction of liver sinusoidal tissues *in vitro*.

6-3-2. PDGF-mediated HSC recruitment to the EC capillary-like structures

The HSC–EC interaction has been extensively studied *in vitro* (DeLeve *et al*., 2008; DeLeve *et al*., 2004; Wirz *et al*., 2008). In terms of liver sinusoid organization, studies using *in vitro* HSC-SEC co-culture have shown that PDGF signaling is critical for capillary organization of SECs (Semela *et al*., 2008). However, little is known regarding the organizational processes of HSC-incorporated structures or the molecular mechanisms underlying the hepatocyte-HSC-EC complex, and they have not been constructed *in vitro*. This study demonstrates that the HSC-incorporated sinusoidal structures arise from HSC migration to pre-formed EC capillary-like structures, and that this process is mediated in part by PDGF signaling (Fig. 6-4), which is consistent with a previous report (Semela *et al*., 2008). Although additional work is required to elucidate the underlying molecular mechanism of HSC recruitment and its effect on EC phenotypic features, this tri-culture model will provide a unique *in vitro* tissue model to

study the organization processes of HSC-incorporated sinusoidal structures and its molecular mechanism.

6-3-3. Up-regulation of hepatic functions in the reconstructed sinusoid-like structures

The HSC-incorporated sinusoidal tissues retained higher levels of albumin secretion (Fig. 6-6) and hepatocyte-differentiated markers (Fig. 6-7) compared to SH-HSC organoids. This up-regulation of hepatic function may be derived from the active interactions between SHs and HSC-incorporated EC capillary-like structures. Various hepatocyte-EC co-culture models have demonstrated that ECs enhance a wide variety of hepatocyte functions by secreting soluble factors (Talamini *et al*. 1998; Jindal *et al*, 2009) and ECM (Ohno *et al*., 2009). In addition, PLGA microporous membranes may enhance hepatocyte–EC interactions. As described above, the PLGA membranes used in this chapter had subcellular thicknesses and high porosity, which may allow for increased transport of soluble factors from ECs to SHs and direct access of SHs to EC-secreted ECM. Previous hepatocyte-NPC co-culture studies have shown that maintenance of the hepatocellular phenotype by NPC requires direct contact for a limited time followed by a sustained soluble signal that has an effective range of <400 μm (Hui *et al*., 2007). The stabilization of hepatocyte function by co-culturing with ECs and HSCs has been shown previously (Nahmias *et al*., 2006; Soto-Gutierrez *et al*., 2010); however, characterization of the organization of HSC-incorporated vascular structures has never been completed. Therefore, I suggest that HSC-incorporated sinusoidal structures might provide a unique *in vitro* tissue model to study interactions between hepatocytes and sinusoids.

In conclusion, liver sinusoidal-like tissues where HSCs were located along EC capillaries were reconstructed in hepatocyte-HSC-EC tri-culture. Use of PLGA microporous membrane enhanced the heterotypic interactions across the membranes, which was essential for organogenesis of functional sinusoidal-like tissues *in vitro*. This

model will provide a structural unit for constructing the functional, thick, and vascularized liver tissues *in vitro*.

6-4. Summary

In liver sinusoids, HSCs line the outer surface of microvessels to form a functional unit with endothelia and hepatocytes. To reconstruct functional liver tissue *in vitro*, formation of the HSC-incorporated sinusoidal structure is essential. Capillary formation of EC was previously demonstrated in tri-culture where a Matrigel angiogenesis assay and SH-HSC co-culture were combined using polymeric microporous membranes. However, the high thickness and low porosity of the membranes limited heterotypic cell–cell interactions, which are essential to form HSC-incorporated structures. A stack-up culture method has been also previously established to reconstruct 3D hepatic tissues using thin and high porous PLGA membranes. Here, I focused on in hepatocyte-HSC-EC tri-culture to reconstruct the HSC-incorporated liver sinusoidal structures *in vitro*. First, the formation of EC capillary-like structures was induced on Matrigel-coated microporous PLGA membranes. Next, the membranes were stacked on hepatic organoids composed of small SHs and HSCs. When pore size and porosity of the membranes were optimized, HSCs selectively migrated to the EC capillary-like structures. This process was mediated in part by PDGF signaling. In addition, the HSCs were located along the outer surface of the EC capillary-like structures with their long cytoplasmic processes. In the HSC-incorporated sinusoidal tissues, SHs retained high levels of differentiated functions, compared to those without ECs. This model will provide a basis for the construction of functional, thick, and vascularized liver tissues *in vitro*.

References

Armulik A, Abramsson A, Betsholtz C. 2005, Endothelial/pericyte interactions, *Circ Res*, **97**: 512–523.

Bader A, Knop E, Kern A, Böker K, Frühauf N, Crome O, Esselmann H, Pape C, Kempka G, Sewing KF. 1996, 3-D coculture of hepatic sinusoidal cells with primary hepatocytes-design of an organotypical model, *Exp Cell Res*, **226**: 223–233.

DeLeve LD, Wang X, Hu L, McCuskey MK, McCuskey RS. 2004, Rat liver sinusoidal endothelial cell phenotype is maintained by paracrine and autocrine regulation, *Am J Physiol Gastrointest Liver Physiol*, **287**: G757–763.

DeLeve LD, Wang X, Guo Y. 2008, Sinusoidal endothelial cells prevent rat stellate cell activation and promote reversion to quiescence, *Hepatology*, **48**: 920–930.

Díaz-Flores L, Gutiérrez R, Madrid JF, Varela H, Valladares F, Acosta E, Martín-Vasallo P, Díaz-Flores LJr. 2009, Pericytes. Morphofunction, interactions and pathology in a quiescent and activated mesenchymal cell niche. *Histol Histopathol*, **24**, 909–969.

Edwards S, Lalor PF, Nash GB, Rainger GE, Adams DH. 2005, Lymphocyte traffic through sinusoidal endothelial cells is regulated by hepatocytes, *Hepatology*, **41**: 451–459.

Friedman SL. 2008, Hepatic stellate cells: protean, multifunctional, and enigmatic cells of the liver, *Physiol Rev*, **88**: 125–172.

Harimoto M, Yamato M, Hirose M, Takahashi C, Isoi Y, Kikuchi A, Okano T. 2002, Novel approach for achieving double-layered cell sheets co-culture: overlaying endothelial cell sheets onto monolayer hepatocytes utilizing temperature-responsive culture dishes, *J Biomed Mater Res*, **62**: 464–470.

Hui EE, Bhatia SN. 2007, Micromechanical control of cell–cell interactions, *Proc Natl Acad Sci U S A*, **104**: 5722–5726.

Hwa AJ, Fry RC, Sivaraman A, So PT, Samson LD, Stolz DB, Griffith LG. 2007, Rat liver sinusoidal endothelial cells survive without exogenous VEGF in 3D perfused co-cultures with hepatocytes. *FASEB J*, **21**: 2564–2579.

Ito A, Honda H, Kamihira M. 2008, Construction of 3D tissue-like structure using functional magnetite nanoparticles, *Yakugaku Zasshi*, **128**: 21–28.

Jindal R, Nahmias Y, Tilles AW, Berthiaume F, Yarmush ML. 2009, Amino acid-mediated heterotypic interaction governs performance of a hepatic tissue model, *FASEB J*, **23**: 2288–2298.

Kasuya J, Tamogami R, Masuda G, Mitaka T, Ikeda M, Sudo R, Tanishita K. 2011, Reconstruction of 3D stacked hepatocyte tissues using degradable, microporous poly (*D,L*-lactide-*co*-glycolide) membranes, *Biomaterials*, **33**: 2693–2700.

Kinard F, Sergent-Engelen T, Trouet A, Remacle C, Schneider YJ. 1997, Compartmentalized coculture of porcine arterial endothelial and smooth muscle cells on a microporous membrane, *In Vitro Cell Dev Biol Anim*, **33**: 92–103.

Lee JS, Semela D, Iredale J, Shah VH. 2007, Sinusoidal remodeling and angiogenesis: a new function for the liver-specific pericyte? *Hepatology*, **45**: 817–825.

Martinez-Hernandez A, Amenta PS. 1993, The hepatic extracellular matrix. II. Ontogenesis, regeneration and cirrhosis, *Virchows Arch A Pathol Anat Histopathol*, **423**: 77–84.

Martinez-Hernandez A, Amenta PS. 1995, The extracellular matrix in hepatic regeneration, *FASEB J*, **9**: 1401–1410.

Matsusaki M, Kadowaki K, Nakahara Y, Akashi M. 2007, Fabrication of cellular multilayers with nanometer-sized extracellular matrix films, *Angew Chem Int Ed Engl*, **46**: 4689–4692.

Nahmias Y, Schwartz RE, Hu WS, Verfaillie CM, Odde DJ. 2006, Endothelium-mediated hepatocyte recruitment in the establishment of liver-like tissue in vitro, *Tissue Eng*, **12**:1627–1638.

Ohashi K, Yokoyama T, Yamato M, Kuge H, Kanehiro H, Tsutsumi M, Amanuma T, Iwata H, Yang J, Okano T, Nakajima Y. 2007, Engineering functional two- and three-dimensional liver systems in vivo using hepatic tissue sheets, *Nat Med*, **13**: 880–885.

Ohno M, Motojima K, Okano T, Taniguchi A. 2008, Up-regulation of drug-metabolizing enzyme genes in layered co-culture of a human liver cell line and endothelial cells, *Tissue Eng Part A*, **14**: 1861–1869.

Ohno M, Motojima K, Okano T, Taniguchi A. 2009, Maturation of the extracellular matrix and cell adhesion molecules in layered co-cultures of HepG2 and endothelial cells, *J Biochem*, **145**: 591–597.

Rosines E, Johkura K, Zhang X, Schmidt HJ, Decambre M, Bush KT, Nigam SK. 2010, Constructing kidney-like tissues from cells based on programs for organ development: toward a method of in vitro tissue engineering of the kidney. *Tissue Eng Part A*. **16**: 2441–2455.

Sato M, Kojima N, Miura M, Imai K, Senoo H. 1998, Induction of cellular processes containing collagenase and retinoid by integrin-binding to interstitial collagen in hepatic stellate cell culture, *Cell Biol Int*, **22**: 115–125.

Semela D, Das A, Langer D, Kang N, Leof E, Shah V. 2008, Platelet-derived growth factor signaling through ephrin-b2 regulates hepatic vascular structure and function, *Gastroenterology*, **135**: 671–679.

Soto-Gutierrez A, Navarro-Alvarez N, Yagi H, Nahmias Y, Yarmush ML, Kobayashi N. 2010, *Cell Transplant*, **19**: 815–822.

Sudo R, Mitaka T, Ikeda M, Tanishita K. 2005, Reconstruction of 3D stacked-up structures by rat small hepatocytes on microporous membranes, *FASEB J*, **19**:1695–1697.

Talamini MA, McCluskey MP, Buchman TG, De Maio A. 1998, Expression of alpha2-macroglobulin by the interaction between hepatocytes and endothelial cells in coculture, *Am J Physiol*, **275**: R203–211.

Wirz W, Antoine M, Tag CG, Gressner AM, Korff T, Hellerbrand C, Kiefer P. 2008, Hepatic stellate cells display a functional vascular smooth muscle cell phenotype in a three-dimensional co-culture model with endothelial cells, *Differentiation*, **76**: 784–794.

Zhang S, Xia L, Kang CH, Xiao G, Ong SM, Toh YC, Leo HL, van Noort D, Kan SH, Tang HH, Yu H. 2008, Microfabricated silicon nitride membranes for hepatocyte sandwich culture, *Biomaterials*, **29**: 3993–400.

Chapter 7. Concluding remarks

7-1. Summary

A tissue-engineered liver needs to be developed as an alternative method to the liver transplantation. In particular, reconstruction of the liver sinusoidal structures is essential since it might lead to a solution of the greatest challenge in liver tissue engineering: obtaining thick and functional engineered liver tissues. However, previous *in vitro* liver cell culture still did not adequately recapture the sinusoidal architectures since they did not focus on the potentially key role of HSCs in the sinusoidal organization. Therefore, this dissertation focused on the elucidation of the HSC's role in the reconstruction of the sinusoidal structures in the SH-HSC-EC tri-culture, and developing a novel engineering strategy for construction of liver sinusoids *in vitro*.

Chapter 4 showed that recapturing the HSC-mediated sinusoidal structures lead to the achievement of the physiological complex composed of SHs, HSCs, and ECs using PET microporous membranes. In addition, it was also shown that the spatial control of HSC behavior by changing the pore size was critical for the reconstruction of the HSC-mediated structures. SHs and HSCs were first isolated from adult rat livers and then cultured on the PET microporous membranes. The SHs proliferated and formed colonies within 14 days. HSCs located between the SH colonies and the membrane. Furthermore, the HSCs penetrated the pores and were distributed on the other side of membrane. ECs were then seeded on the other side of the membranes. At this stage, HSC behavior was controlled by the membrane pore size, which was critical for achieving the HSC-mediated structures. With 1.0-μm pores, HSCs could extend their processes to the other side of the membrane through the pores, but their nuclei were failed to pass through the pores. Such HSCs were successfully intercalated between

layers of hepatocytes and ECs, owing to the limited HSC behavior. In addition, this *in vivo*-like structure was maintained for at least 40 days. This hepatocyte-HSC-EC complex enabled us to investigate the roles of HSCs, as both facilitators and integrators of hepatocyte–EC communications. Specifically, we confirmed that HSCs mediated hepatocyte–EC communications in terms of EC morphogenesis. When cytoplasmic processes of quiescent HSCs were adjacent to ECs, while the HSC bodies remained on the hepatocyte side of the membrane, the ECs changed morphologically, whereas under other co-culture conditions there was no morphological change. Thus, the spatial control of HSC behavior was shown to be essential to achieve HSC-mediated functional complex by using the PET microporous membranes.

In chapter 5, engineering strategy for achievement capillary formation was developed in the SH-HSC-EC complex. The effect of the direct HSC–EC contacts on EC capillary formation was first investigated in the SH-HSC-EC complex which was established in the chapter 3. EC capillary morphogenesis was induced by overlaying Matrigel on an EC layer. Direct HSC–EC contacts inhibited EC capillary morphogenesis, suggesting that the HSC–EC contacts may be an important factor in capillary formation. Following these results, I next tested the hypothesis that, in addition to spatial control, temporal control of HSC behavior is also important in achieving capillary morphogenesis in the tri-culture. ECs responded to the induction of capillary morphogenesis before the formation of direct HSC–EC contacts, while the ECs remained to form monolayers when capillary morphogenesis was induced after the HSC–EC contacts were established. When capillary morphogenesis was successfully achieved in the tri-culture, HSCs tended to preferably localize near the pre-formed capillary-like structures, resulting in the reconstruction of liver sinusoidal structures. In these structures, hepatocyte maturation was partially induced. Thus, both spatial and temporal control of HSC behavior was revealed to be a key engineering strategy for the

vascularization of engineered liver tissues *in vitro*.

In liver sinusoids, HSCs surround the outer surface of the EC capillary structures. In chapter 6, to reconstruct the HSC-incorporated capillary structures, the heterotypic cell–cell interactions across the membranes were improved. PLGA microporous membranes were fabricated and their topography such as thickness, pore size, and porosity were optimized. When the membrane with optimized pore size and porosity was used, HSCs selectively migrated to the EC capillary-like structures and that this process was mediated in part by PDGF signaling. In addition, these HSCs surrounded the outer surface of the EC capillary-like structures by their long cytoplasmic processes, resulting in the reconstruction of the liver sinusoid-like structures. Furthermore, SHs within the structures exhibited the mRNA transcription of hepatic-differentiation markers and retained a relatively high level of albumin secretion. Thus, PLGA microporous membranes facilitated the interactions between HSCs and EC capillary structures, which was essential for the reconstruction of the HSC-incorporated functional sinusoid-like tissues *in vitro*.

To briefly summarize the above (Fig. 7-1), in chapter 4 and 5, the spatio-temporal control of HSC behavior was revealed to be essential to reconstruct liver sinusoid-like tissues. In addition, HSCs in the liver sinusoid-like tissues not only structurally but also functionally bridged between hepatocyte tissues and EC capillary-like structures. In the following chapter 6, PLGA microporous membranes were used and this had two aims. The first aim was to accelerate the heterotypic cell–cell interactions. The subcellular thicknesses and high porosity of the PLGA membranes promoted the HSC–EC interactions, resulting in construction of HSC-incorporated functional sinusoid-like tissues. Another aim of using the PLGA membranes was their application to the future implantation therapy (Fig. 7-2). PLGA is a biodegradable material that is commonly

used in clinical practice. Although the significant *in vitro* degradation of the membranes was not observed in this study, the membrane will be degraded after the implantation. Thus, the findings in this dissertation will provide a basis for clinical application of the tissue-engineered liver constructs as an alternative method to the liver transplantation.

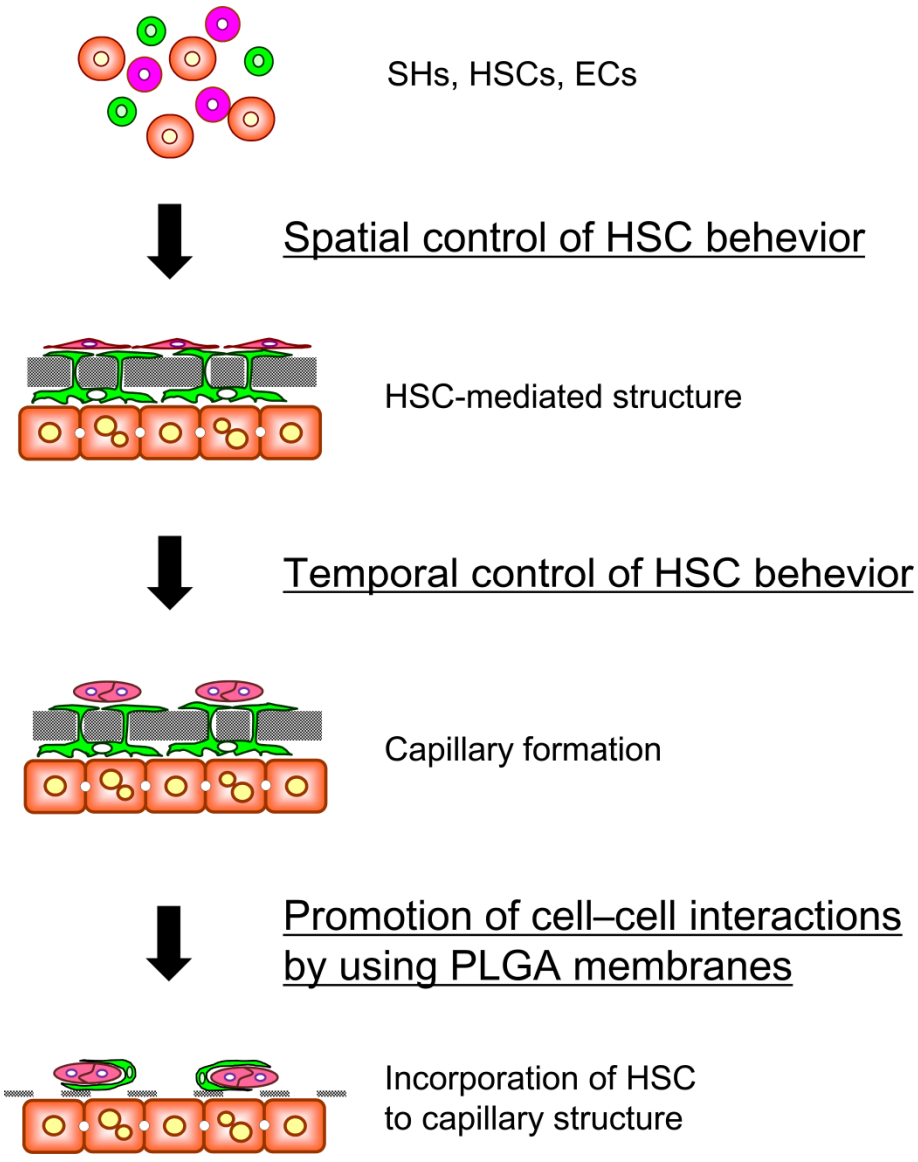

Figure 7-1. Reconstruction of liver sinusoidal tissues *in vitro.*

7-2. Future prospects

This dissertation demonstrated the construction of a structural unit of liver sinusoidal tissues using biodegradable PLGA microporous membranes. Thicker liver tissues containing sinusoidal beds will be available by multiple stacking of this unit (Fig. 7-2). In addition, in order to reconstruct transplantable thick liver tissues *in vitro*, a novel culture system where the sinusoidal beds can be anastomosed with an *ex vivo* perfusion system needs to be developed. ECs are known to be self-organized into capillary structures with luminal structures in 3D collagen gel culture (Davis *et al*., 2007; Vailhé *et al*., 2001; Yamamura *et al*., 2007). Combining a perfusable 3D culture of ECs with the multiple stacking of the unit will solve the above issue.

Besides the clinical application of this culture system, it has a potential application as physiological and pathological liver culture models. In this dissertation, the hepatocyte differentiated functions were shown to be in part elevated in the reconstructed sinusoidal tissues. However, little is still known whether the sinusoidal tissue organization also affects phenotypes and functions of the other cell types. Previous *in vivo* and *in vitro* studies have shown that HSCs and SECs significantly affect their phenotypes and functions with each other, which is closely linked with their structural association (DeLeve *et al*., 2004; DeLeve *et al*, 2008; Lee *et al*, 2007). However, due to the lack of appropriate *in vitro* culture models, little is known about dynamic relationships between their structural changes and their phenotypic and functional changes. The elucidation of this open question would have significant implication for therapeutic development for liver fibrosis, whose progress might result in cirrhosis and liver cancer. Cirrhosis and liver cancer are now among the top ten causes of death worldwide (Bosetti *et al*, 2007). Chapter 6 shows that HSCs surrounded the EC capillary structures, which might induce some phenotypic and functional alterations of these cell types. A comprehensive temporal study of the cellular

phenotypes and functions in this tri-culture system would help us understand the dynamic relationships between the sinusoidal tissue organization and the cellular phenotypes and functions.

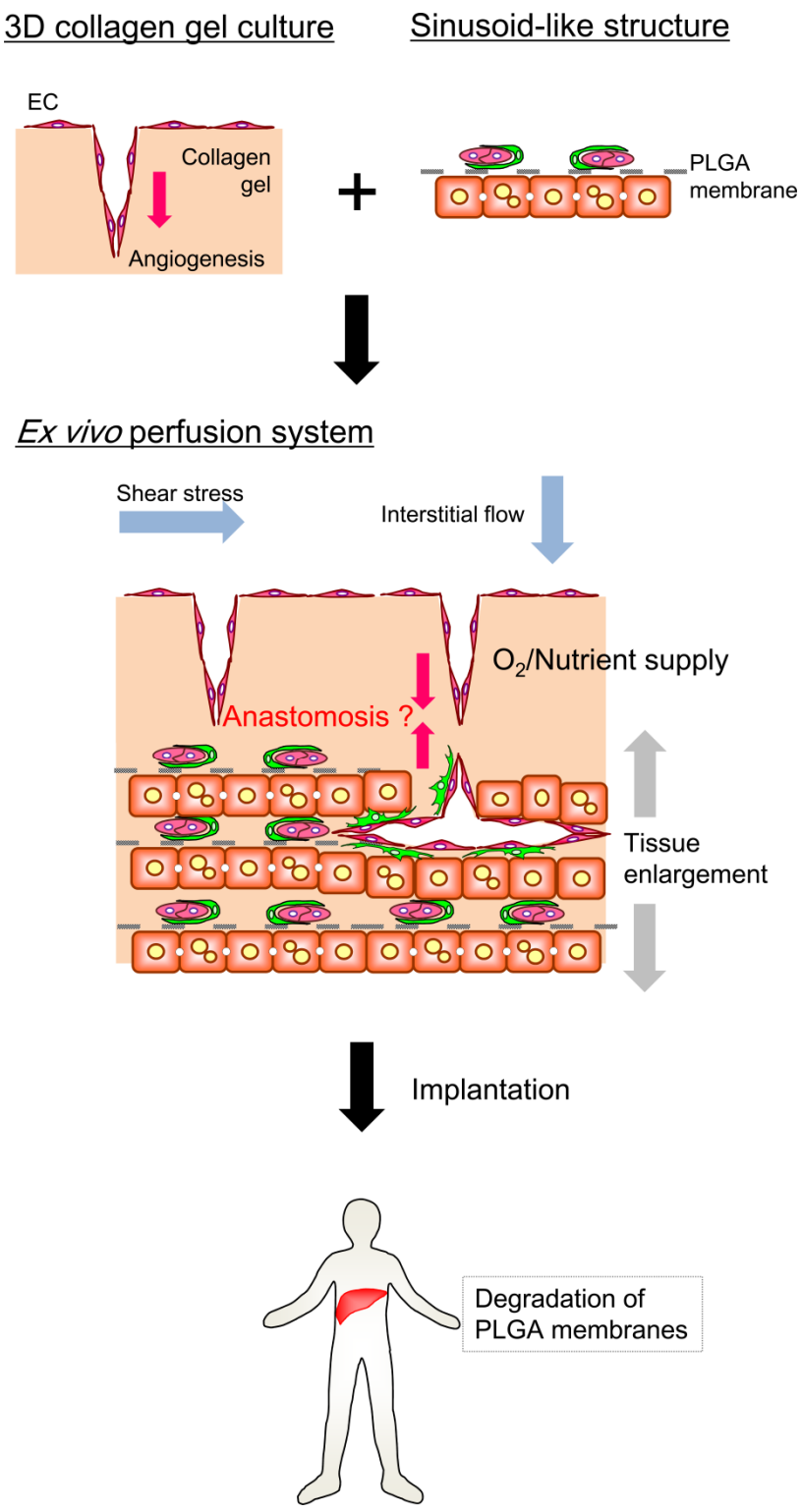

Figure 7-1. The application of reconstructed sinusoidal tissues to future implantation therapy.

References

Bosetti C, Levi F, Lucchini F, Zatonski WA, Negri E, La Vecchia C. 2007, Worldwide mortality from cirrhosis: an update to 2002, *J Hepatol*, **46**: 827–839.

Davis GE, Koh W, Stratman AN. 2007, Mechanisms controlling human endothelial lumen formation and tube assembly in three-dimensional extracellular matrices, *Birth Defects Res C Embryo Today*, **81**:270–285.

DeLeve LD, Wang X, Hu L, McCuskey MK, McCuskey RS. 2004, Rat liver sinusoidal endothelial cell phenotype is maintained by paracrine and autocrine regulation, *Am J Physiol Gastrointest Liver Physiol*, **287**: G757–763.

DeLeve LD, Wang X, Guo Y. 2008, Sinusoidal endothelial cells prevent rat stellate cell activation and promote reversion to quiescence, *Hepatology*, **48**: 920–930.

Lee JS, Semela D, Iredale J, Shah VH. 2007, Sinusoidal remodeling and angiogenesis: a new function for the liver-specific pericyte?, *Hepatology*, **45**: 817–825.

Vailhé B, Vittet D, Feige JJ. 2001, *In vitro* models of vasculogenesis and angiogenesis, *Lab Invest*, **81**:439–52.

Yamamura N, Sudo R, Ikeda M, Tanishita K. 2007, Effects of the mechanical properties of collagen gel on the *in vitro* formation of microvessel networks by endothelial cells, *Tissue Eng*, **13**:1443–1453.

Bibliography

Publications

1. Junichi Kasuya, Ryo Sudo, Toshihiro Mitaka, Mariko Ikeda, Kazuo Tanishita. Hepatic stellate cell-mediated three-dimensional hepatocyte and endothelial cell tri-culture model. *Tissue Engineering Part A*. **17** (3-4): 361–370, 2011.

2. Junichi Kasuya, Ryo Sudo, Genta Masuda, Toshihiro Mitaka, Mariko Ikeda, Kazuo Tanishita. Reconstruction of 3D stacked hepatocyte tissues using degradable, microporous poly(*D,L*-lactide-*co*-glycolide) membranes. *Biomaterials*. **33** (9): 2693–2700, 2012.

3. Junichi Kasuya, Ryo Sudo, Toshihiro Mitaka, Mariko Ikeda, Kazuo Tanishita. Spatio-temporal control of hepatic stellate cell-endothelial cell interactions for reconstruction of liver sinusoids *in vitro*. *Tissue Engineering Part A* (in press).

4. Junichi Kasuya, Ryo Sudo, Ryu Tamogami, Genta Masuda, Toshihiro Mitaka, Mariko Ikeda, Kazuo Tanishita. Reconstruction of hepatic stellate cell-incorporated liver sinusoidal structures in small hepatocyte tri-culture using microporous membranes. (submitted for publication).

Proceedings (International)

1. Junichi Kasuya, H Asami, Ryo Sudo, Toshihiro Mitaka, Mariko Ikeda, Kazuo Tanishita. Design of multilayered coculture system composed of small hepatocytes, liver stellate cells and sinusoidal endothelial cell. *Third Asian Pacific Conference on Biomechanics*, Tokyo, Japan, November, 2007.

2. Junichi Kasuya. 3D tri-culture model for liver regenerative medicine. *The 2nd International Symposium on Symbiotic, Safe and Secure System Design, Advances in System Design Project Research*, Kanagawa, Japan, February, 2010.

3. Junichi Kasuya, Ryo Sudo, Toshihiro Mitaka, Mariko Ikeda, Kazuo Tanishita.

Hepatic stellate cell-mediated three-dimensional hepatocyte and endothelial cell tri-culture model for a physiological liver experimental model. *Sixth World Congress on Biomechanics*, Singapore, Singapore, August, 2010.

4. Junichi Kasuya. Developing a novel approach for vascularization of engineered-liver tissue. *The 3rd International Symposium on Symbiotic, Safe and Secure System Design, Advances in System Design Project Research*, Kanagawa, Japan, February, 2011.

5. Junichi Kasuya, Ryo Sudo, Toshihiro Mitaka, Mariko Ikeda, Kazuo Tanishita. Spatio-temporal control of hepatic stellate cell–endothelial cell interactions for reconstruction of vascularized liver constructs *in vitro*. *The Asia Pacific Chapter of the Tissue Engineering and Regenerative Medicine Meeting 2011 (TERMIS-AP 2011)*, Singapore, Singapore, August, 2011.

Proceedings (Domestic) *written in Japanese

1. 粕谷 淳一，浅見 裕之，須藤 亮，三高 俊広，池田 満里子，谷下一夫．類洞内皮細胞と小型肝細胞を用いた共培養モデルの評価．第 14 回肝細胞研究会，鹿児島，2007 年 6 月．

2. 粕谷 淳一，浅見 裕之，須藤 亮，三高 俊広，池田 満里子，谷下一夫．小型肝細胞，星細胞，および類洞内皮細胞を用いた 3 次元積層共培養モデルの評価．第 46 回日本生体医工学会大会，兵庫，2008 年 5 月．

3. 粕谷 淳一，須藤 亮，三高 俊広，池田 満里子，谷下一夫．生体外における 3 次元肝組織再構築．日本生体医工学会専門別研究会バイオメカニクス研究会第１２６回研究会，埼玉，2008 年 11 月．

4. 粕谷 淳一，須藤 亮，三高 俊広，池田 満里子，谷下一夫．小型肝細胞，星細胞，血管内皮細胞による 3 次元積層共培養系の構築．日本機械学会 第 21 回バイオエンジニアリング講演会．北海道，2009 年 1 月．

5. 粕谷 淳一，須藤 亮，三高 俊広，池田 満里子，谷下一夫．小型肝細胞，星細胞，および血管内皮細胞による 3 次元共培養モデル．第 8 回日本再生

医療学会総会．東京，2009 年 3 月．

6. 粕谷 淳一，隅井干城，須藤 亮，三高 俊広，池田 満里子，谷下一夫．肝再生を目標とした小型肝細胞と血管内皮細胞による 3 次元共培養モデルの構築．第 48 回日本生体医工学会大会，東京，2009 年 4 月．

7. 粕谷 淳一，須藤 亮，三高 俊広，池田 満里子，谷下一夫．小型肝細胞，星細胞，血管内皮細胞による 3 次元積層共培養系の構築．第 16 回肝細胞研究会，山形，2009 年 6 月．

8. 粕谷 淳一，須藤 亮，三高 俊広，池田 満里子，谷下一夫． Hepatic stellate cell-mediated three-dimensional hepatocyte and endothelial cell tri-culture model. 第 49 回日本生体医工学会大会，大阪，2010 年 3 月．

9. 粕谷 淳一，須藤 亮，三高 俊広，池田 満里子，谷下一夫．星細胞－血管内皮細胞間接触による血管形態形成の制御．第 18 回肝細胞研究会，東京，2011 年 6 月．

Awards

1. APAB Young Investigator Award at AP Biomech 2007. *Third Asian Pacific Conference on Biomechanics, Asian Pacific Association for Biomechanics*, November, 2007.

2. Tissue Engineering & Regenerative Medicine SYIS-AP Young Investigator Awards, SYIS-AP Best Oral Presentation Third Prize. *The Asia Pacific Chapter of the Tissue Engineering and Regenerative Medicine Meeting 2011 (TERMIS-AP 2011)*, August, 2011.

Scholarships*written in Japanese

1. 財団法人旭硝子奨学会　2009 年度奨学生

2. 財団法人 村田海外留学奨学会　第 43 期奨学生

Acknowledgement

The research activities for this thesis were carried out at the School of Integrated Design Engineering, Keio University, under the guidance of Prof. Kazuo Tanishita.

First of all, I am deeply grateful to my supervisor Prof. Tanishita whose comments and suggestions were of inestimable value for my study. He gave me great suggestions from the standpoint of bioengineering and helped me step back to look at the overall big picture. Special thanks also go to Prof. Mariko Ikeda and Prof. Ryo Sudo whose opinions and information have helped me very much throughout the production of this study.

I would also like to express my gratitude to Prof. Toshihiro Mitaka for invaluable comments and suggestions from the standpoint of medical biology.

I also owe my gratitude to my thesis committee members Prof. Atsushi Hotta and Prof. Shogo Miyata.

This work could not have been possible without the contribution from so many wonderful people I worked with. I especially thank Mr. Genta Masuda for his grateful help for the experiments using PLGA microporous membranes. One of the most challenging parts of this study was working with the membranes. Its fabrication and operation was made much more manageable with his help. I'm also really indebted to the members of Tanishita-Sudo lab, especially the members of Cell Group in the lab for their technical supports.

I would also like to express my gratitude to all of my friends, especially to Ms. Yoko Sakai. This work could not have been possible without for her moral support and warm encouragements.

And last but not the least; I would like to express my deepest gratitude to my family for their unwavering love and support. My sincere gratitude to all of you for encouraging me–I could not have done this without you.

March 2012

Junichi Kasuya.

Junichi Kasuya